EFFECT OF THE JOINT ADDITION OF ALUMINUM AND MOLYBDENUM ON THE PRECIPITATION AND RECRYSTALLIZATION IN HSLA STEELS

by

DANNY ANDERSON

A Thesis Submitted to the Faculty of Graduate Studies and Research in Partial Fulfilment of the Requirements for the Degree of Master of Engineering.

Department of Mining and Metallurgical Engineering
McGill University
Montreal, Canada

November 1986

ABSTRACT

Three microalloyed steels of a series of six were hot compressed at constant true strain rates in the temperature range 875 to 925° to determine their high temperature flow behaviour. Of these 0.07% C + 1.25% Mn based steels, those containing additions of (i) 0.20% Mo and (ii) 0.20% Mo + 0.08% Al were tested as a part of this study. The results of a fourth steel containing 0.08% Al were introduced for purposes of comparison.

The influence of aluminum and molybdenum in solid solution on the yield strength of the steels was measured over the experimental temperature and strain rate range prior to the occurrence of precipitation. On an equal atom fraction basis, the molybdenum addition appeared to have a greater solute strengthening effect than aluminum. Results show that the addition of 0.08% Al (total) retards the onset of recrystallization in the plain C and 0.20% Mo steels. This further effect is believed to result from dynamic precipitation. The PTT curves determined for the Al and Al-Mo steels suggest that the addition of molybdenum accelerates the onset of dynamic precipitation. Comparison with a similar steel containing 0.30% Mo and 0.065% Al indicated that the substitution of aluminum for some of the molybdenum does not improve the hot deformation behaviour of the steel to suit controlled rolling applications. This may, in part, be due to difficulties in controlling the steelmaking practices (the level of aluminum in solution as opposed to total amount is difficult to control, as was observed to be the case here).

RESUME

Des tests de compression à haute température variant entre 875 et 925°C et à vitesse de déformation vraie constante ont été effectués sur trois d'une série de six aciers microalliés. De ces six aciers à base de 0.07 % C et 1.25 % Mn, ceux contenant des additions de (i) 0.20 % Mo et (ii) 0.20 % Mo + 0.08 % Al ont fait l'objet de cette étude. Les données provenant d'un quatrième acier contenant 0.08 % Al ont été introduites pour fins de comparaison.

L'influence de l'aluminium et du molybdène en solution solide sur la limite élastique des aciers a été measurée pour chaque température et vitesse de déformation utilisée avant l'apparition de précipitation provoquée par la déformation. Pour une même fraction atomique, la présence de molybdène sous forme de soluté a paru apporter un plus grand effet de renforcement que celle de l'aluminium. Les résultats indiquent que l'addition de 0.08 % Al (total) retarde le début de la recrystallization dans l'acier au carbone ainsi que celui contenant 0.20 % Mo. Cet effet additionnel semble provenir d'une précipitation dynamique. Les courbes précipitation-temps-température (PTT) déterminées pour les deux aciers contenant de l'aluminium suggèrent que l'addition de molybdène accélèrent le début de la précipitation dynamique. Une comparaison avec un acier similaire contenant 0.30 % Mo et 0.065 % Al a indiqué que le remplacement partiel du molybdène par de l'aluminium n'améliore pas le comportement à chaud de l'acier pour satisfaire à des applications en laminage controllé. Ceci peut, en partie, être dû aux difficultés rencontrer lors de la production d'acier (contrairement à la quantité totale d'aluminium présente dans l'acier, le niveau en solution est difficile à controller, tel qu'observé dans ce cas-ci).

ACKNOWLEDGEMENTS

The author wishes to express his gratitude to his thesis supervisor Professor M. G. Akben for her guidance, encouragement and support. Appreciation goes to Professor J. J. Jonas for use of the experimental equipment. He thanks his fellow graduate students for their interest and for providing a pleasant atmosphere in which to work. He is also grateful to B. Bacroix and A. Macchione for their stimulating support and attention.

He is indebted to CANMET for providing the experimental materials and financial support and particularly to Dr. G. E. Ruddle for his interest and technical assistance. He also acknowledges the scholarship from the Faculty of Graduate Studies.

Finally, he expresses his gratitude to L. J. Vroomen and Louis C. Vroomen for their continuous assistance with the use of the computer programs and Martin Knoepfel, George Dedic and George Tewfik for specimen preparation and for assistance with the repair of the experimental equipment.

TABLE OF CONTENTS

LIST OF FIGURES

LIST OF TABLES

CHAPTER 1

INTRODUCTION

One of the most important developments in ferrous metallurgy in this century may well be the large scale production of high-strength low-alloy (HSLA) steels. These steels constitute a class of engineering materials which feature simultaneously a high strength-to-weight ratio, superior toughness and reasonable weldability (1, 2). Production of steels with these properties depends strongly on the control of softening mechanisms such as recovery and recrystallization which occur during some stages of rolling. Many of the advances associated with the development of HSLA steels result from the application of controlled rolling. In this process, microalloying additions as well as thermomechanical processing are utilized in order to achieve a desired combination of mechanical properties through microstructural control. The controlled rolling of HSLA steels is a relatively inexpensive production technology (3). The total microalloy content of these steels seldom exceeds 0.1% by weight. Most importantly, the associated thermomechanical processing precludes the need for further heat treatment (Fig.1.1).

Microalloying elements such as Mo, Nb, Ti and V are added to HSLA steels as solutes but also as carbonitride forming agents which precipitate in the austenite phase inside the finishing stages of rolling. By controlling this precipitation, it is possible to retard or arrest recovery and recrystallization, enabling the production of a "pancaked" austenite grain structure. Upon transformation, such a structure provides a maximum number of ferrite nucleation sites, resulting in a fine ferrite grain size. The fine ferrite grain size is responsible for the high strength and superior toughness of microalloyed steels at application temperatures. Yield strengths in the range 350 to 700 MPa may be achieved in the as-rolled condition, thereby doubling the strength levels of mild steels (4). The simultaneous attainment of high

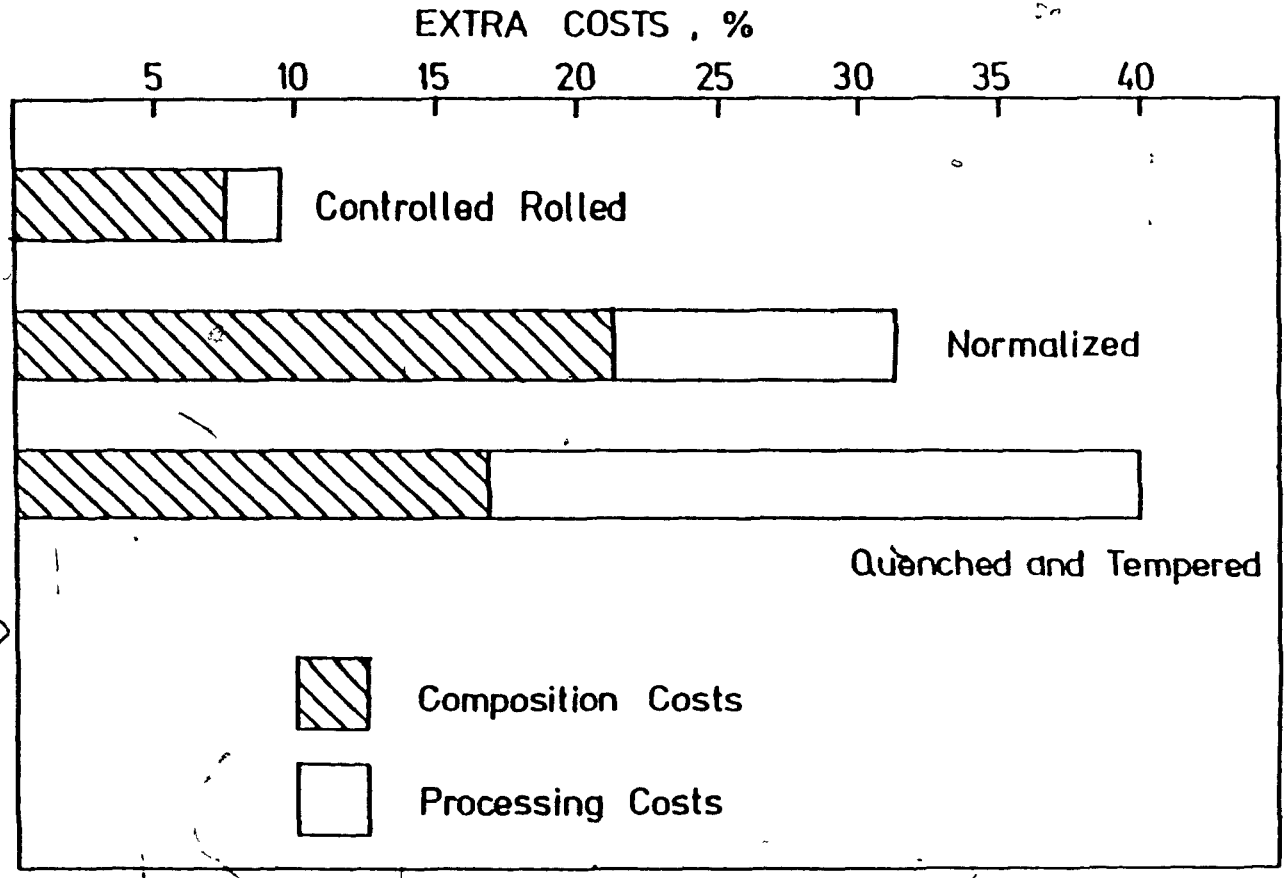

Figure 1.1 Additional composition and processing costs associated with: (i) controlled rolling, (ii) normalizing, and (iii) quenching and tempering, compared to conventional hot working of C-Mn steels (after Parrini et al (3)).

strength, superior toughness and reasonable weldability has resulted in the increasing demand for these economical materials for use in natural gas transmission pipelines, ship plates, off-shore drilling platforms and automotive applications (5).

The microalloying elements added to HSLA steels are known to retard austenite recrystallization and whether they fulfill their purposes as solutes or as precipitate formers is fairly well understood today. Molybdenum is generally added to microalloyed steels containing niobium and/or vanadium to enable higher strength levels to be attained. Aluminum is recognized as a widely used deoxidating agent and reacts with nitrogen to form AlN. Despite their widespread uses, the effect of molybdenum added jointly with aluminum on the microstructural processes taking place during controlled rolling, i.e. the recrystallization of austenite and the strain-induced precipitation of AlN in this case, is not well known. The primary objective of the present study is to determine the effect of AlN precipitation on the onset of dynamic recrystallization during the high temperature deformation of microalloyed austenite. A subsidiary aim is to investigate the influence of molybdenum addition on the kinetics of AlN precipitation. Comparison between the results of this work with the ones obtained in a previous study will reveal if the partial substitution of Al for the more expensive Mo can make the steel suitable to satisfy controlled rolling applications. Finally, by measuring the influence of the Al and Mo additions on the yield strength, i.e. on the ease of dynamic recovery, prior to the occurence of strain-induced precipitation, the experiments will permit the determination of the relative influence of the microalloying elements in solution.

Although the investigation is concerned with the initiation of dynamic recrystallization and dynamic precipitation, the relative influence of the microalloying additions on the static processes, of greater interest under industrial rolling conditions, can be established from these experiments.

CHAPTER 2

LITERATURE REVIEW

2.1 DEVELOPMENT OF CONTROLLED ROLLING

2.1.1. Historical Settings

Half a century ago, the design of high strength structural steels was based around the tensile strength of the material. Steel members were being shaped in hot rolling mills where the temperature was kept as high as possible (6) and the required tensile strength was achieved by increasing the levels of elements such as carbon, manganese (7, 8), silicon, phosphorus and by sometimes adding chromium, nickel or copper (9). The process gave the steels a coarse ferrite grain structure and, together with the high levels of alloy additions present, resulted in poor toughness, weldability, formability and increased cost.

By the early 1950's, it was demonstrated that a fine ferrite grain size leads to a simultaneous increase in yield strength and a decrease in the Impact Transition Temperature (I.T.T.) (10-12). This finding accelerated the wide scale introduction of normalized steels featuring finer grain sizes (13). It was not yet appreciated that the influence of manganese on grain refinement was through decreasing the austenite to ferrite transformation temperature. Normalized steels were produced with small amounts of grain refining agents such as aluminum and later on, molybdenum, niobium, titanium and vanadium (14). At that time, the so-called High Strength Low Alloy (HSLA) and plain carbon steels were produced in similar ways.

Forming operations may or may not have been followed by heat treatments to produce the required properties. Such procedures led to a coarse as-rolled austenite grain size and the resulting strength and impact properties were not very good. The solution to the problem came when it was realized that hot rolling could not only be a shaping method but also a thermomechanical process capable of improving the properties of hot-rolled

steels. One of the pioneer works was done by Domnarfvets Jernverk in Sweden around 1940 in which the finish rolling temperature was substantially lower than that employed in conventional practice (15). Such a technique produced a fine austenite and consequently a fine ferrite grain size while preserving the benefits of precipitation strengthening. This process, which eliminated the need of further heat treatment, was called "controlled rolling" in 1958 by Vanderbeck (15). Several years passed before controlled rolling was universally accepted, mainly because of the insufficient knowledge of the mechanisms involved (16).

Since the mid 1960's, controlled rolling has been increasingly utilized to produce HSLA steels. Several factors are responsible for its large scale applications. These include increasing the understanding of the role of microalloy additions (e.g. Nb, Ti and V) to HSLA steels during controlled rolling, the energy crisis of the 1970's as well as the increasing demands by the oil and gas industry for steels with high yield strengths, superior fracture toughness and improved weldability. Today, control-rolled HSLA steels are used in a wide range of applications such as pipelines, bridges, ships and transportation vehicles (7, 13). Some of the major metallurgical phenomena involved in controlled rolling are reviewed in the following sections.

2.1.2. Concept of Controlled Rolling

The concept of controlled rolling consists of monitoring the rolling process parameters such that the required product properties are obtained without any further heat treatments. Properties such as high strength and good toughness are achieved simultaneously by refining the ferritic grain structure. Hence, by controlling the interpass times, the temperature, the rate and the amount of deformation per pass, steels are now finish rolled at temperatures lower than in conventional rolling in order to refine the microstructure.

This thermomechanical process is often considered to have three (17) or four stages (18). These stages are reheating (or soaking), roughing, finishing and if the product is sufficiently thin, coiling (17, 19-23). The basic

metallurgical principles of the first three stages are illustrated in Fig. 2.1 and are discussed individually in the following sections.

2.1.2.1. Reheating

Also called soaking, this primary stage consists of reheating the material at temperatures in the range 1100 to 1300 ^{o}C before initiating the rolling process. The purpose of this operation is to obtain a uniform initial grain size throughout the material and to dissolve the required microalloy carbonitrides present in the steel. The latter is often the criterion to be satisfied in determining the minimum reheating temperature, particularly in conventional controlled rolling.

The choice of any reheating temperature should be carefully determined since it concerns both economic and metallurgical aspects of the process. Hence, high reheating temperatures, which are often necessary, should be avoided when possible because of their greater energy requirements and also, because of the longer holding times needed to cool the material to the desired rolling temperatures. High reheating temperatures yield relatively large grains. Although their refinement requires large amounts of reduction, lighter rolling loads are needed due to the material being softer. On the other hand, the use of low reheating temperatures yields relatively small austenite grains and consequently, allows for "easy" grain refinement. This is partly because the amount of deformation required for the onset of recrystallization decreases with smaller initial grain sizes. Reheating temperatures below the carbonitride solution temperature can also be used. In this case, smaller austenite grains can be produced due to the control of grain coarsening brought about by undissolved microalloy precipitates (25). However, these undissolved precipitates lower a) the amount of solutes (in supersaturation) and b) the overall contribution of precipitation upon retarding recrystallization during the later stages of rolling. They also reduce the amount of precipitation available for strengthening in the ferrite phase (25).

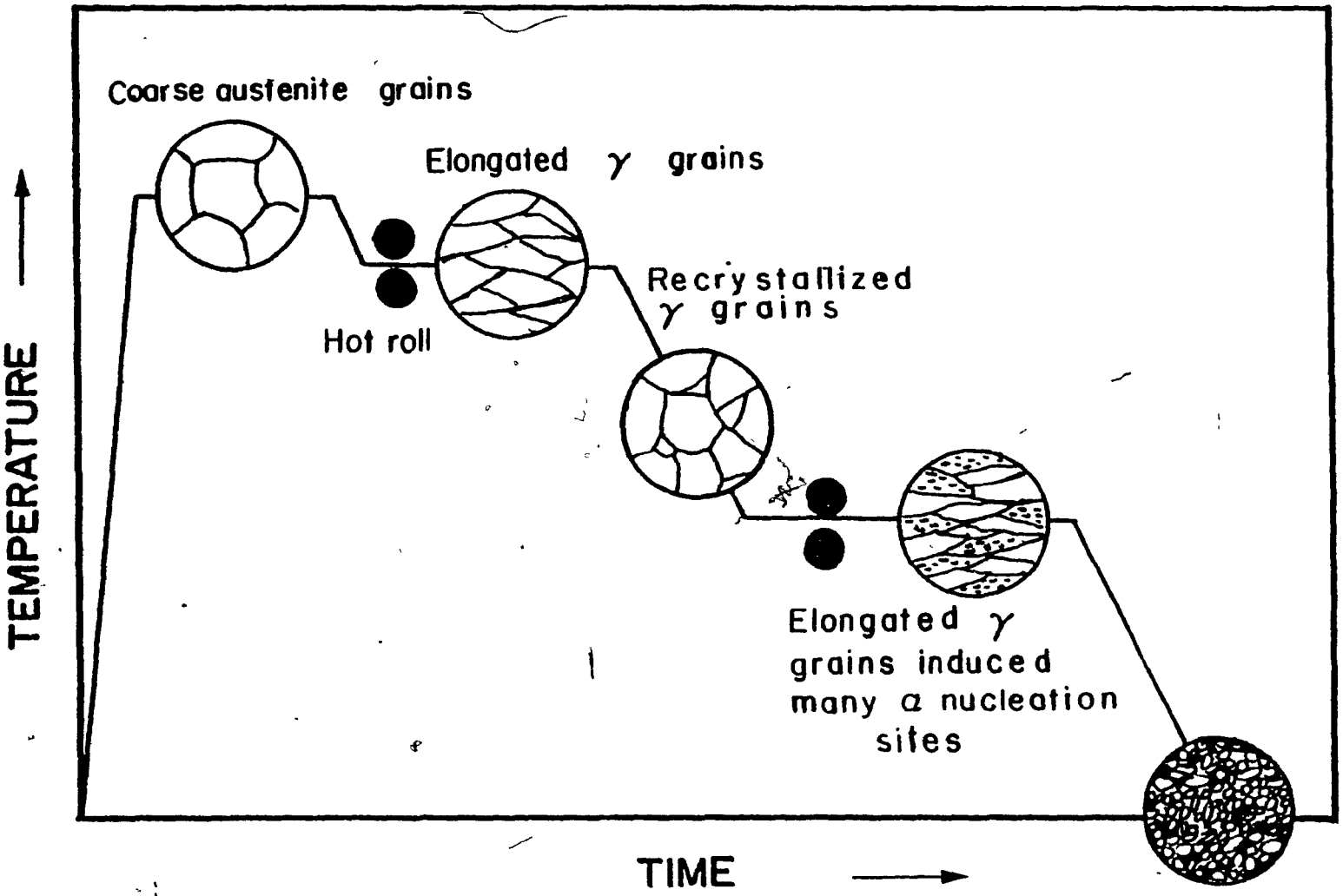

Figure 2.1 Schematic illustration of the controlled rolling process and the resulting microstructure.

2.1.2.2. Roughing

Once the reheating stage is completed, the material is cooled down to the temperature at which the rolling process is initiated. The series of reductions carried out in the high temperature range (roughly 1150 to about 950°C) constitutes the roughing stage, where several cycles of recrystallization are generated in order to refine the austenite grains. Two regions can be distinguished in this temperature range. The primary one, ranging from 1150 to 1050°C, is a region where static recrystallization takes place very rapidly (within seconds or less) and is followed by some grain growth. This range is shown in Fig. 2.2 as Region I. Below 1050°C, the static recrystallization kinetics are somewhat slower. In the cases where the time required for the completion of static recrystallization becomes comparable to the interpass times, incomplete or partial recrystallization may result, leading to an undesirable grain structure. This is shown in Fig. 2.2 as Region II, path A. However, a proper selection of the strain and strain rate permits the occurence of complete static recrystallization (Region II, path B) and continuation of roughing down to approximately 950°C. The final state of the grain structure after roughing ideally consists of refined but relatively large austenite grains.

2.1.2.3 Finishing

As the rolling temperature decreases further, a point is reached where complete static recrystallization is no longer possible within the interpass times. A transition must therefore take place from the roughing to the finishing stage.

In the latter one, an elongated and heavily deformed austenite grain structure is ideally produced without the occurence of any recrystallization (Fig. 2.2, Region III). For this purpose, the temperature at which finishing starts must be below that at which strain induced precipitation can produce a sufficient volume fraction of small particles to prevent, or at least delay, the beginning of recrystallization. The success of the finishing stage also depends on the amount of deformation per pass. Hence, as finishing proceeds and the strains of several passes are accumulated, recrystallization times get

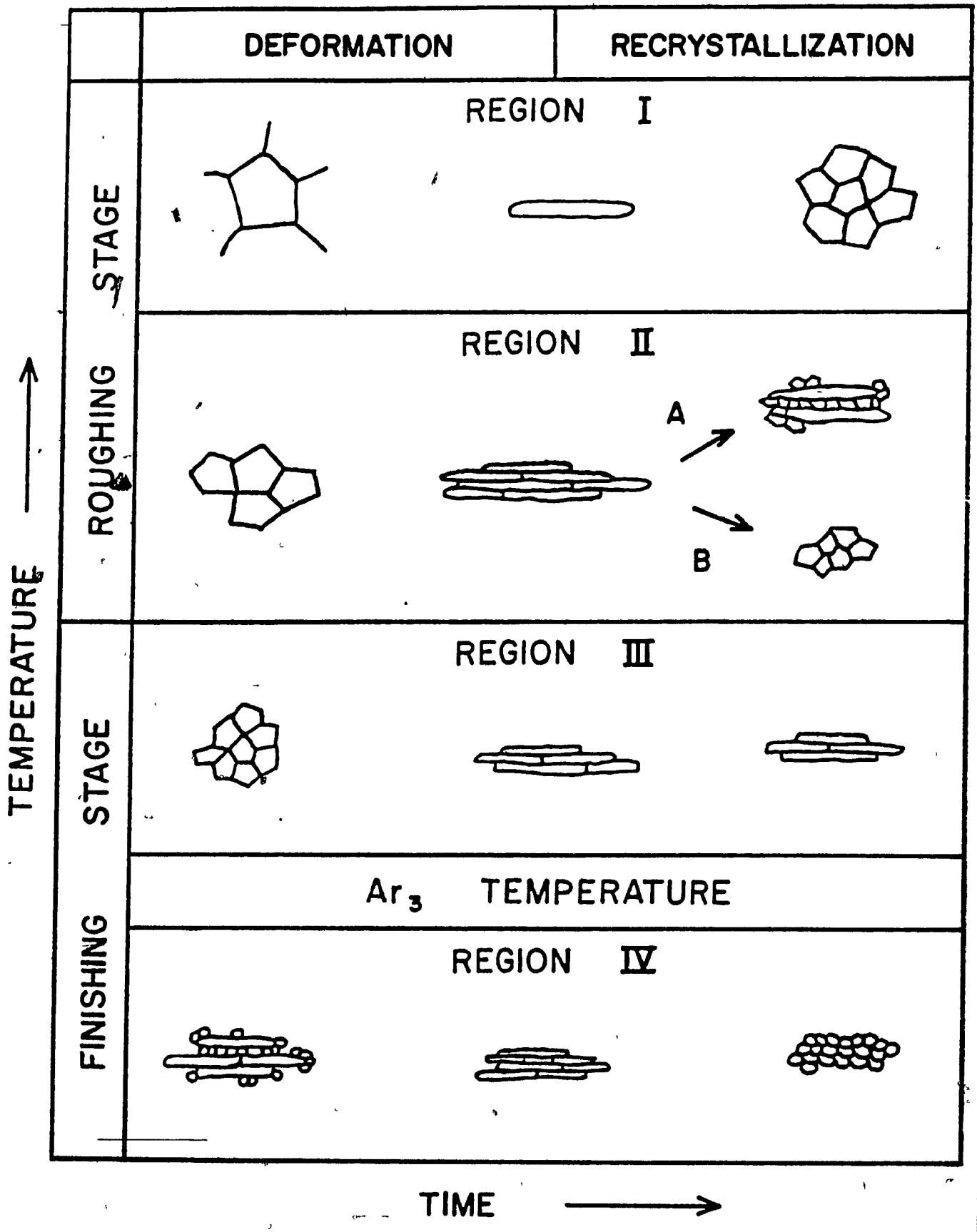

Figure 2.2 Changes in austenite grains during controlled rolling.

shortened. However, the accumulation of strains in a large number of series of small passes at decreasing temperatures produces a more effective retardation than a small number of series of large reductions (26). This presumably arises because additional nucleation of precipitates takes place after each pass as a result of the decreasing solubility. On the other hand, small reductions per pass (i.e. < 10 - 14 %) followed by holding times at high temperatures can generate a phenomenon known as abnormal grain growth resulting in the formation of non-uniform coarse grains (27-29). It becomes important to carefully establish the reductions per pass if an extremely fine grained or heavily flattened austenite structure is to be obtained. This type of structure exhibits a very high ratio of grain boundary area/volume which, upon transformation, favours the nucleation of fine polygonal ferrite.

Finally, a fourth region in the controlled rolling process appears when finishing is carried out below the transformation temperature from austenite to ferrite Ar_3 (Fig. 2.2, Region IV). The resulting refinement of ferrite structures accompanied by the effect of substructure formation and separation can both improve the strength and lower the FATT (Fracture Appearance Transition Temperature) (6, 28).

During normal controlled rolling, all of the microalloying elements do not precipitate in austenite. This leads to precipitation in ferrite during cooling with resulting precipitation hardening. The dispersion of fine precipitates may, under certain circumstances, increase the ferrite nucleation rate and also help to restrict the growth of the ferrite grains after transformation (6, 28). In this way, grain sizes of about 5 μm may be obtained in thin plates of commercially controlled rolled HSLA steels (6, 30).

2.1.3. Cooling

Cooling constitutes a natural and integral part of controlled rolling. Its control can yield excellent results in terms of economy, productivity and material properties. Rapid cooling rates tend to lower the transformation temperature, prevent austenite recrystallization prior to transformation and reduce the extent of carbonitride precipitation in austenite (7). The resulting enhanced precipitation in ferrite is both a source of ferrite grain refinement

and improved precipitation strengthening due to the formation of finer precipitates at low temperatures. Also, the decrease in the transformation temperature helps reduce ferrite grain coarsening.

In principle, this leads to an excellent combination of strength and toughness. Nevertheless, when the cooling rates are too high, toughness may be reduced as a result of bainite formation. The optimum cooling rates must therefore be determined in connection with the hardenability of steel.

2.2 SOFTENING MECHANISMS INVOLVED IN CONTROLLED ROLLING

The whole concept of controlled rolling rests on the ability to control the relevant softening processes. The latter have a significant effect on the hot strength of austenite and are of vital importance in determining the final properties of a hot rolled steel. These processes can act during deformation, i.e. inside the roll gap, or during the interpass time, which is the time between two successive rolling passes. Softening takes place inside the roll gap by dynamic recovery and occasionally by dynamic recrystallization. The restoration processes that occur during the interpass times are static recovery, static recrystallization and occasionally metadynamic recrystallization (31). The predominant softening mechanism depends on the interaction between processing parameters such as the temperature, strain and strain rate. It is also affected by material parameters such as grain size, stacking fault energy and precipitation characteristics (32, 33). Each of these softening mechanisms is examined in more detail below.

2.2.1. Softening in the Roll Gap

2.2.1.1. Dynamic Recovery

The mechanism of recovery involves the motion and annihilation of point defects and of point defect agglomerates. This softening process leads to a reduction in the dislocation density and therefore decreases the yield strength of the material.

In the early stages of hot deformation, the flow stress rises as the dislocation density increases in the material. The initially equiaxed grains become elongated and, following some rearrangement and annihilation of dislocations, equiaxed substructures begin to form inside these grains. The extent of subgrain formation increases with increasing temperature and decreasing strain rate (34, 35).

Beyond the formation of substructures, further straining can lead to either a stabilization of the structure or an accumulation of dislocations depending on the stacking fault energy of the material and the formation conditions. In high stacking fault energy materials, such as Al and bcc metals, the rate of work hardening gradually decreases with strain until the flow stress reaches a steady state. The resulting grains are more elongated but the subgrains maintain a constant size and shape. This condition of essentially constant dislocation density is due to a balance between the rates of dislocation creation and annihilation (36).

In moderate or low stacking fault energy materials, such as steel in the austenite phase, smaller subgrains develop with very tangled boundaries. In this case, dynamic recovery alone is not able to reduce the dislocation density to stable levels during deformation (36). The rate of dislocation accumulation becomes relatively high and sufficient strain energy can be stored within the subgrains to initiate dynamic recrystallization.

2.2.1.2. Dynamic Recrystallization

Once a critical dislocation density has been exceeded during deformation, dynamic recrystallization takes place and produces a drop in both dislocation density as well as flow stress. The exact location on the flow curve where this process begins is not exactly known. Extensive metallographic observations have indicated that dynamic recrystallization is initiated at a critical strain which is about five-sixths the strain corresponding to the peak in flow stress (37). The latter, referred to as peak strain, is slightly higher than the critical strain because, while the first nuclei are softening the material locally, the remaining part continues to get stronger (17, 38, 39). However, for most practical purposes, this difference

can be neglected and the peak strain can be regarded as the critical strain for the initiation of recrystallization (40, 41).

The predominant nucleation sites for dynamic recrystallization are at the grain boundaries where dislocation densities are high (42) however, deformation bands within the grains and subgrains can also act as nucleation sites (43). The size of the dynamically recrystallized grains is not influenced by the initial grain size before straining but is primarily controlled by a combination of the temperature and strain rate known as the Zener-Holloman "Z" parameter:

$$Z = \dot{\epsilon} \exp\left(\frac{Q}{RT}\right)$$

where $\dot{\epsilon}$: Strain Rate (s^{-1})

Q: Activation Energy (cal/g mole)

R: Universal Gas Constant 1.987 cal/(^{O})(mole)

T: Testing Temperature ^{O}K:

Finer recrystallized grains are produced from conditions giving higher values of Z such as high strain rates and low temperatures (43, 44). The peak strain for a given composition increases with increasing strain rate and decreasing temperature (45, 46). It also increases with increasing initial grain size even though the latter has no influence on the dynamically recrystallized grain size (43, 44).

Comparison of the reductions performed in a rolling pass with the critical strain for dynamic recrystallization in austenite indicates that dynamic recrystallization is most likely to occur during the early rolling passes, when the temperatures are high and the strain rates relatively low, and that it is more probable in plain carbon than in microalloyed steels. However, under these conditions, static recrystallization is also extremely rapid and is likely to occur between passes, so that it may be difficult to accumulate the dislocation densities required to initiate dynamic recrystallization.

The role played by dynamic recrystallization during industrial rolling is not yet known and requires more research. Nevertheless, many

authors (47-49) discount the possibility of dynamic recrystallization taking place during plate rolling, although in strip rolling, where the reduction per pass is higher, this mechanism may play a significant role (41).

2.2.2. Softening During the Interpass

2.2.2.1. Static Recovery

In this primary restoration process, the subboundaries become sharper and the dislocation density within the subgrains is reduced with little change in the shape or size of these.

Static recovery occurs when the material is unloaded and it does not involve an incubation time (39). The main factors affecting the recovery rate are the temperature, strain, strain rate and the addition of alloying elements. The rate of recovery increases as the temperature, strain and strain rate are increased (39). Static recovery is particularly important in the no-recrystallization stage of controlled rolling because it is the predominant softening mechanism.

2.2.2.2. Static Recrystallization

This type of recrystallization appears after the material is unloaded. It results in the replacement of the strained microstructure by new strain-free grains, with a large number of dislocations being absorbed by the migrating grain boundaries (50).

The critical strain required for the onset of static recrystallization is usually small (of the order of 10%) (39). Once it is exceeded, an incubation time must elapse before recrystallization proceeds. Both the incubation time and the rate of static recrystallization are influenced by the strain, strain rate, temperature and initial grain size. Finer initial grains and higher strain rates decrease the incubation time and increase the rate of recrystallization (24). The recrystallized grain size depends on the initial grain size and more particularly on the specific grain boundary area since grain boundaries are the favoured sites for the nucleation of new grains (17, 38, 51).

Finer recrystallized grains are produced by deformation at higher

strain rates and lower temperatures; such combinations correspond to higher values of Z, the temperature corrected strain rate. This parameter, together with the amount of deformation, control the driving force for recrystallization.

Due to the small amounts of critical strain required, static recrystallization is the most important recrystallization process to occur in controlled rolling. By controlling its progress during the interpass times, the desirable austenite microstructure can be obtained during the roughing stage of the rolling process.

2.2.2.3. Metadynamic Recrystallization

The third type of recrystallization observed is called metadynamic and it also occurs after the material is unloaded. However, it differs from the static type by the fact that dynamic recrystallization must have been initiated before the interruption of straining (52). This also implies that nuclei are already present when the load is removed and therefore, no incubation time is involved (53).

Metadynamic recrystallization proceeds very rapidly upon termination of deformation but, nucleation for static recrystallization can still take place in regions where dynamically formed nuclei are not present. The conditions favouring metadynamic recrystallization are the same as those described for the dynamic type.

2.2.3. Formation of Mixed Grain Structure

The success of conventional controlled rolling rests in the ability to achieve a fine and uniform grain structure. Unfortunately, control rolled steels sometimes exhibit a mixed grain structure consisting of fine and coarse ferrite grains which seriously deteriorates the low temperature mechanical properties. The formation of mixed (or duplex) ferrite-pearlite microstructures depends directly on the state of austenite prior to transformation. There are several reasons on how the austenite structure results in a mixed grain size. In 1968, Jones and Rothwell reported that where partial recrystallization occurs, mixed grain structures were produced

by preferential recrystallization at austenite grain boundaries, grain interiors being left unrecrystallized (23). This situation is encountered in rolling when recrystallization times are comparable to the interpass times. Another cause of mixed grain structure resides in the occurence of abnormal grain growth. This phenomenon is observed when very light reductions per pass, which are too weak to promote overall recrystallization, are applied (54). Once a mixed grain structure is formed, it usually cannot be eliminated unless there are many further rolling passes (55). By being further rolled, the recrystallized regions in the vicinity of the prior grain boundaries tend to preferentially recrystallize since they have a smaller grain size than the unrecrystallized regions inside the grains. The resulting microstructure seriously deteriorates the toughness of the material. It is therefore important to design the rolling schedule such as to avoid the formation of a mixed grain structure. It is possible to prevent partial recrystallization by applying reductions per pass smaller than the critical strain for recrystallization. This critical reduction depends on the temperature and the initial grain size of the material. As described later, the onset of recrystallization can be delayed by the addition of microalloying elements.

Limiting the strains can lead to abnormal grain growth. The prevention of abnormal grain growth requires the reduction per pass to be greater than 10 to 14 %, particularly when delay periods are included in the schedules (29). The above suggest that, whenever the times required to obtain complete recrystallization become comparable to, or longer than, the interpass times, a compromise in rolling reductions per pass should be established to prevent the occurence of both abnormal grain growth and partial recrystallization.

2.3 ROLE OF MICROALLOYING ADDITIONS IN CONTROLLED ROLLING

The importance of microalloying additions to steel comes from their contribution to strength and toughness in the control rolled product. Specific elements such as Al, Mo, Nb, Ti and V help retard recovery, recrystallization

and sometimes suppress grain growth. Their beneficial action, when present as either solutes and/or carbonitride precipitates, is briefly summarized in the following.

2.3.1. Effects of Microalloying Additions as Solutes

The presence of microalloying elements such as Al, Mo, Nb, V and Ti in solution retard recovery in deformed austenite and consequently delay the onset of recrystallization. However, they have less influence on the progress of recrystallization once it is initiated. The retarding effect of the elements in solution has been attributed to the following factors:

- The presence of solute atoms on slow moving grain boundaries can generate a "solute drag force" which then impedes their motion and retards recrystallization (56).
- Direct segregation of solute atoms on dislocations can affect the rate of recovery (57).
- Substitutional solute atoms can interact with the interstitial C and N to create dipoles which then interfere with the motion of dislocations. This makes the dislocation rearrangement and subgrain formation more difficult and it delays both nucleation and recrystallization (5).
- Solute additions can change the alloy's stacking fault energy. A decrease in the stacking fault energy reduces the possibility of cross-slip, which makes recovery more difficult (39).

Together with their retardating influence on recrystallization, the elements in solution also increase the strength of a material. This solid solution strengthening is strongly dependent on the mobility of the foreign atoms, which makes it less effective at elevated temperatures. While in the case of substitutional atoms the high temperature strength of austenite increases with increasing alloy content (58, 59), the effect brought about by interstitial atoms can be neglected (58-60).

2.3.2. Effects of Microalloying Additions as Precipitates Formers

Below the relevant solution temperatures, microalloying elements such as Al, Mo, Nb, V and Ti have a strong tendency to form stable carbide and/or nitride precipitates. The resulting precipitation is controlled by two factors: supersaturation and diffusivity of the precipitate forming elements. Supersaturation provides the driving force for precipitation and in this case, determines the free energy of the system. Diffusivity strongly depends on temperature and whether or not the material is recrystallized. Two of the most important factors that influence the properties of materials are the size and the distribution of precipitates. When particles are large and widely spaced, they generate local lattice distorsions during deformation which create nucleation sites for recrystallization. The resulting increase in local dislocation density then promotes the recrystallization process. When the precipitates are fine and dispersed, they can retard recrystallization by different mechanisms:

- They create a dragging force on the moving grain boundaries and thus inhibit grain boundary migration during grain growth (7, 61, 62).
- They pin the dislocations and hinder their rearrangement into subgrains or mobile high angle boundaries (63).
- They increase the homogeneity of the dislocation distribution and thus prevent the local nucleation of new grains (39, 63).

Precipitation can take place during (dynamic) or after deformation (static and strain induced precipitation). In steels, precipitation can occur in austenite, ferrite or during the austenite to ferrite transformation.

2.3.2.1. Precipitation in Austenite

In austenite, the choice of the reheating temperature has an important effect since it determines whether the precipitates are dissolved or not. Complete dissolution of precipitates is desirable. In this way, the full potential of precipitation thermomechanical processing becomes available. However, this is somewhat offset by the fact that high reheating temperatures can lead to coarse initial austenite grain sizes. On the other

hand, undissolved precipitates, resulting from low soaking temperatures, can inhibit the grain growth of the initial austenite grains (7, 19) but, they can also promote recrystallization if sufficiently large. Precipitation in undeformed austenite is relatively slow and is most likely to occur at grain boundaries. However, a major acceleration of precipitation is caused by deformation and the resulting strain induced precipitates, which appear preferentially on subgrain boundaries developed during straining (64, 65), retard both the onset and progress of recrystallization (20). The extent of the delay depends on the degree of supersaturation of the precipitating species, and on temperature, strain and strain rate (21).

In addition to the effect of deformation, the influence due to the presence of "quaternary" elements on precipitation is of importance. For example, Mn, Mo or V can slow down the onset and progress of precipitation of Nb in austenite. This is due to the decrease in the activity coefficients of the precipitating elements associated with the presence of Mn, Mo and V (66-69).

2.3.2.2. Interphase Precipitation

The microalloying elements in solid solution which do not precipitate in austenite can precipitate while the austenite to ferrite transformation is taking place. In this case, the precipitates form along the advancing austenite-ferrite phase boundary (22, 70). When the boundary moves to a new location, the precipitates are left behind in a sheet-like array. This type of precipitation is enhanced by high solute solubility and high Ar_3. The final microstructure consists of numerous sheets of precipitates, where each sheet denotes the location of the interphase boundary during the course of transformation. The spacing correlates with the cooling rate through the transformation. As the cooling rate is increased, the rows become more closely spaced and the precipitates more effective as dispersion strengtheners (71).

2.3.2.3. Precipitation in Ferrite

Precipitation also occurs in ferrite, preferentially on dislocations and subgrain boundaries (72). Compared with the particles precipitated in austenite, the ones formed in ferrite contribute more strongly to the strengthening due to their finer size. They also prevent the migration of ferrite boundaries during cooling, resulting in further grain refinement (71).

Precipitation in austenite versus precipitation during or after transformation are two competing processes since the particles formed in austenite reduce the amount of microalloying elements available for precipitation in ferrite. A cooling schedule which promotes grain refinement, uses a large proportion of microalloying elements for the control of austenite grain size. As a result, ferrite precipitation hardening is minimized (73). The ideal controlled rolling schedule would therefore take into consideration the required amount of grain refinement and precipitation hardening, and would control precipitation in order to obtain the desired product properties.

2.3.3. Effects of Individual Microalloying Elements

All microalloying elements added to HSLA steels are not equally effective in controlled rolling. Aluminum is found to retard the recrystallization of austenite, in part by the precipitation of AlN (74). Depending on where they form, the AlN precipitates can have different consequences on the behaviour of the steel. When deposited on the austenite grain boundaries, the particles can lead to embrittlement (75-78) or to a decrease in hot workability (79-81). By contrast, when formed as fine particles on dislocations, they can retard both the nucleation of new grains, as well as their subsequent growth in a manner somewhat analogous to the effect of Nb(CN) or VN. Similar to titanium, aluminum has a favorable influence on hot ductility (82). Molybdenum is known to strengthen the ferrite matrix by solid solution hardening (83, 84) and to delay austenite recrystallization through a strong solute effect (85, 86). The solute retarding influence of molybdenum is intermediate between that of niobium, which has the greatest, and of vanadium, which has the smallest effect on an equal atom fraction basis (57). The presence of molybdenum in austenite

contributes to a decrease in the carbon and nitrogen activity coefficients which in turn reduces the driving force for carbonitride precipitation in austenite. When present alone in austenite, molybdenum does not precipitate but with vanadium, titanium and niobium, it forms co-precipitates (85, 87, 88). Niobium is considered as highly effective in controlled rolling since it strongly retards the recrystallization of austenite (40, 66, 89). This is due in part to its solute effect and also, to its strong tendency to form carbonitride precipitates in austenite as well as in ferrite (48, 66, 90). The addition of titanium (up to 0.02%) allows the precipitation of very stable TiN during solidification (91). These prevent austenite grain coarsening during reheating up to 1200-1300°C. At higher concentrations, e.g., 0.1 to 0.2%, the precipitation of TiC takes place at lower temperatures in austenite and delays recrystallization (92). Precipitation hardening can also be obtained by the precipitation of TiC in ferrite. The retarding influence of vanadium on recrystallization is much weaker than that of niobium (66). First, its influence in solution is much smaller when compared to niobium but also, the greater solubility of VN in austenite makes this nitride completely soluble at common reheating temperatures (48, 93, 94). For these reasons, vanadium cannot contribute much to the austenite grain refinement at usual N levels. Nevertheless, vanadium contributes in a substantial way to ferrite strengthening and is often added together with niobium.

2.4 METHODS OF FOLLOWING PRECIPITATION IN AUSTENITE

A major difficulty in following the behaviour of austenite in HSLA steels is due to the instability of that phase at room temperature for many steel chemistries. Different methods of following the progress of precipitation in austenite exist today. These are classified as direct or indirect depending on whether they take place at high or room temperatures.

2.4.1. Direct Methods

A mechanical method was conceived by Weiss (40, 89, 95) to determine the PTT curves of two niobium HSLA steels in the undeformed (static), predeformed and deforming (dynamic) states of the material. The method involves isothermal, constant true strain rate, uniaxial compression testing. The peak strain (ϵ_p) determined from the resulting flow curves is the parameter used to establish the precipitation start (P_s) and finish (P_f) times. After a soak at the solution temperature, the sample is cooled to the test temperature and one of three procedures is applied:

1) It can be held for various times and then tested at a given strain rate. This provides data about static precipitation.
2) The samples may be predeformed at a selected strain rate to a pre-determined strain, held for various times and the deformation resumed, possibly at another strain rate. This method is used to follow precipitation in the predeformed static case, i.e. strain induced precipitation.
3) Finally, samples can be tested without any interruption over a range of strain rates to study dynamic precipitation.

These procedures are described in full detail in the papers of Weiss and Jonas (40, 89, 95, 96). For the purpose of the present investigation, which is focused on dynamic recrystallization and precipitation, the third method appears as the most appropriate. In this case, the P_s and P_f times are calculated from the peak strain ϵ_p vs. log strain rate $\dot{\epsilon}$ curves as represented in Fig. 2.3. The precipitation-time-temperature (PTT) curves obtained by this method are in good agreement with the ones determined by other methods (47). The differences observed are due mostly to variances in chemical composition or heat treatment (i.e. initial austenite grain sizes). Other mechanical testing methods involve use of constant crosshead speed instead of constant true strain rate (94).

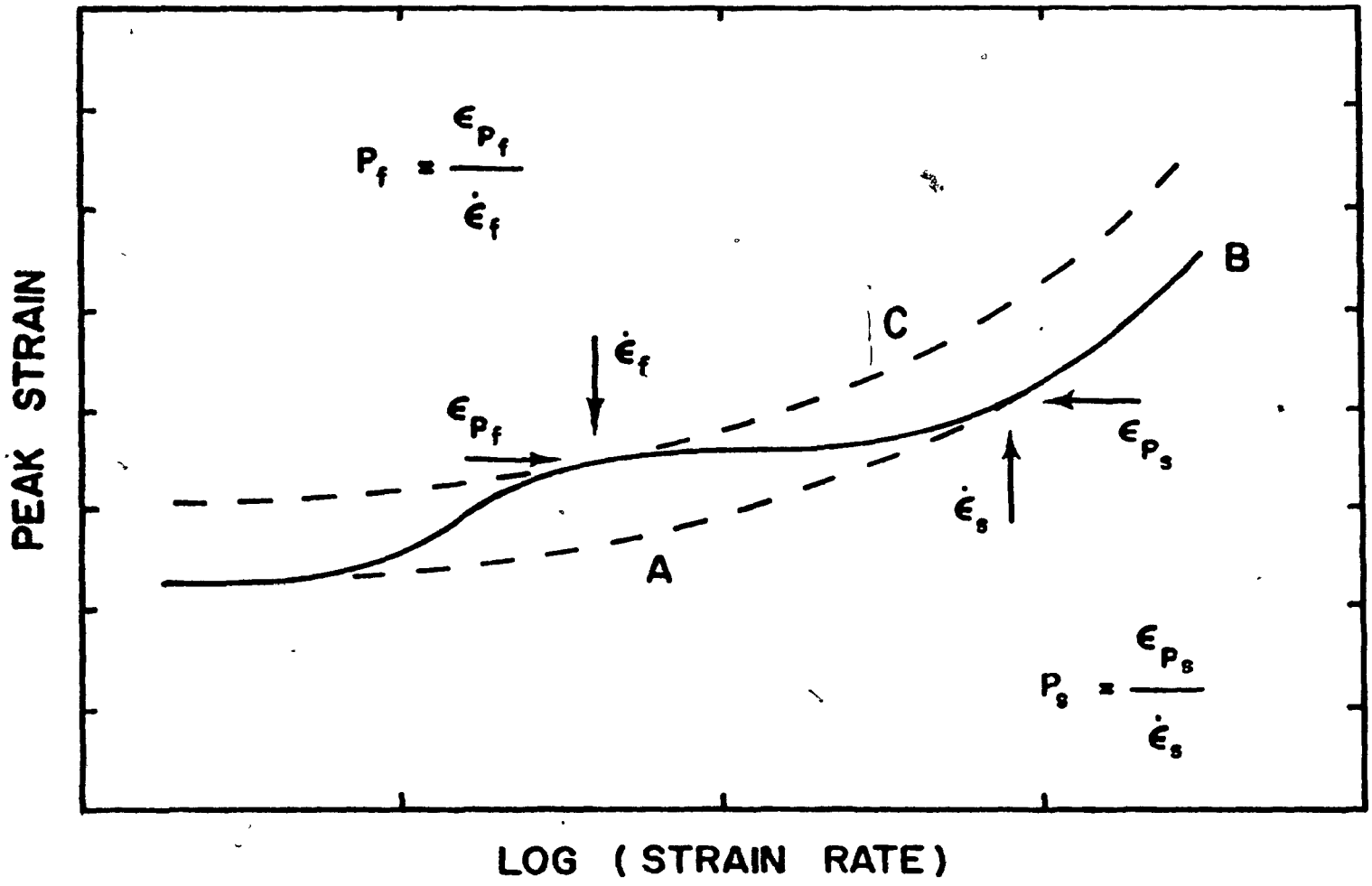

Figure 2.3 Schematic ϵ_P vs log $\dot{\epsilon}$ curve to demonstrate the method of determining P_s and P_f.

2.4.2. Indirect Methods

Some of the indirect methods are summarized below:

- The physical property measurement methods involve the measurement of electrical resistivity, which is sensitive to the structure of the material and thus, to the presence of precipitates (97); measurement of the volume fraction and size distribution of precipitates by x-ray diffraction (73); measurement of thermoelectric potential and of martensite transformation temperature M_s (98).

- The mechanical property measurement methods involve microhardness measurements (41, 99). (Precipitation in the austenite range reduces the amount of carbonitride available for precipitation in the ferrite, resulting in a loss of secondary hardening.)

- Quantitative metallography and microscopy can produce information concerning the size, volume fraction and shape of the individual precipitates (94, 100).

- Quantitative chemical methods, for example chemical extraction, can be useful to calculate the amount of precipitates present at the different stages of aging (101). For instance, Watanabe et al. attempted to determine the composition and crystalline structure of Nb (CN) with such a method (84). They had the subsidiary aim of checking for the presence of molybdenum in the carbonitrides in a series of Mo-Nb microalloyed steels.

Each of the indirect methods has the disadvantage, however, that it is not carried out at the temperature at which the information is wanted. By contrast, the mechanical direct method has two advantages. One is that testing is in the phase of interest (i.e. the austenite phase) and the other one is that bulk, rather than local, properties are measured, so that sampling errors are reduced. When followed by electron microscopy, this technique can provide the most detailed and reliable information enabling the determination of the PTT curves. It is the approach which has been selected for the present study.

CHAPTER 3

EXPERIMENTAL MATERIALS AND PROCEDURE

3.1 EXPERIMENTAL MATERIALS

With the purpose of investigating the effects of the addition of molybdenum alone and with aluminum on the kinetics of dynamic recrystallization and precipitation, three microalloyed steels were tested. These were of a series of nine 0.07% C, 1.25% Mn steels prepared by the Physical Metallurgy Research Laboratories of the Department of Energy, Mines and Resources, Canada.

The chemical compositions of the reference plain C, Mo, Al (102) and Al-Mo steels are listed in Table 3.1. The first two steels were issued from the same base material while the last ones came from a different stock. The other materials (Al-Nb steels) were studied concurrently as a part of another M. Eng. research (102).

3.1.1. Specimen Preparation

The samples were machined from 13 mm thick plates with the compression axis aligned along the rolling direction as shown in Fig. 3.1.

The specimens had a diameter and height of 7.9 and 11.8 mm respectively. These dimensions were based on the load capacity and the cross-head speed range of the testing gear and on previous experience with the equipment (98, 103-105). To prevent barrelling and enhance uniform deformation, the end faces of the samples were concentrically grooved to retain the glass lubricants used during high temperature compression (103, 104).

The glass lubricants help to minimize friction between the end faces of the sample and the SiN compression platens. The groove design was based on previous investigations which showed that best results are obtained with flat bottomed grooves (96, 103) As shown in Fig. 3.2 the grooves are wider at their bases than at the ridges between them. This configuration allows for the gradual release of the stored lubricant as the specimen/platen interface area increases during the deformation.

Table 3.1 Chemical Composition (wt.%) of the Steels Tested

Steel	C	Mn	Mo	Al	N	Si
PLC	0.072	1.22	0.010	0.015	0.010	0.165
Mo	0.070	1.25	0.215	0.015	0.010	0.155
Al	0.072	1.25	—	0.080	0.006	0.210 *
Al-Mo	0.070	1.32	0.205	0.075	0.006	0.230
ALL	P: 0.01	S: 0.01	Cr: 0.035			

* After Wang (102)

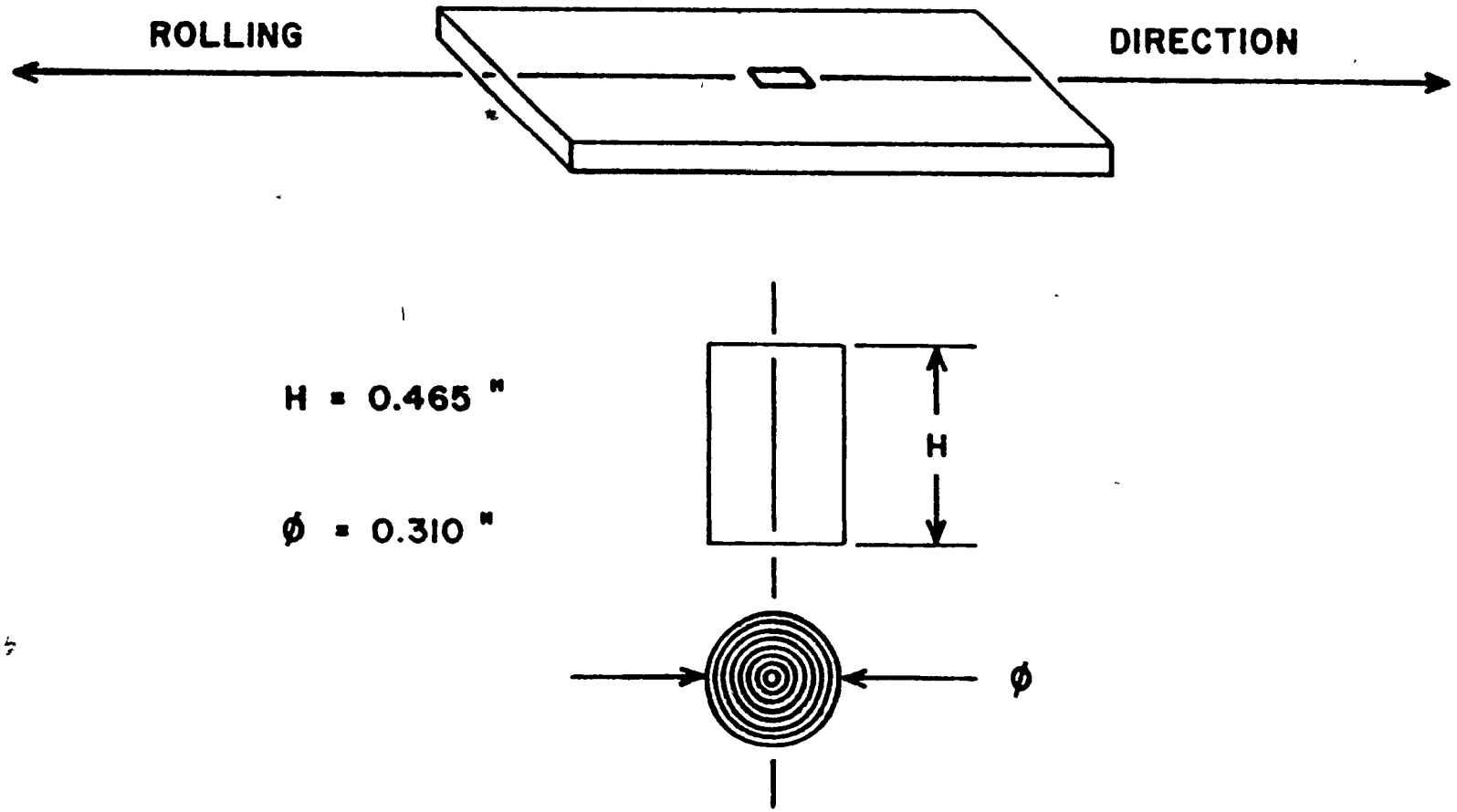

Figure 3.1 Geometry of a compression test sample.

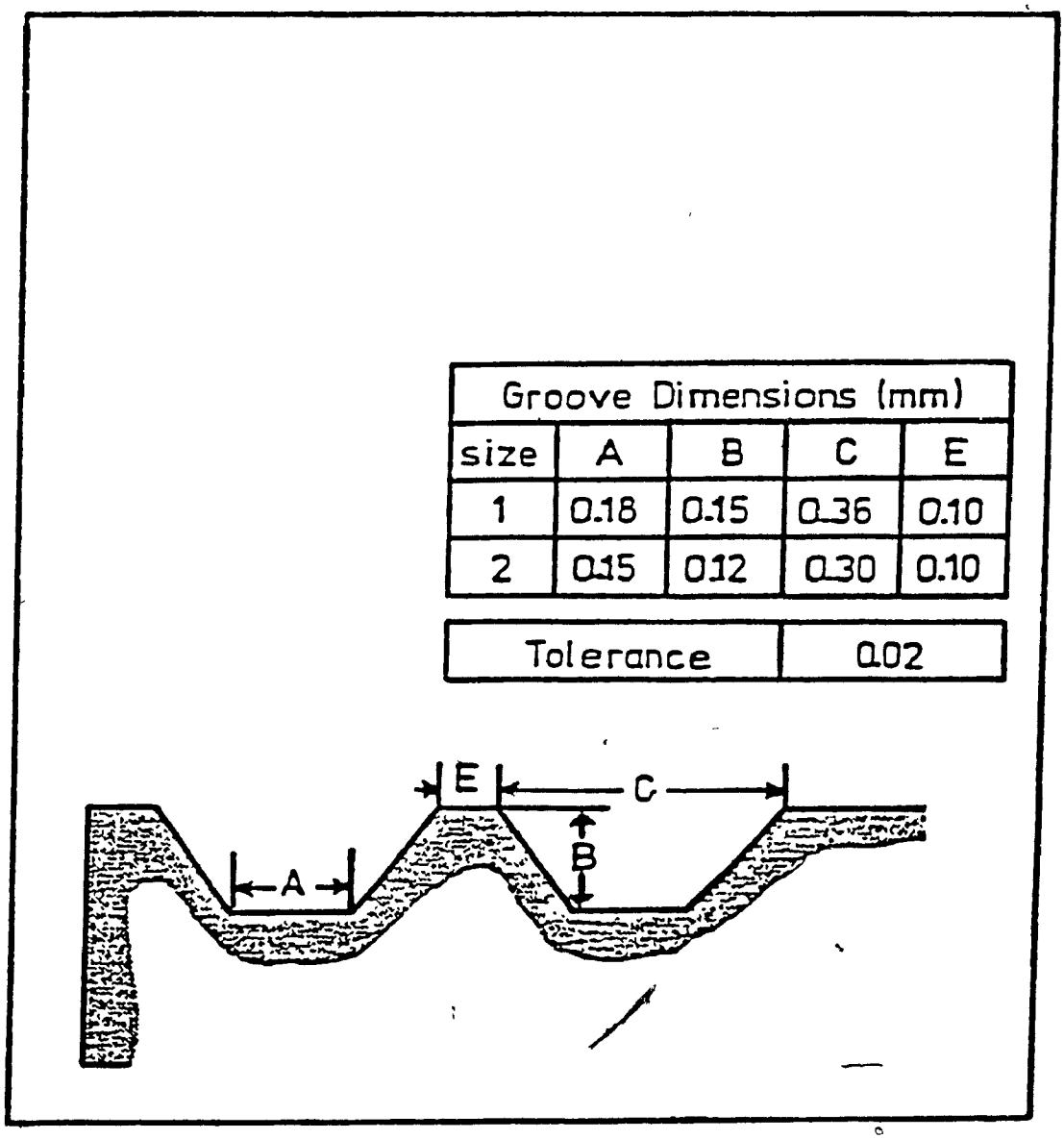

Figure 3.2 Details of the groove design on the end faces of a compression sample (after Weiss (96)).

3.2 EXPERIMENTAL PROCEDURE

3.2.1. Heat Treatment

All the specimens were heat treated for two hours at 1000°C under a vacuum atmosphere and then water quenched. The purpose of this heat treatment was to eliminate any rolling texture present in the as-received materials which could lead to non-homogeneous deformation. Following this normalizing treatment, each sample was austenitized for thirty minutes in the test chamber immediately before the deformation.

The choice of the austenitization temperature for each steel was based on two considerations:

1) To ensure the complete dissolution of the aluminum nitride (AlN).
2) To obtain approximately the same initial austenite grain size in all of the steels.

Details on the above two requirements follow.

3.2.2. Determination of the Solution Temperatures

In order to produce the maximum precipitation in the steels containing Al, all the AlN precipitates present at room temperature were dissolved during a solution heat treatment. The solution temperature was calculated according to the formula given by Darken (106):

$$\log (Al)\ (N) = -\frac{7400}{T} + 1.95$$

Here (Al) and (N) are the concentrations in weight per cent of Al and N respectively and T is the absolute temperature.

Using the above equation, the equilibrium solution temperature for the two steels containing Al was estimated to be 1114°C. To ensure complete dissolution, the minimum austenitization temperature was raised by at least 40°C above the calculated one. The austenitization temperatures and the resulting austenite grain sizes for the three microalloyed steels and the plain C steel are listed in Table 3.2.

Table 3.2 Austenitization Temperatures and Austenite Grain Sizes for the Steels Tested

Steel	Calculated Solution Temperature (^{o}C)	Austenitization Temperature Selected (^{o}C)	Corresponding Austenite Grain Size (μm)
Pl. C	——	1060	90
Mo	——	1060	95
Mo - Al	1114	1150	95
Al (102)	1114	1180	100

3.2.3. Initial Grain Size Measurement

Following the vacuum annealing heat treatment, a series of samples from the three steels investigated was austenitized for 30 minutes at different temperatures after which, each specimen was immediately quenched in ice water. The samples were then cut in two by a 11-1180 Buehler Isomet low speed diamond saw to prevent overheating of the surfaces. Once mounted in bakelite MM 112, the specimen surfaces were hand ground using successively 120, 240, 400 and 600 grit silicon carbide papers and polished with 6 and 1 μm diamond compounds for the final finish.

Two different etchants were used to reveal the prior austenite grain boundaries. The first one was Villela's reageant (107):

5 ml HCl

1 gr. of picric acid (wet)

20 drops of wetting agent (Teepol)

for 100 ml of ethanol (95 %).

The second reagent was a modified version of Villela's solution:

1 gr. of picric acid (wet)

20 drops of wetting agent (Teepol)

for 100 ml of distilled water. This solution was heated to a temperature between 50 and 70°C. The grain sizes were determined by the intercept method (ASTM #E112) using a circular 200 mm length grid. Measurements on five different pictures covering different areas of the same specimen were used. The microstructure of the investigated steels excluding the Al steel, quenched from different soaking temperatures, are shown in Fig. 3.3.

To enable a comparison of these results and those from the work of Bacroix (57), an initial austenite grain size of 100 μm was selected. The evolution of the austenite grain size as a function of reheating temperature is shown in Fig. 3.4.

3.2.4. Compression Testing Equipment

In order to determine the dynamic recrystallization and precipitation kinetics of the steels, high temperature compression tests were carried out at constant true strain rates ranging from 7.4×10^{-5} to 7.4×10^{-1} s^{-1}. The basic design of the Instron test frame modified for constant

Figure 3.3a Undeformed microstructure of the plain C steel at 1060°C after 1800 s.
Magnification: 125x

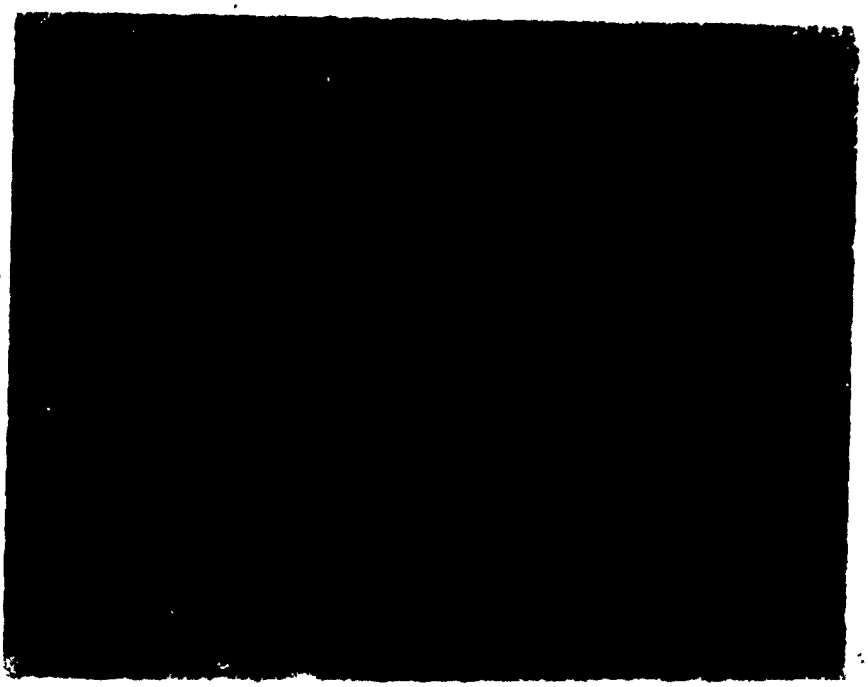

Figure 3.3b Undeformed microstructure of the Mo steel at 1075°C after 1800 s.
Magnification: 63x

Figure 3.3c Undeformed microstructure of the Al-Mo steel at 1150° after 1800 s.
Magnification: 100x

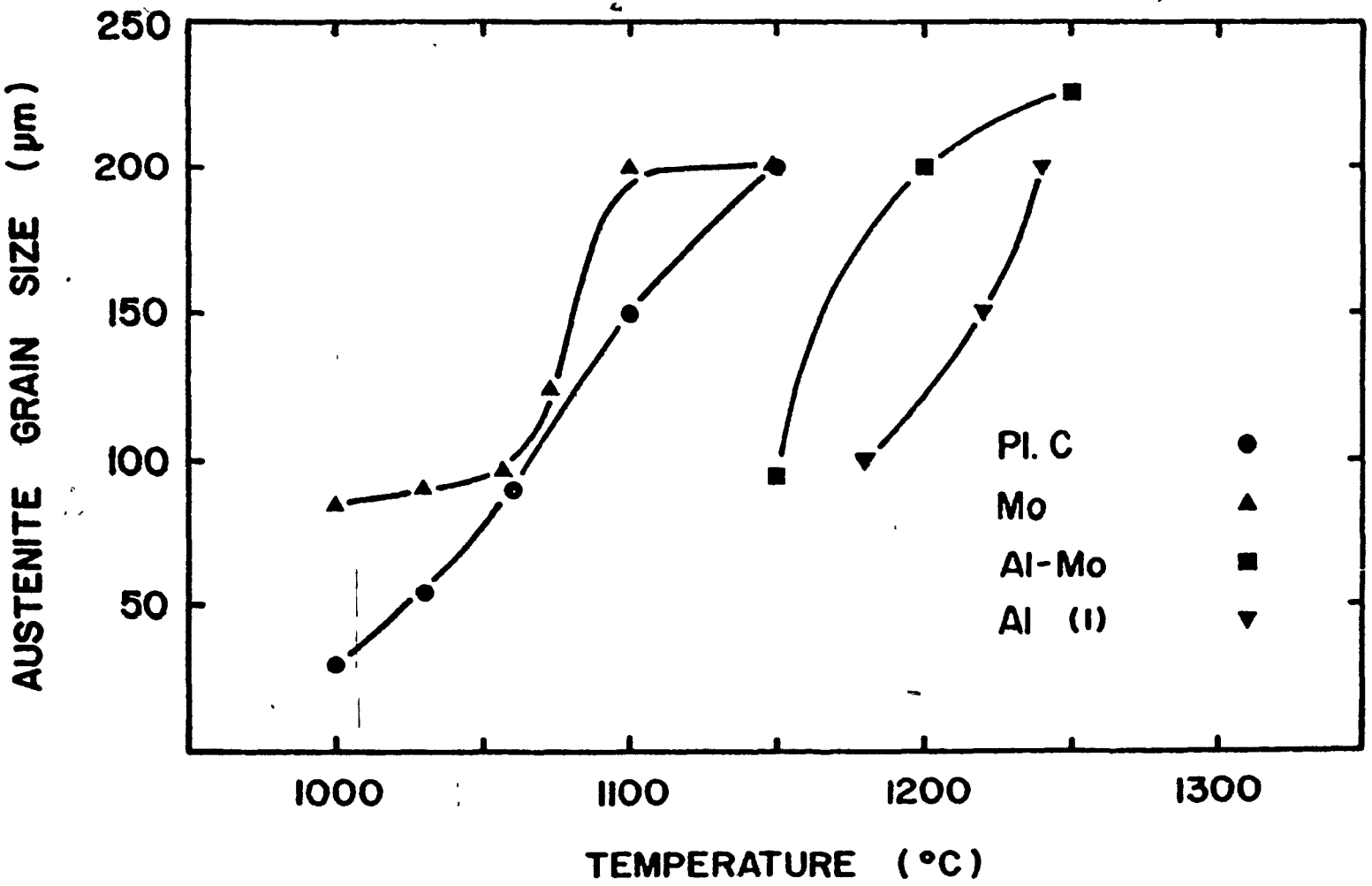

Figure 3.4 Dependence of the austenite grain size on temperature for the three microalloyed steels and the plain C steel.

true strain rate deformation, has been described in detail elsewhere (40, 89, 95, 108). The important features of the test system are the loading members consisting of an upper ram assembly which is connected to the moving cross-head and a stationary lower anvil attached to the load cell (Fig. 3.5). The specimen and tools were surrounded by an Inconel muffle which allowed for testing in either a vacuum of about 10^{-3} Torr, or in an argon atmosphere.

SiN inserts were placed at the contact surfaces of both the ram and the anvil. They were held in position by superalloy retaining collars. The smoothly ground SiN inserts provided flat and hard compression surfaces for deformation.

The tests were performed with the aid of a Honeywell 4020 process control computer. The load measurements were taken from the load cell and the displacement measurements from a Linear Variable Displacement Transducer (LVDT). The LVDT rod was attached to the moving cross-head and the coil to the Instron frame. These data were stored by the computer on a scratch file. True stress/true strain plots were obtained immediately after each test, after which the data were transferred on tape for permanent storage, so that they could be recalled at will at a later date.

The high temperatures required were obtained by means of a Satec split 3-zone platinum resistance furnace with a capacity of 14.5 amperes per zone. This furnace was connected to a Leeds and Northrup Electromax III Series 6435 controller.

A final point of interest is the specimen ejection mechanism, which allows the user to quench a sample within 4 seconds of completing a test.

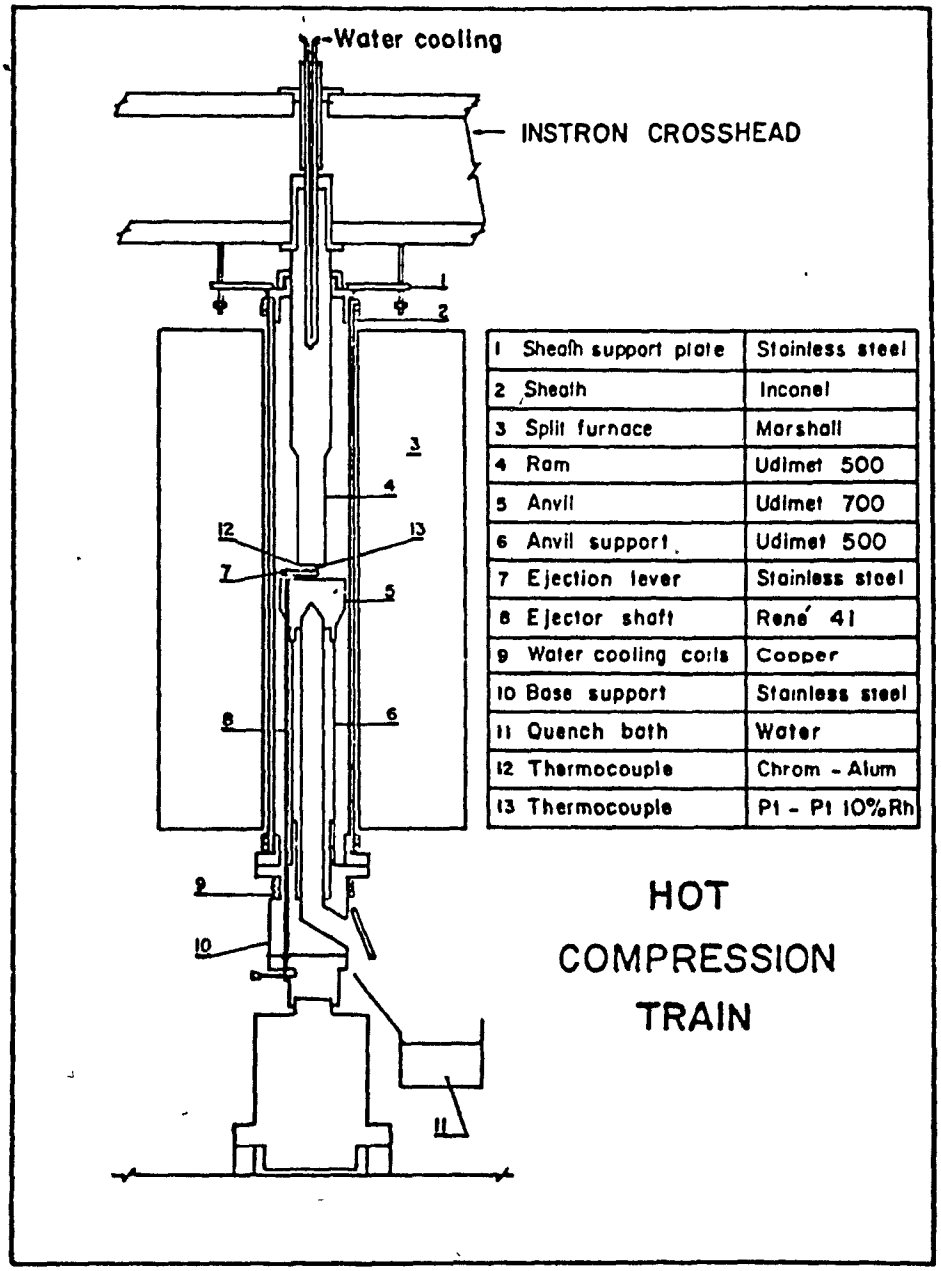

1 Sheath support plate	Stainless steel
2 Sheath	Inconel
3 Split furnace	Marshall
4 Ram	Udimet 500
5 Anvil	Udimet 700
6 Anvil support	Udimet 500
7 Ejection lever	Stainless steel
8 Ejector shaft	René 41
9 Water cooling coils	Copper
10 Base support	Stainless steel
11 Quench bath	Water
12 Thermocouple	Chrom - Alum
13 Thermocouple	Pt - Pt 10%Rh

Figure 3.5 . - Cross-section of the hot compression testing frame (after Weiss (96)).

CHAPTER 4

EXPERIMENTAL RESULTS

The aims of this study were the following:

1) To evaluate the solute strengthening produced by the single and joint addition of Al and Mo to microalloyed steels.
2) To establish the PTT (Precipitation-Time-Temperature) curves for the steels tested in order to investigate the effect of Mo on AlN precipitation kinetics.
3) To examine the possibility of substituting Al for some of the more expensive microalloy additions (such as Mo) made to steels produced by controlled rolling.

To determine the PTT curves for the microalloyed steels, compression tests were conducted at constant true strain rates ranging from 5.6×10^{-5} to 0.1 s^{-1} in isothermal conditions at 875, 900 and 925°C. The thermal history preceding compression tests is described in Chapter 3.

4.1 EXPERIMENTAL FLOW CURVES

A selection of typical flow curves for the three steels investigated at 875, 900 and 925°C, is presented in Figs. 4.1 to 4.3. The curves reveal that the materials yield, work harden to a maximum stress and the flow stress then decreases due to dynamic recrystallization. Since recrystallization is a nucleation and growth process, its progress requires time. The higher the strain rate, the shorter is the time required to reach a given strain. It follows that higher peak strains are necessary to initiate recrystallization at higher strain rates. At 900°C, a raise in the strain rate from 1.4×10^{-4} to $1.4 \times 10^{-1} s^{-1}$ results in increasing the peak strain by a factor of 2.3 for the plain C steel; 1.8 for the Al steel tested by Wang (102); 2.2 for the Mo steel and 1.8 for the Al-Mo steel. The rank of these factors in decreasing order is plain C, Mo, Al and Al-Mo steel, with the latter two being approximately the same. The meaning of these factors is briefly discussed in the next chapter.

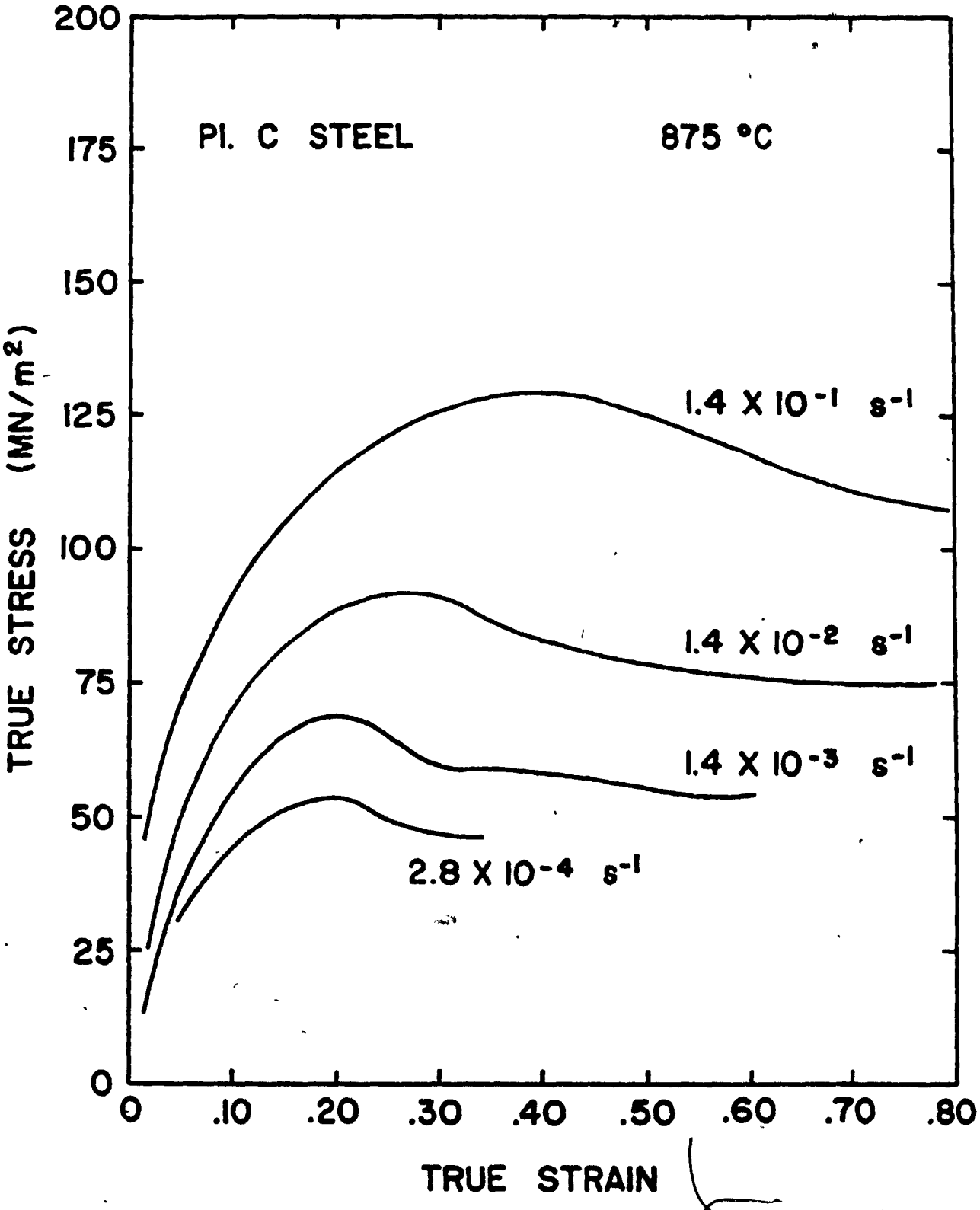

Figure 4.1a Flow curves for the plain C steel at 875°C over the range of strain rates investigated.

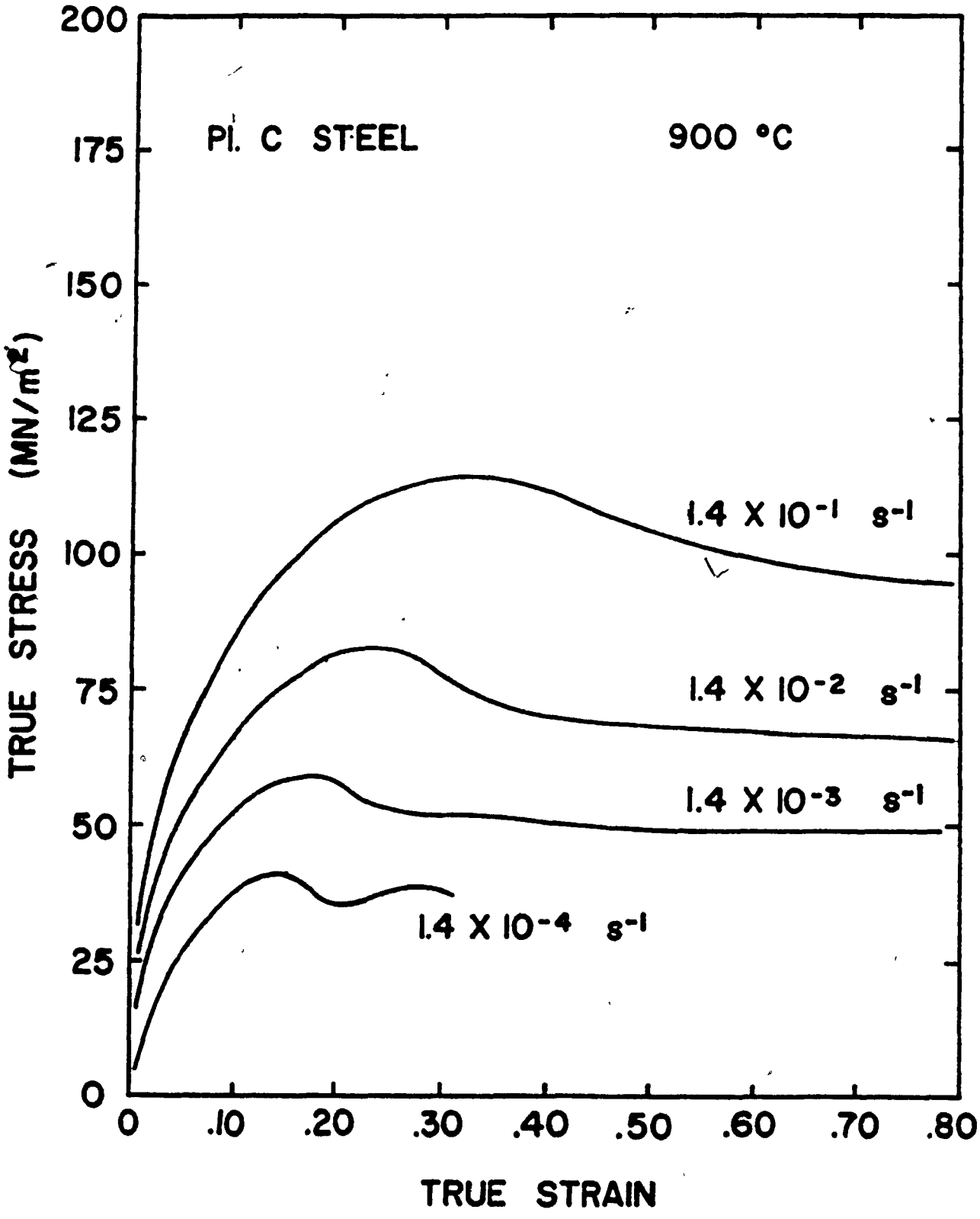

Figure 4.1b Flow curves for the plain C steel at 900°C over the range of strain rates investigated.

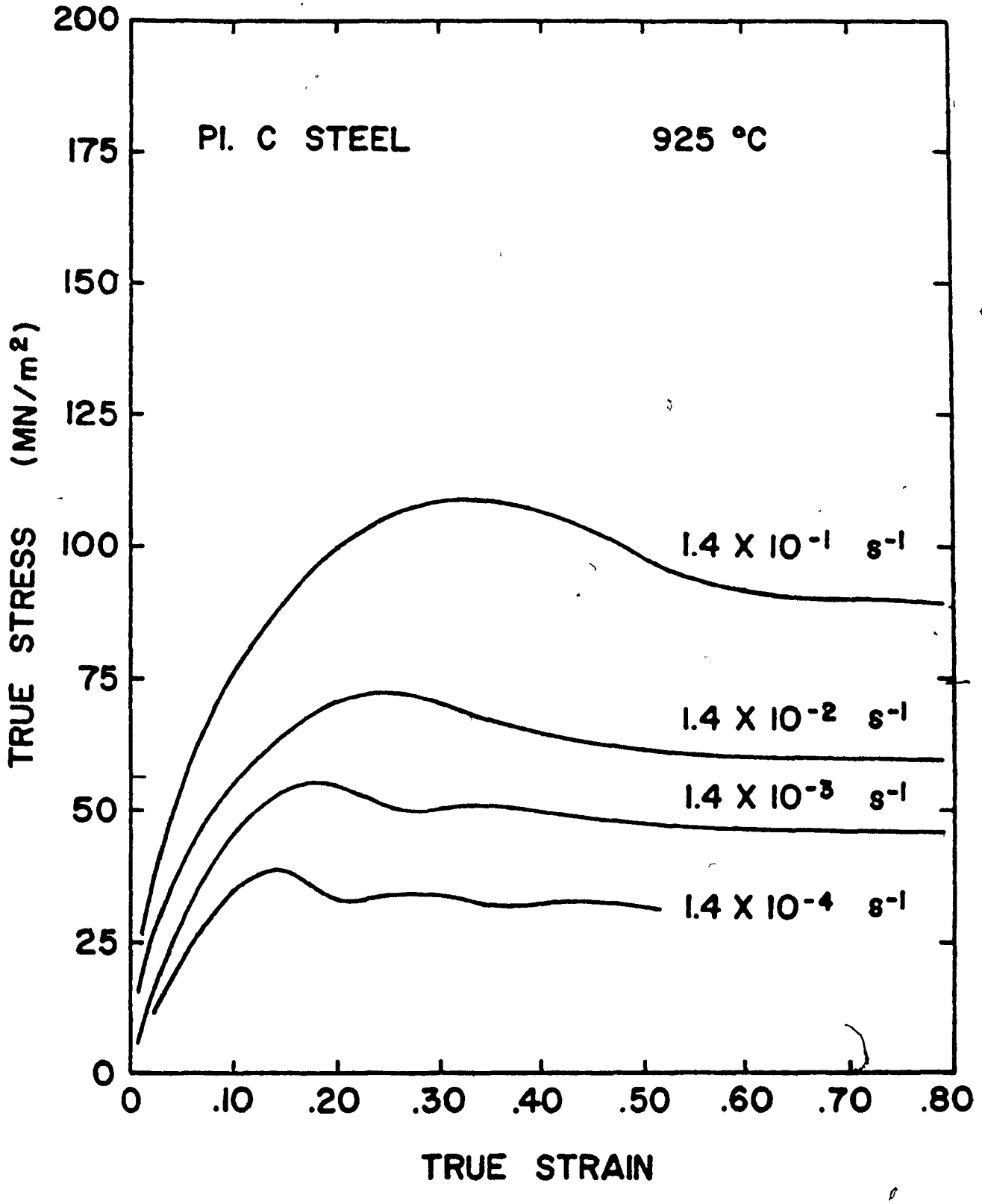

Figure 4.1c Flow curves for the plain C steel at 925°C over the range of strain rates investigated.

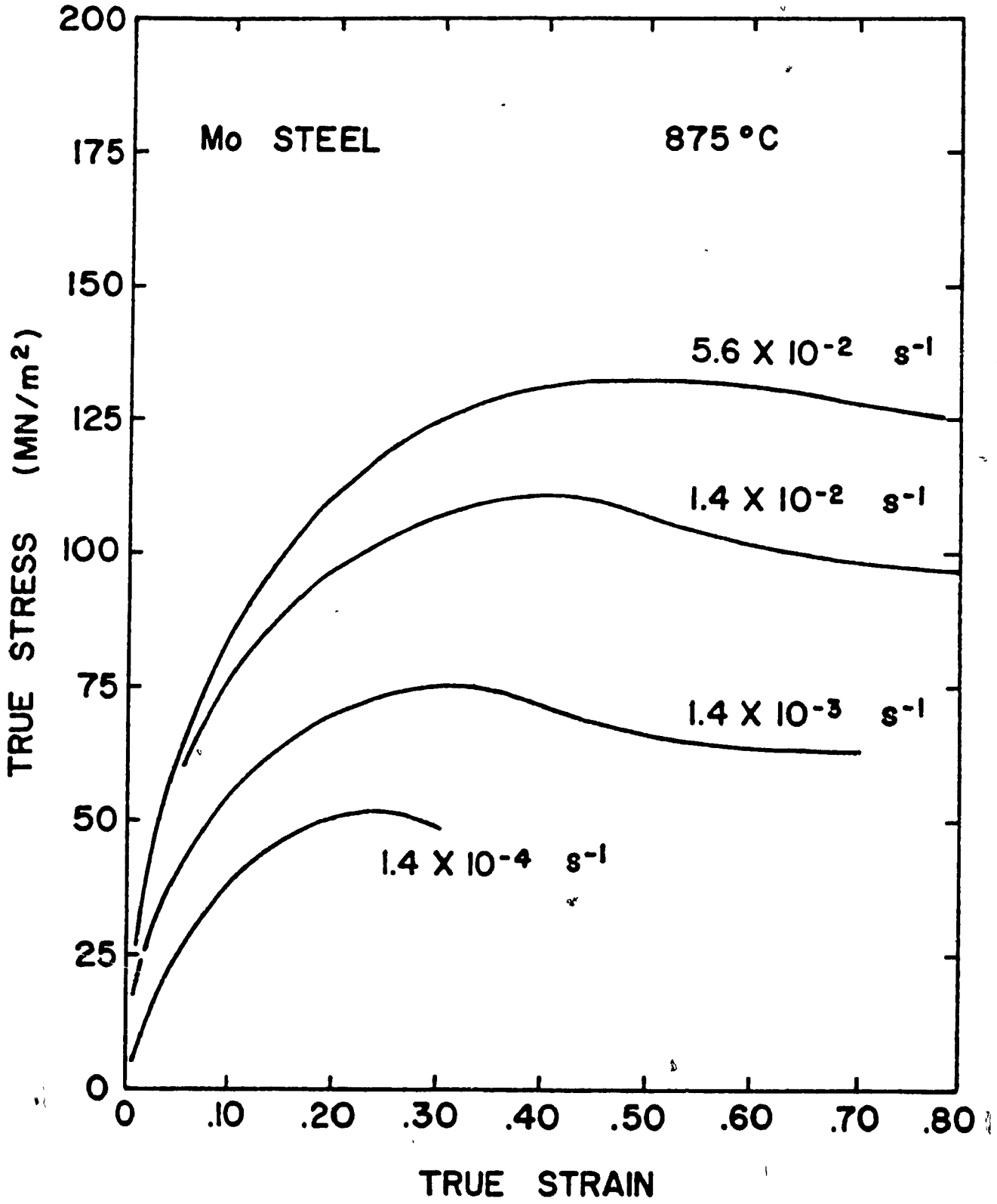

- Figure 4.2a Flow curves for the Mo steel at 875°C over the range of strain rates investigated.

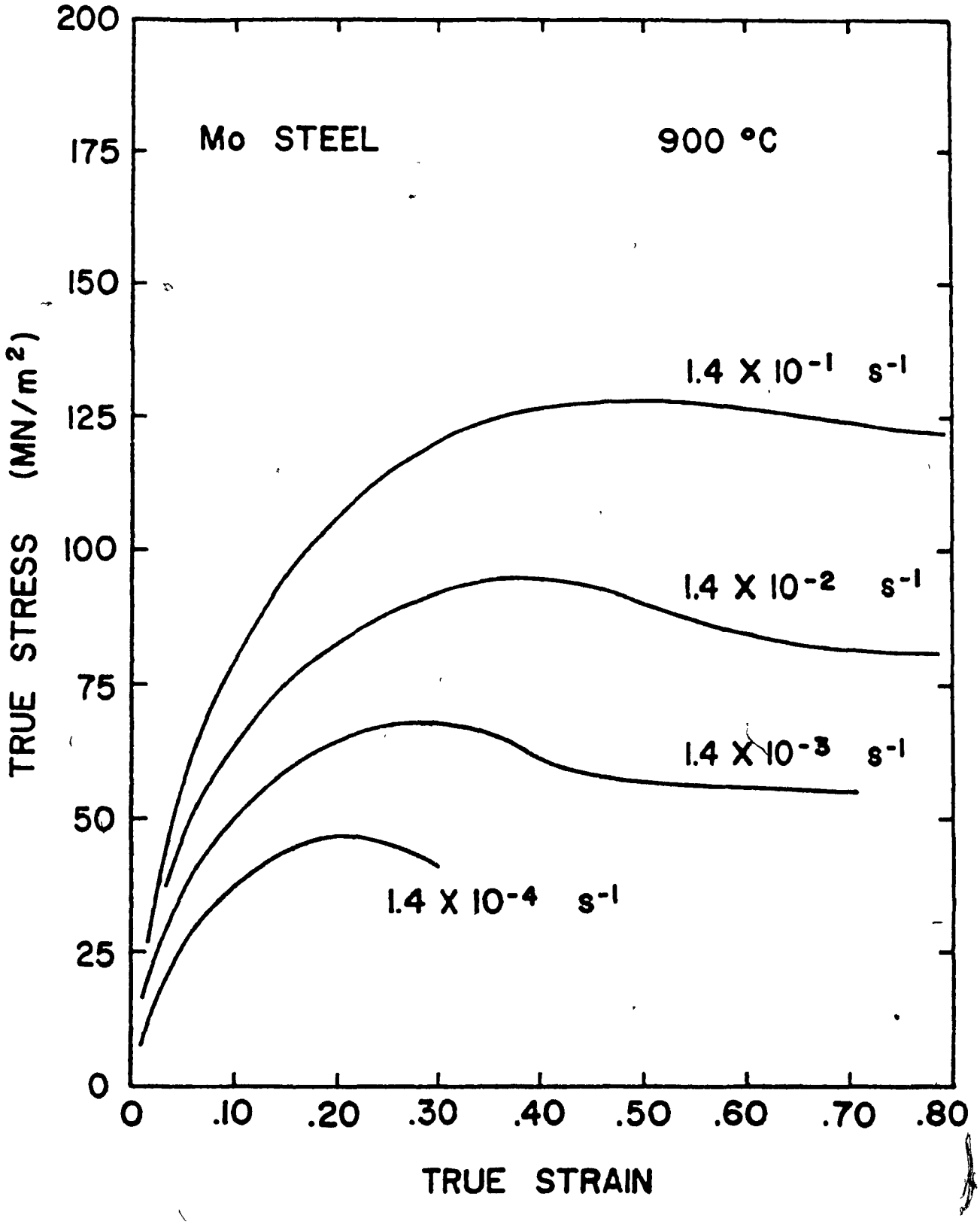

Figure 4.2b Flow curves for the Mo steel at 900°C over the range of strain rates investigated.

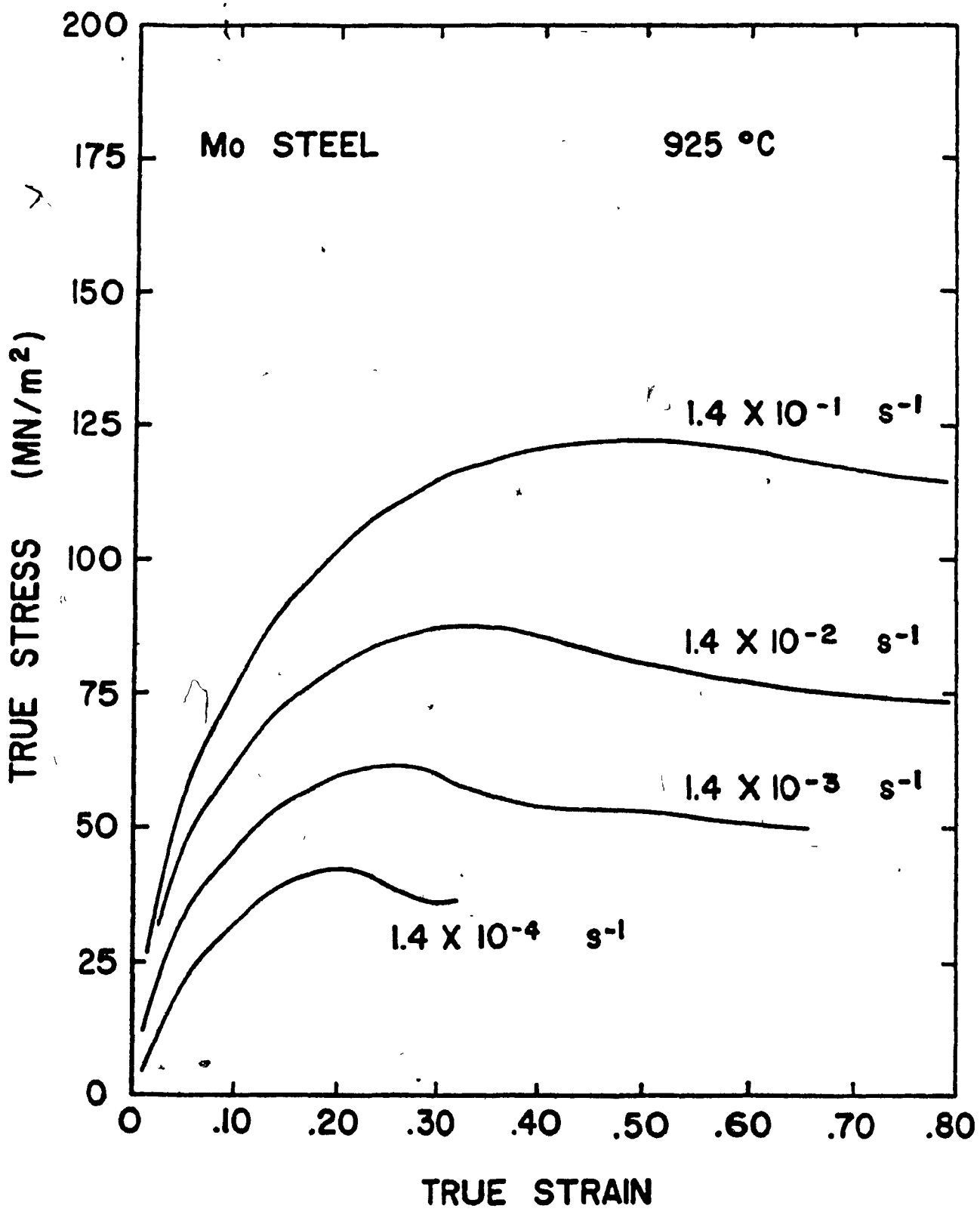

Figure 4.2c Flow curves for the Mo steel at 925°C over the range of strain rates investigated.

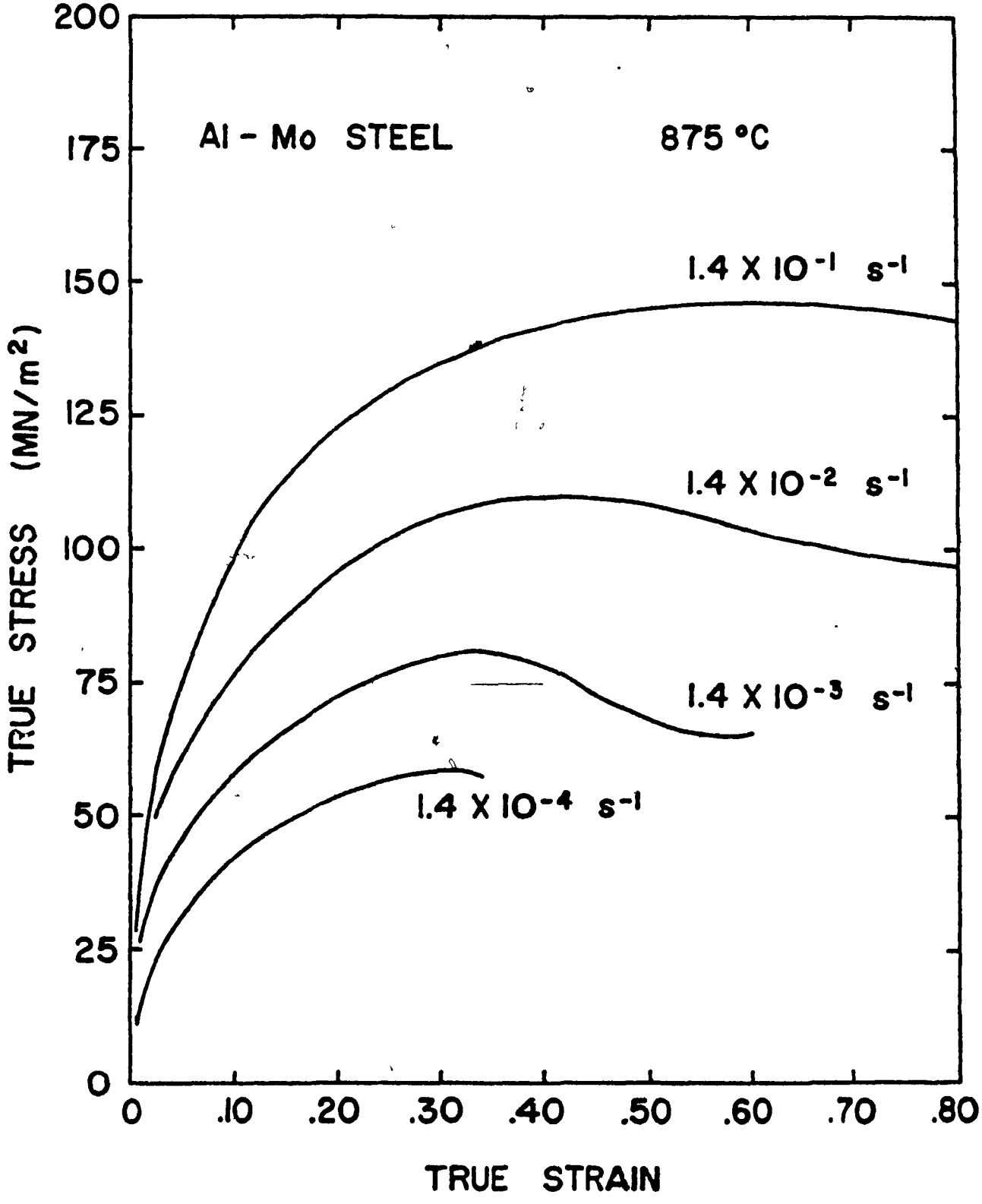

Figure 4.3a Flow curves for the Al-Mo steel at 875°C over the range of strain rates investigated.

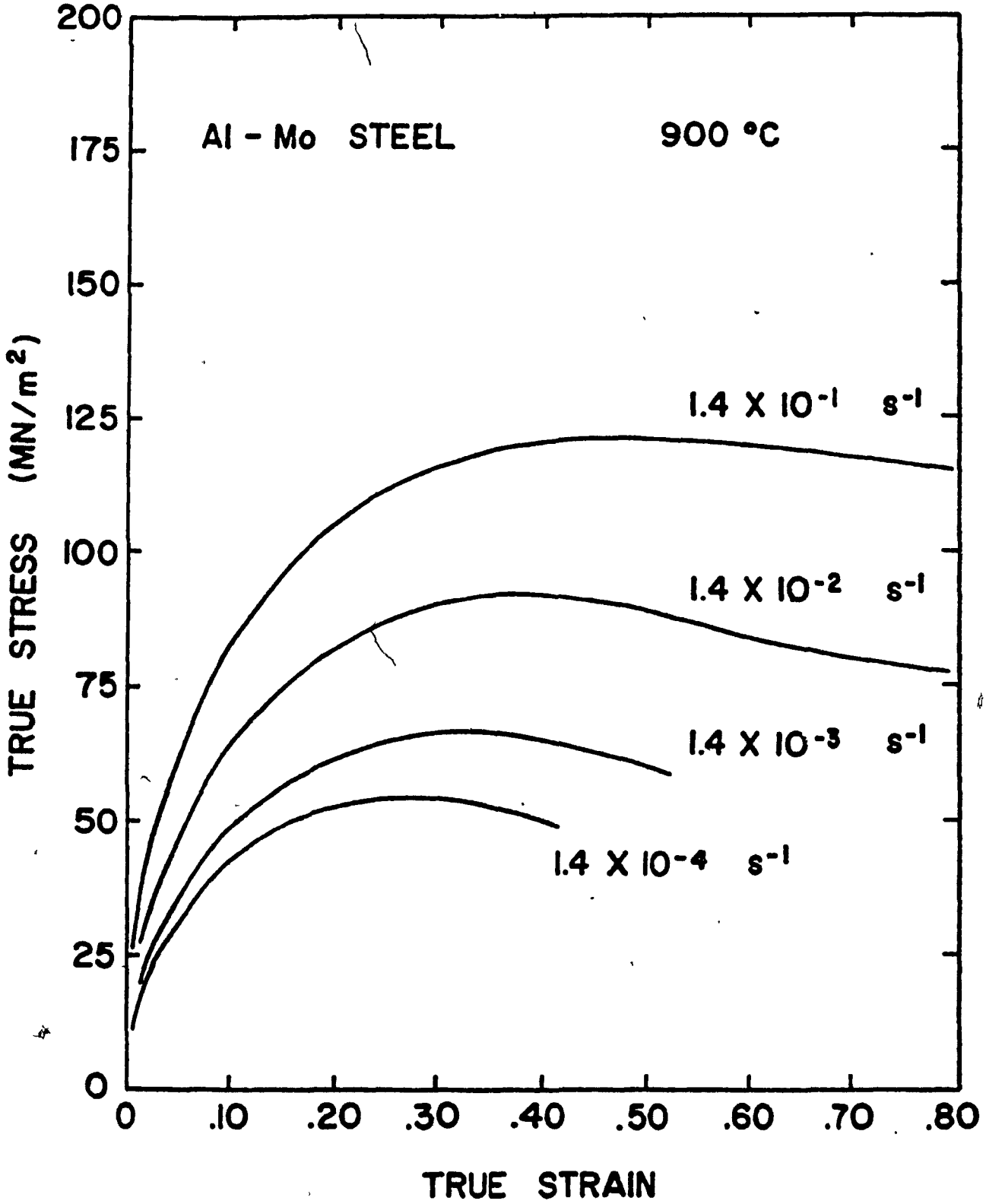

Figure 4.3b Flow curves for the Al-Mo steel at 900°C over the range of strain rates investigated.

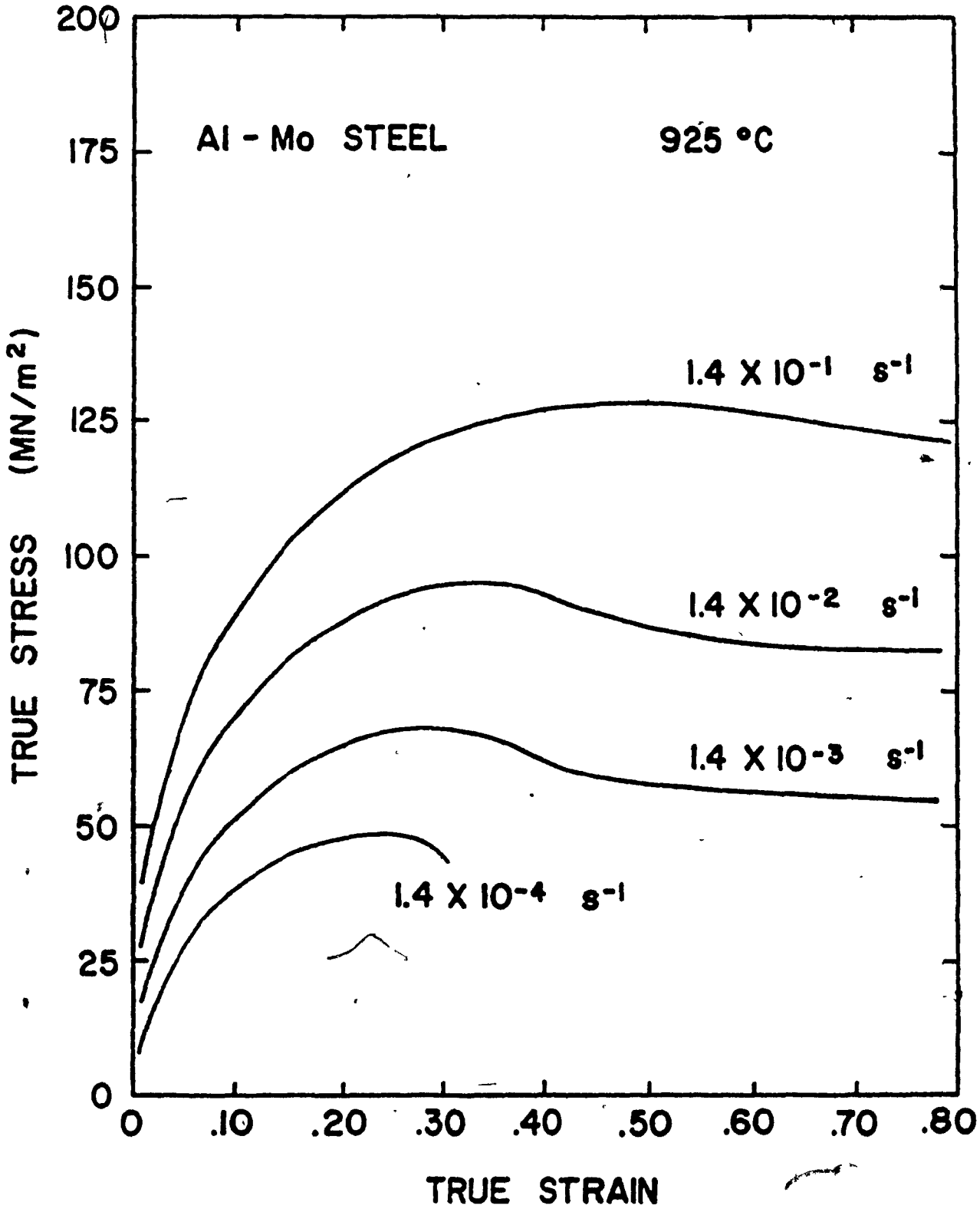

Figure 4.3c Flow curves for the Al-Mo steel at 925°C over the range of strain rates investigated.

The flow curves for the four steels are presented in Fig. 4.4 such that comparison of the influence of the microalloying elements on the peak stresses and strains can be made easily. Here, the curves for the Al steel concurrently studied by Wang (102) are included.

Figs. 4.4 (a) and (b) regroups tests that were conducted at 900°C at strain rates of $1.4 \times 10^{-1} s^{-1}$ and $5.6 \times 10^{-4} s^{-1}$ respectively.

At the relatively high strain rate of $1.4 \times 10^{-1} s^{-1}$, the deformation time is too short for precipitation to take place before the onset of dynamic recrystallization (Fig. 4.4 (a)). In this case, the observed differences in peak strain can only be attributed to the presence of the microalloying elements in solution. The results suggest that, when added to the plain C steel, Al alone does not retard recrystallization but simply increases the peak stress (115 to 122 MN/m^2). The addition of Mo, however, delays the onset of recrystallization (the peak strain increases from 0.33 to 0.50) and also raises the peak stress to 128 MN/m^2. The same amount of retardation is found when both Al and Mo are added but the gain in peak stress is somewhat lower than with the Mo steel (121 MN/m^2). By contrast, when these tests were performed at the much lower strain rate of $5.6 \times 10^{-4} s^{-1}$ (Fig. 4.4 (b)), enough time should have been available for precipitation to precede dynamic recrystallization. The observed influences of the microalloying elements on recrystallization can be explained by their presence as both solutes and precipitates.

The flow curves of Fig. 4.4 (b) show a different picture than the ones of Fig. 4.4 (a) and suggest that the addition of Al to the plain C steel brings both an increase in peak stress (53 to 62 MN/m^2) and in retardation of dynamic recrystallization (0.17 to 0.24). The addition of Mo presents almost the same effect as Al. Finally, the joint presence of Al and Mo seems to boost the peak strength to 68 MN/m^2 and move the peak strain to 0.32.

4.2 STRAIN RATE DEPENDENCE OF PEAK STRAIN

The strain rate dependence of the peak strain is shown in Fig. 4.5 for the plain C, Mo and Al-Mo steels at the three temperatures of interest.

The results for the Al steel tested by Wang (102) are included for sake of comparison. The peak strain increases smoothly with strain rate for

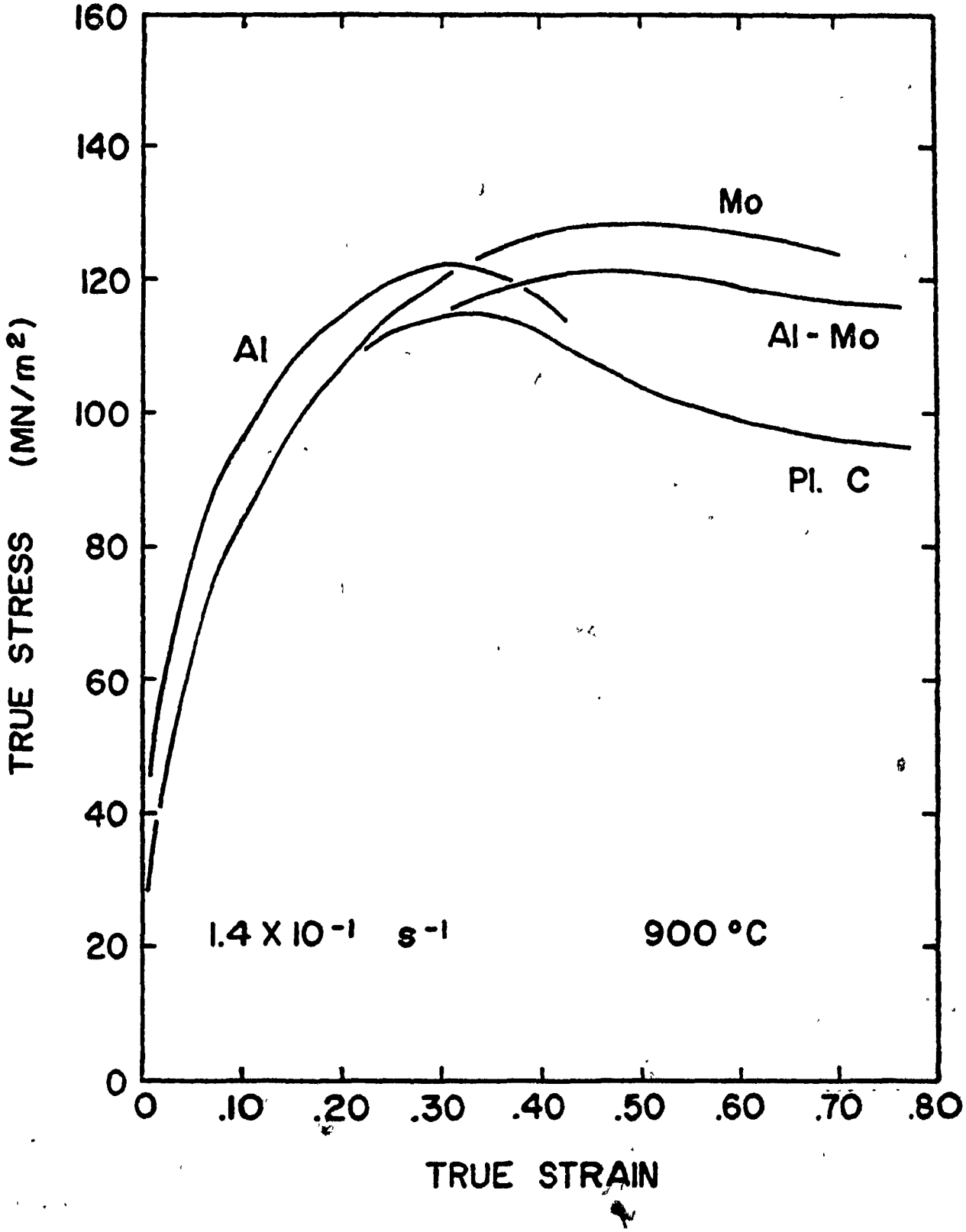

Figure 4.4a Influence of Al and/or Mo addition on the flow curves of a series of microalloyed steels tested at a strain rate of $1.4 \times 10^{-1}\ s^{-1}$ and 900°C.

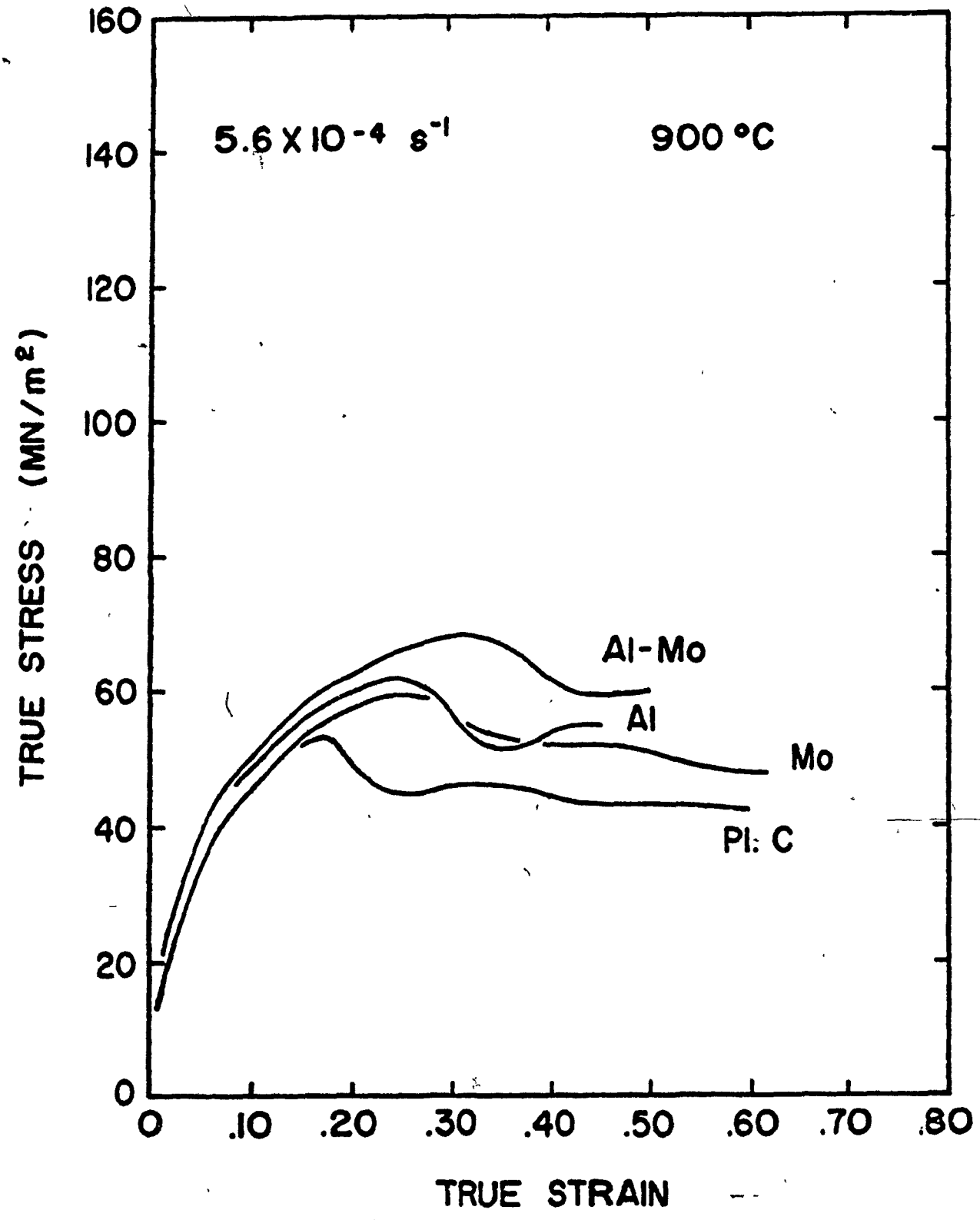

Figure 4.4b Influence of Al and/or Mo addition on the flow curves of a series of microalloyed steels tested at a strain rate of $5.6 \times 10^{-4}\ s^{-1}$ and 900°C.

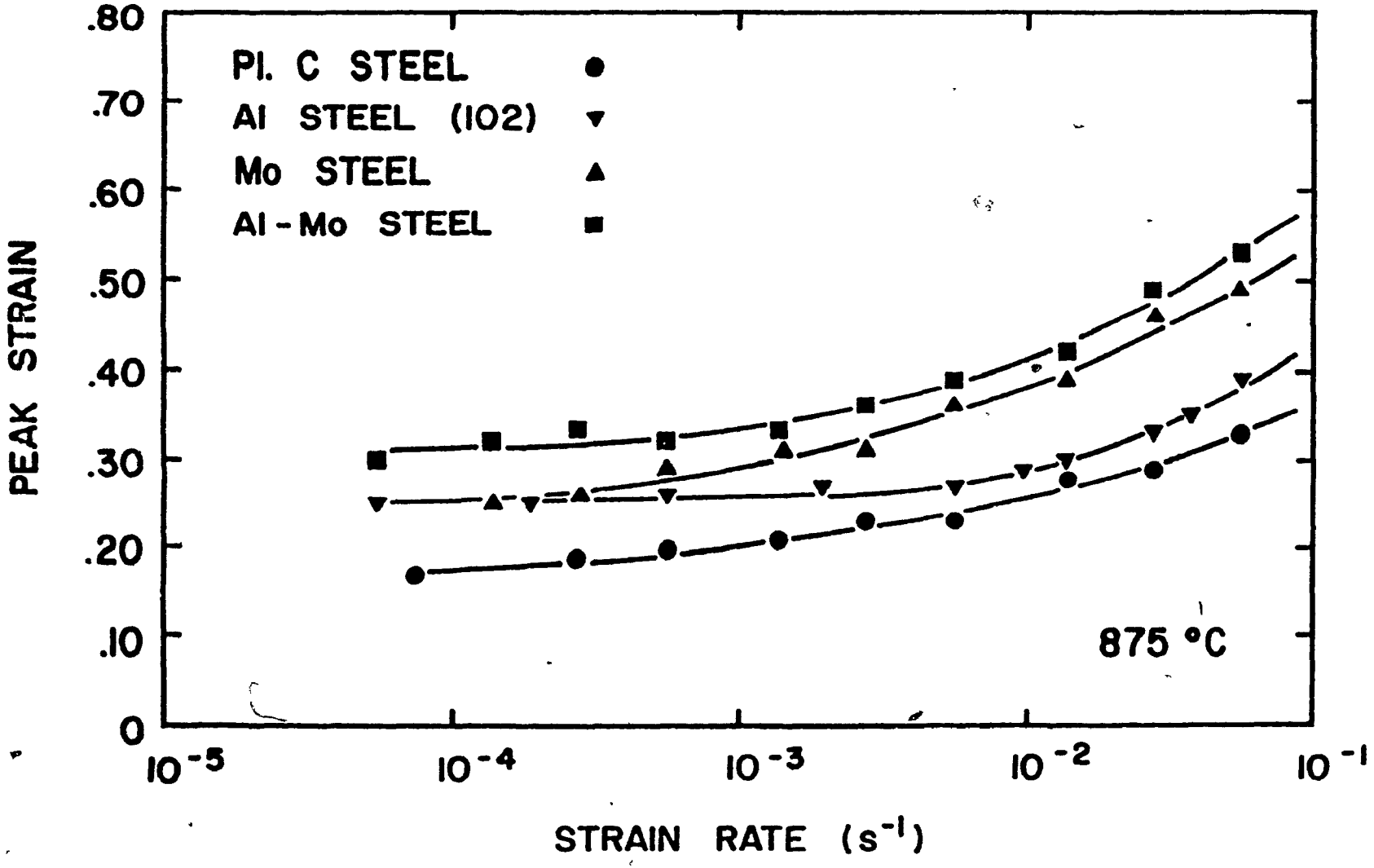

Figure 4.5a Dependence of peak strain on strain rate at 875°C for the three microalloyed steels and the plain C steel.

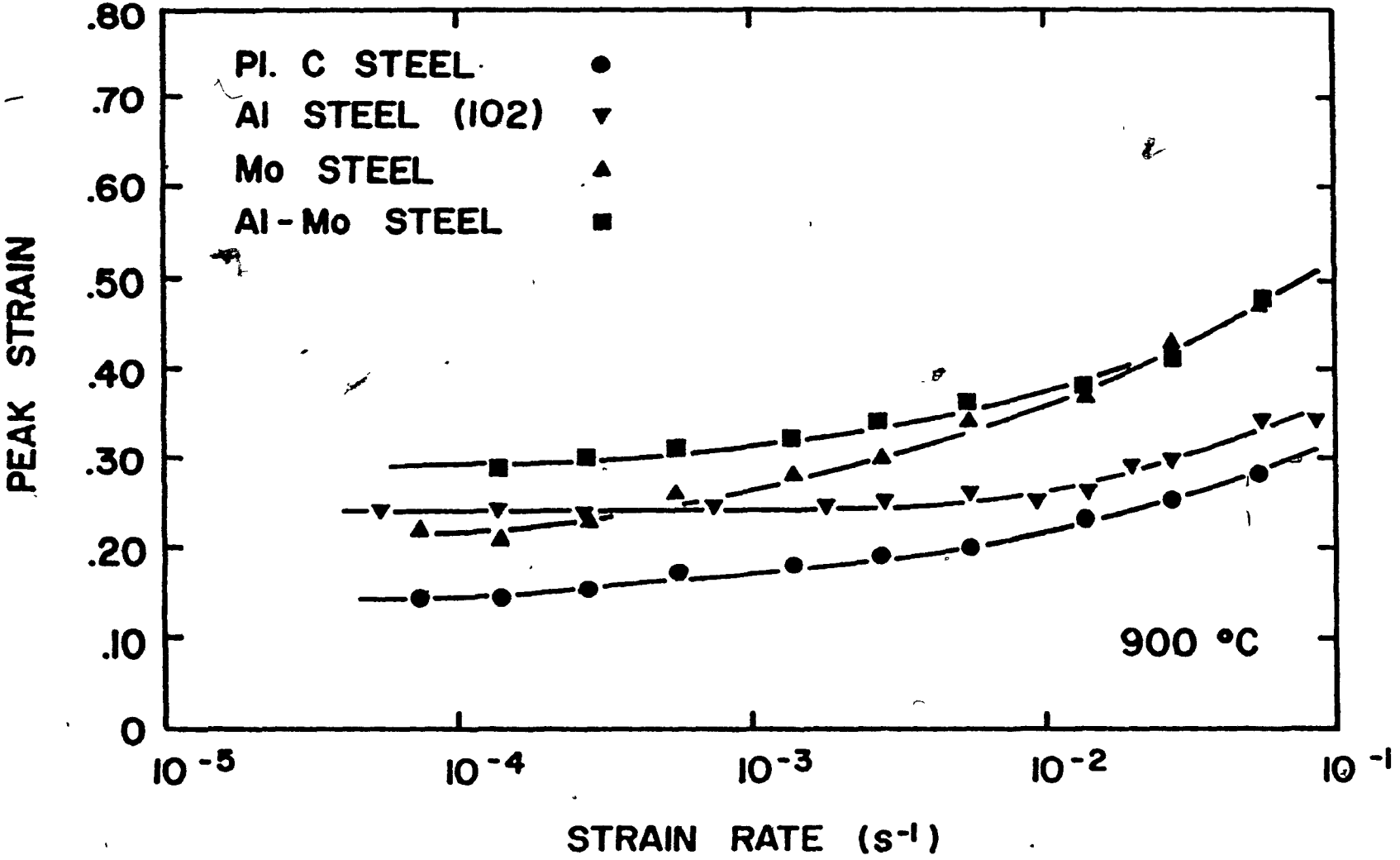

Figure 4.5b Dependence of peak strain on strain rate at 900°C for the three microalloyed steels and the plain C steel.

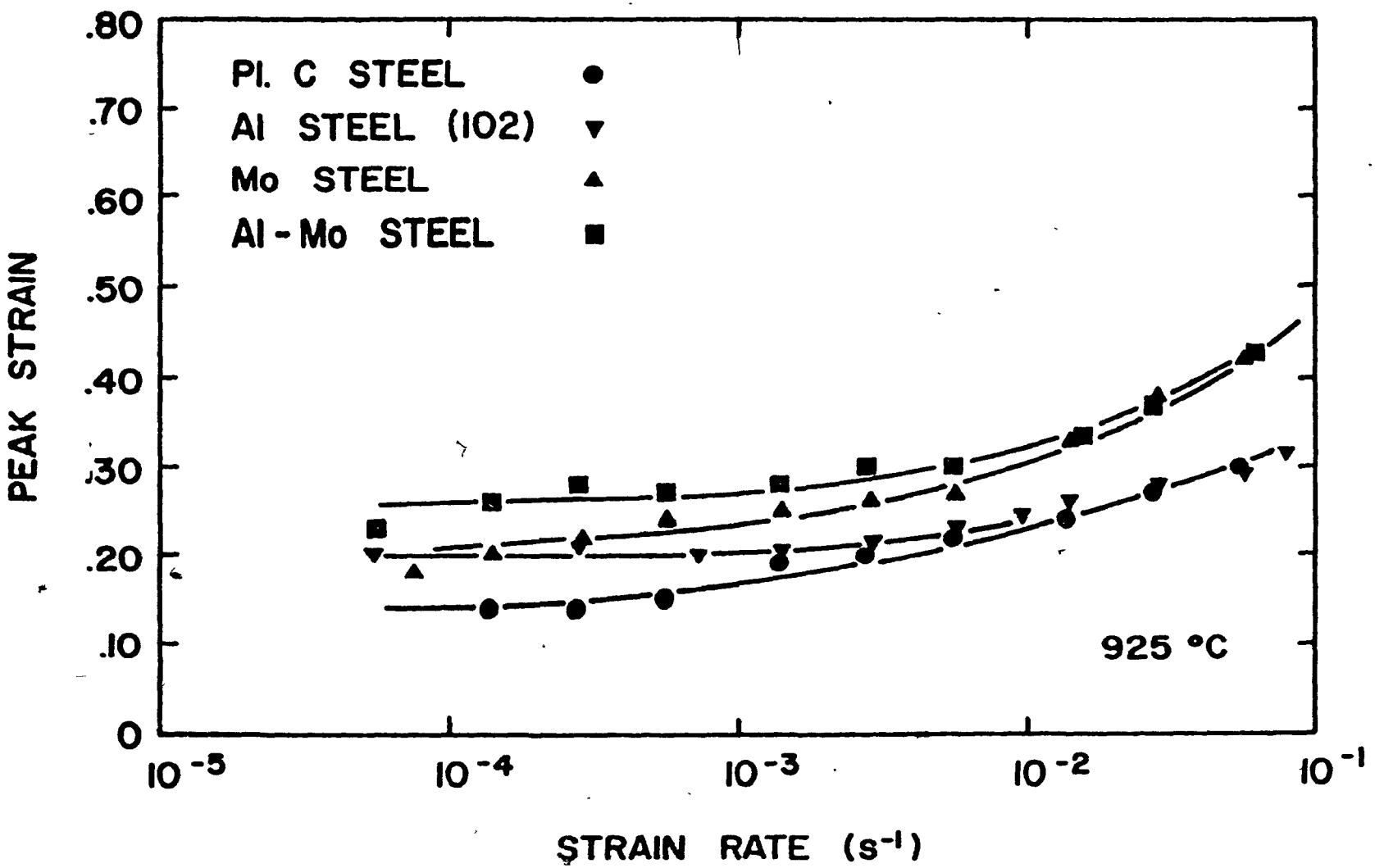

Figure 4.5c Dependence of peak strain on strain rate at 925°C for the three microalloyed steels and the plain C steel.

the plain C steel and the dependence is qualitatively similar at the three temperatures. The curves for the microalloyed steels display two important features:

First, there is an overall shift of the curves towards higher values of ϵ_p in comparison with the plain C steel. This indicates that dynamic recrystallization is delayed by the addition of the microalloying elements and the overall shift is attributed to the effect of these elements acting as solutes. (The behaviour of the Al steel at 925° is an exception).

Second, in the cases of the Al-Mo steel and more particularly the Al steel, a deviation from the trend (slope) of the reference Mo and plain C steels respectively is observed at low strain rates ($<10^{-3}s^{-1}$). The curves of the Al and Al-Mo steels "level off" at somewhat higher strain rates than the ones of the plain C and Mo steels.

The latter observation suggests that an additional contribution in retarding dynamic recrystallization comes from the microalloying elements possibly acting as dynamically formed precipitates.

From the curves displayed in Fig. 4.5, the relative effect of composition in retarding dynamic recrystallization is expressed in increasing order as Al, Mo and Al-Mo. It is interesting to note the limited solute effect of 0.08 wt.% Al on dynamic recrystallization. Its weak delaying contribution is well demonstrated when added to the plain C steel (Al steel) or to the Mo steel (Al-Mo steel). Note here that 0.08 wt.% Al is the total Al content. The soluble Al levels are under study and are expected to be less (80 %) than that amount. By contrast, the addition of 0.20 wt.% Mo to the plain C steel strongly delays the occurence of dynamic recrystallization. This effect might result solely from the presence of Mo as solute since almost exclusively no data have been reported in the literature concerning the precipitation of Mo(C,N) in high temperature austenite (57). However, the results of a recent study carried out by L'Ecuyer et al. on a Mo steel revealed the presence of Mo rich precipitates (109). Electron microscopy was performed on unstrained as well as deformed samples which were immediately quenched from the test temperature. The precipitation of complex Mo carbides (Mo_xC_y) took place around existing nuclei. In this Mo steel, these nuclei where found to be TiN particles resulting from the presence of residual Ti from the stock used to

make the steel. The above findings suggest that Mo might not only act as a solute but also, as a precipitate former in high temperature austenite.

The occurence of precipitation, which is suggested by the deviation on the curves of both the Al and Al-Mo, is not very clear under present conditions. At the low strain rate end of the ϵ_p vs log $\dot{\epsilon}$ curves (Fig. 4.5), no sign of convergence for both the Al and the Al-Mo steels is observed towards the slope of the reference plain C and Mo steels respectively. Testing at lower strain rates was not possible due to experimental difficulties. The idea of convergence is better visualized in the schematic of Fig. 4.6. Such convergence would indicate the end of precipitate formation and the growing influence of particle coarsening. The occurence of precipitation remains to be verified by microscopy.

4.3 STRAIN RATE DEPENDENCE OF PEAK STRESS

The dependence of peak stress on strain rate and composition is shown in Fig. 4.7. The curves indicate a trend for increasing peak stress with increasing strain rates. These dependences incorporate both those of the yield stress (described later) and those of the amount of work hardening accumulated between yielding and the attainment of the peak.

The yield stress and the peak stress during high temperature straining are influenced by the alloying elements in solution. However, due to the relatively long straining times involved, newly formed precipitates can affect the work hardening rate. These precipitates can pin the dislocations and retard recrystallization, leading to higher values of peak stress.

The results obtained at 875 and 925°C reveal that the magnitude of the peak stress increases with decreasing temperature and follows the increasing order of Pl.C., Al, Mo and Al-Mo steel. A clear distinction is difficult at 900°C although the microalloyed steels clearly display higher stresses than the plain C material.

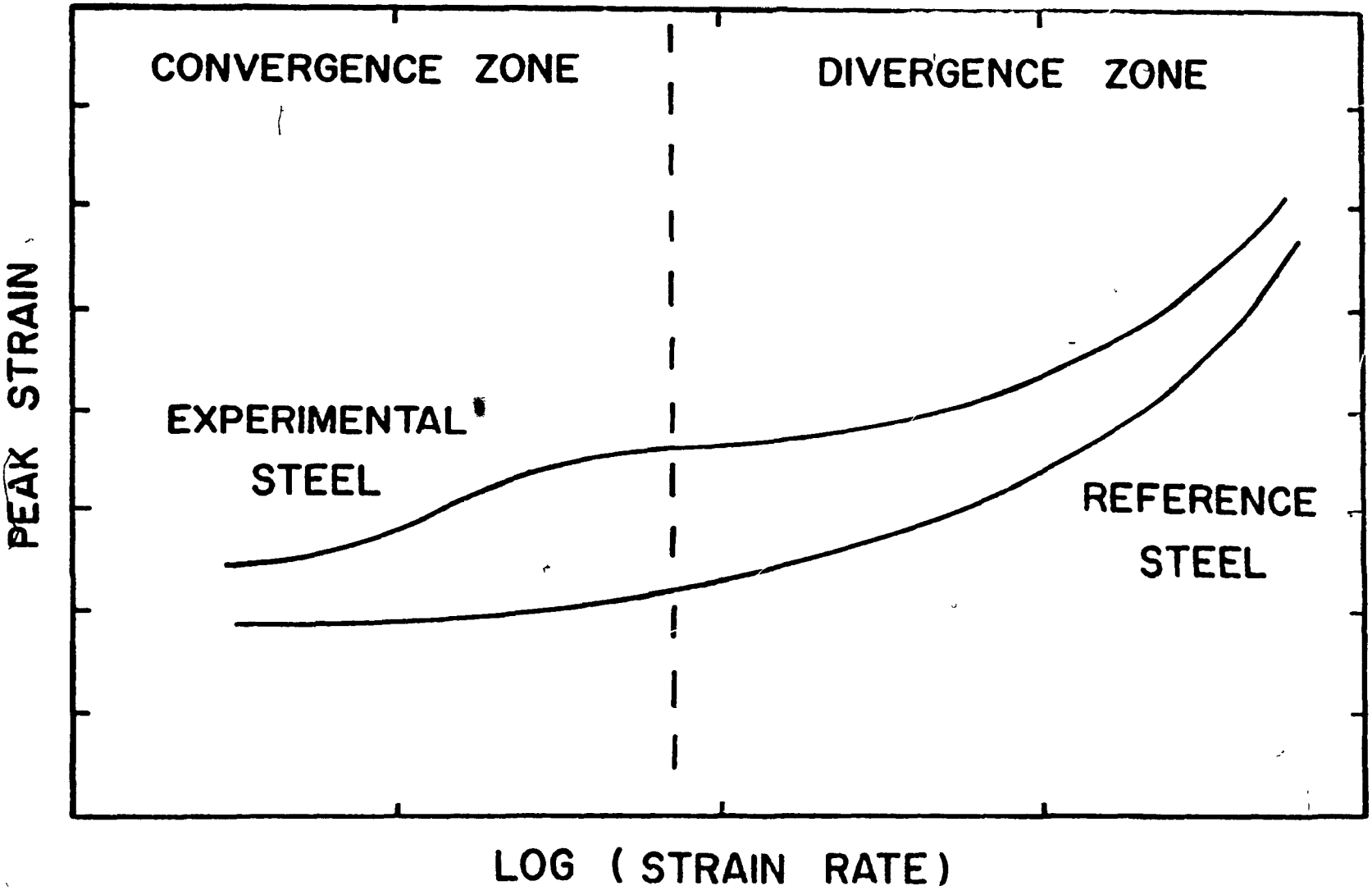

Figure 4.6 Schematic representing the convergence and the divergence zones of two curves.

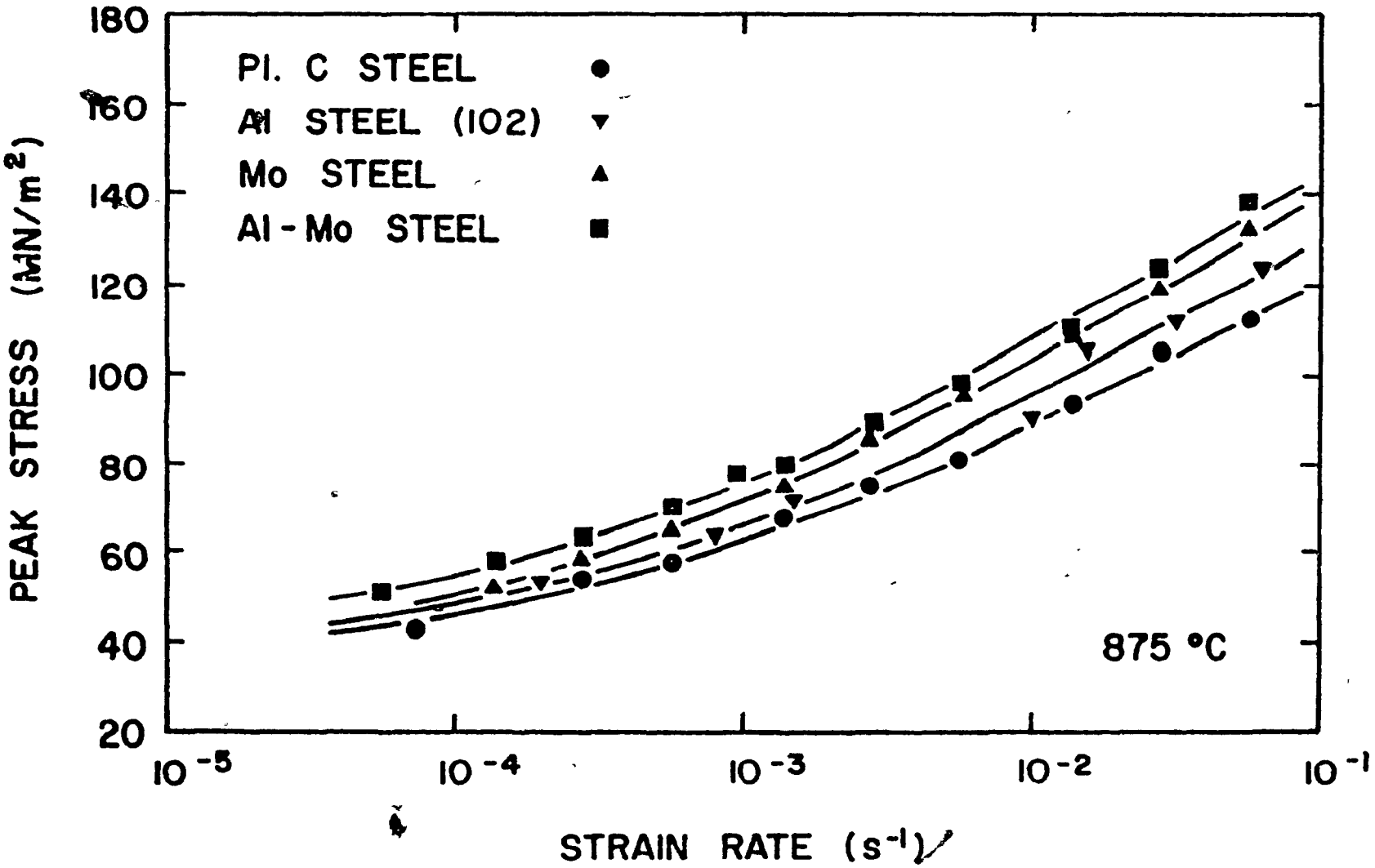

Figure 4.7a Dependence of peak stress on strain rate at 875°C for the three microalloyed steels and the plain C steel.

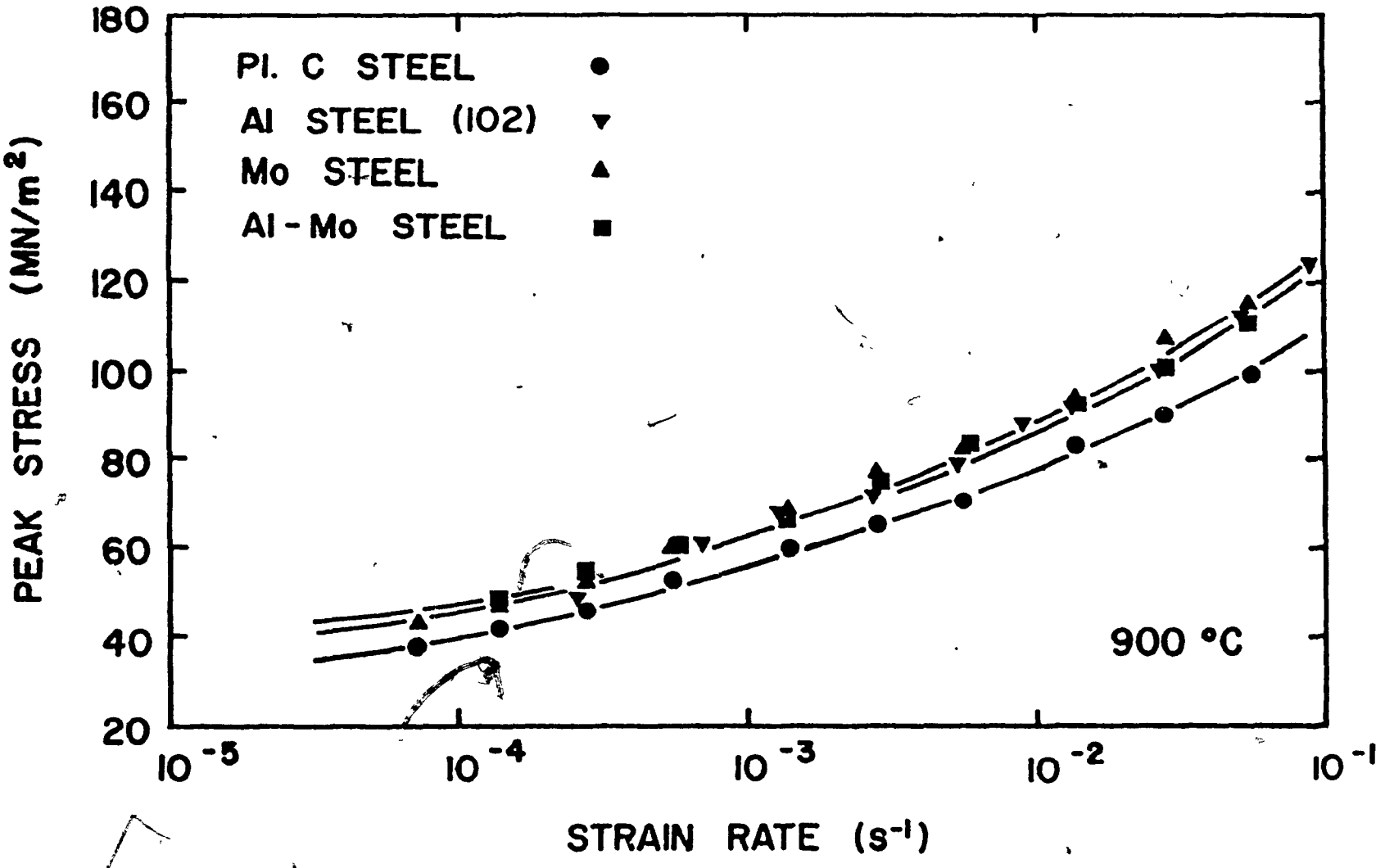

Figure 4.7b Dependence of peak stress on strain rate at 900°C for the three microalloyed steels and the plain C steel.

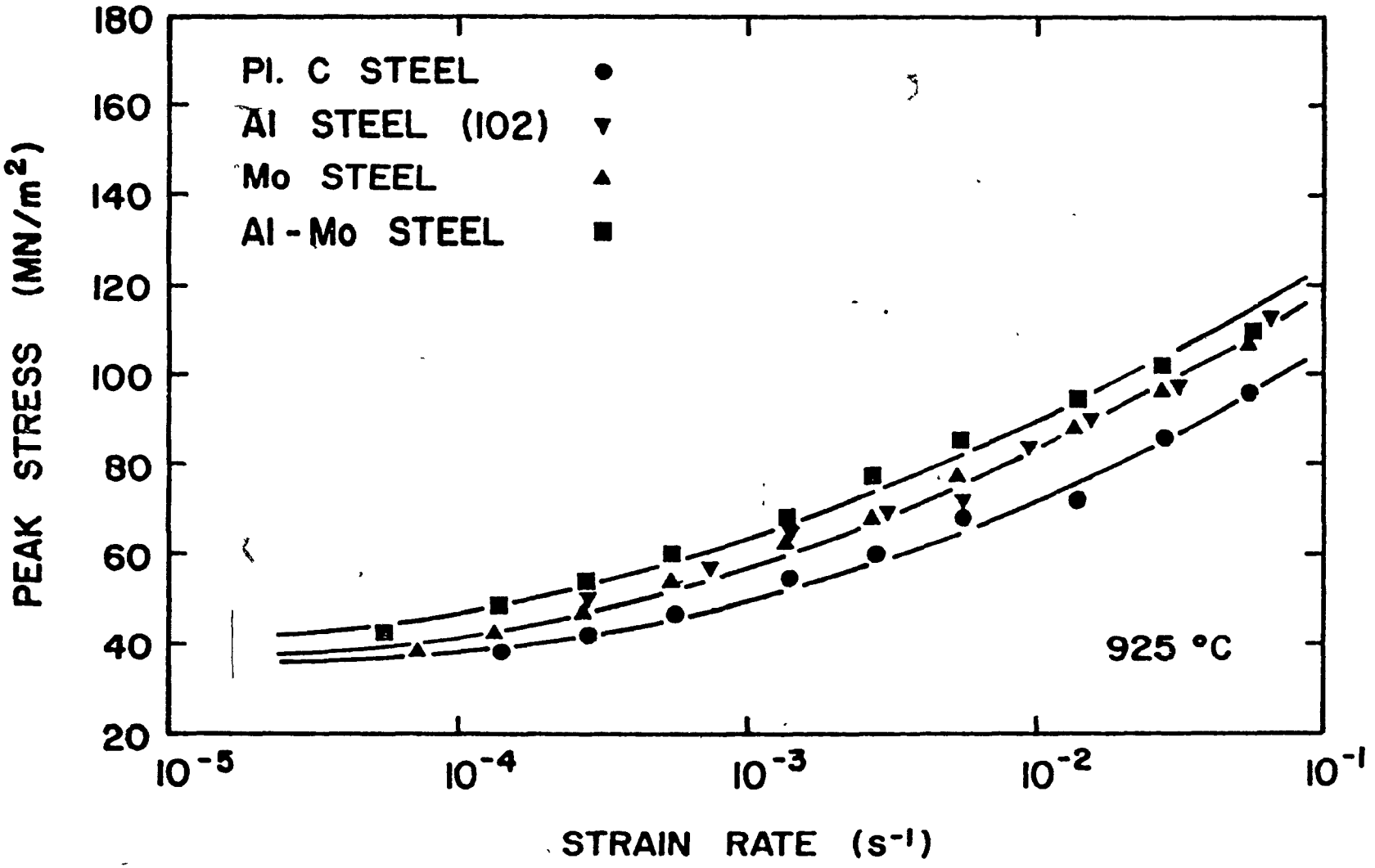

Figure 4.7c Dependence of peak stress on strain rate at 925°C for the three microalloyed steels and the plain C steel.

4.4 HIGH TEMPERATURE STRENGTHENING

4.4.1. Strain Rate Dependence of Yield Stress

Using a 0.2% offset technique, the yield stresses of the four steels were measured over the range of temperatures and strain rates investigated. As the plastic strain associated with macroscopic yield is small (first 1 to 3% of total strain) and rapidly attained, the magnitude of the yield stress is unaffected by strain induced precipitation (96). The difference between the yield stress levels of the various steels can then be attributed solely to the alloy additions which are present in the form of solutes. The strain rate dependence of the yield stress is presented in Fig. 4.8.

Since there is a considerable degree of scatter in the data of Fig. 4.8, the order of increasing yield stress is difficult to establish directly from the curves. To enable a more precise assessment of the dependence of the flow stress on composition, the average value of strengthening for each temperature and strain rate was calculated as described below.

4.4.2. Strengthening Produced by Al and Mo Additions

The relative solute strengthening ΔS_a was calculated using the formula:

$$\Delta S_a = \frac{\sigma_y^x - \sigma_y^{ref}}{\sigma_y^{ref}} \times \frac{0.1}{at.\%x} \times 100$$

Here σ_y^{ref} and σ_y^x are the yield stresses for the reference steel and that containing the element x, respectively. The values of the strengthening parameters ΔS_a and ΔS_w (the latter normalized to 0.1 weight % addition of the element x) are presented in Table 4.1. The strongest solute strengthening is produced by the addition of molybdenum (13.1% per 0.1 at. % in the Al-Mo steel), followed by aluminum, (6.5% in the Al-Mo Steel), molybdenum (6.0% in the Mo steel) and aluminum (1.3% in the Al steel). On a weight % basis, aluminum brings more strengthening than molybdenum (13.4% compared to 7.6%) when added to the Al-Mo steel. It should be noted here that the Al levels used in the calculations were based on the total Al levels. The soluble Al levels are currently being determined. It is expected that these levels are lower. In that event, the effect of Al as a solute would be

Table 4.1 High Temperature Strengthening Produced by Al and Mo Additions

Element	% Strengthening Per 0.1 at.%	% Strengthening Per 0.1 wt.%
* Al (in Al Steel)	1.3	2.6
Al (in Al-Mo Steel)	6.5	13.4
Mo (in Mo Steel)	6.0	3.5
* Mo (in Al-Mo Steel)	13.1	7.6

* Based on G. L. Wang's data, Ref. 102.

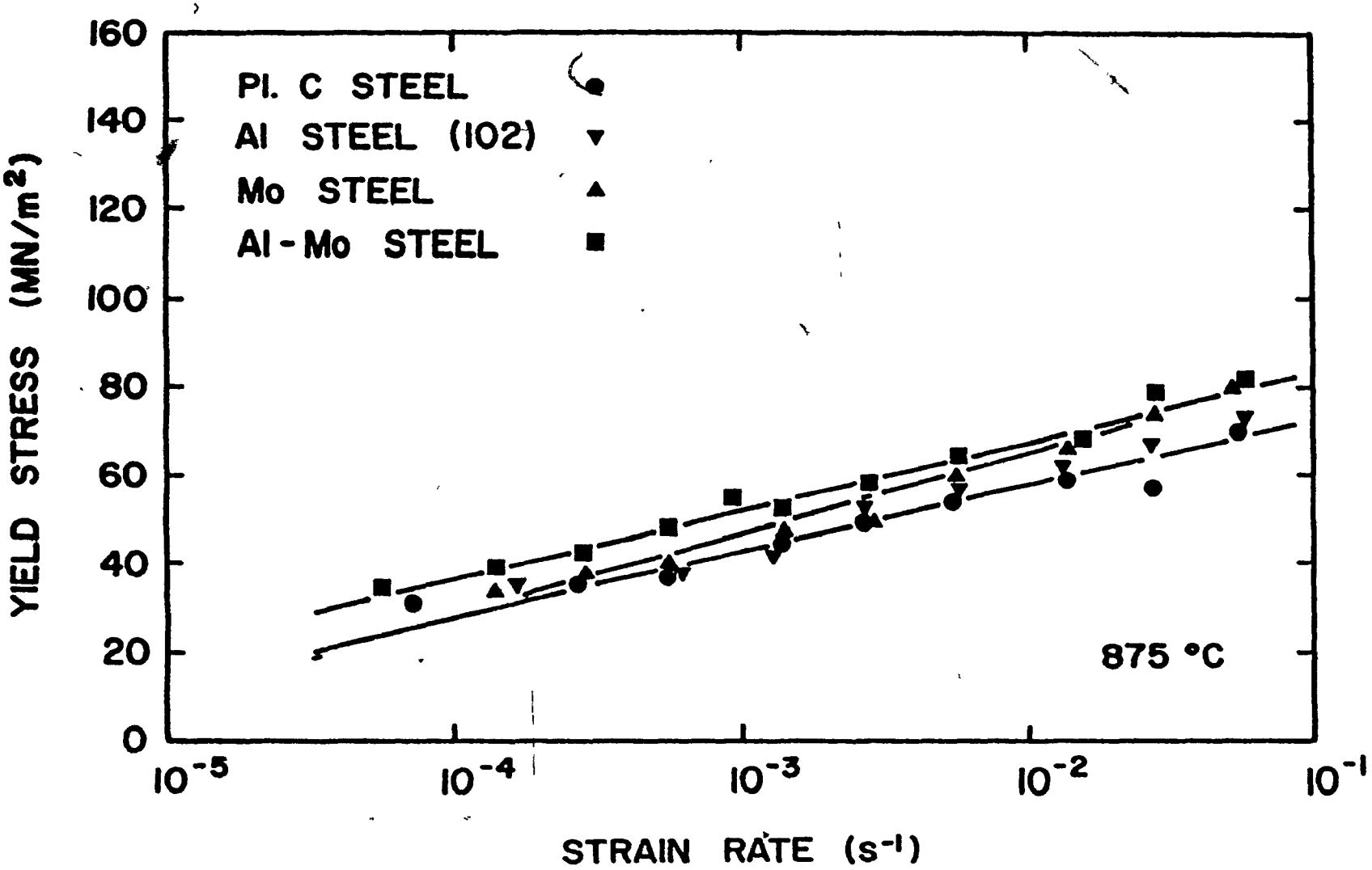

Figure 4.8a Dependence of yield stress on strain rate at 875°C for the three microalloyed steels and the plain C steel.

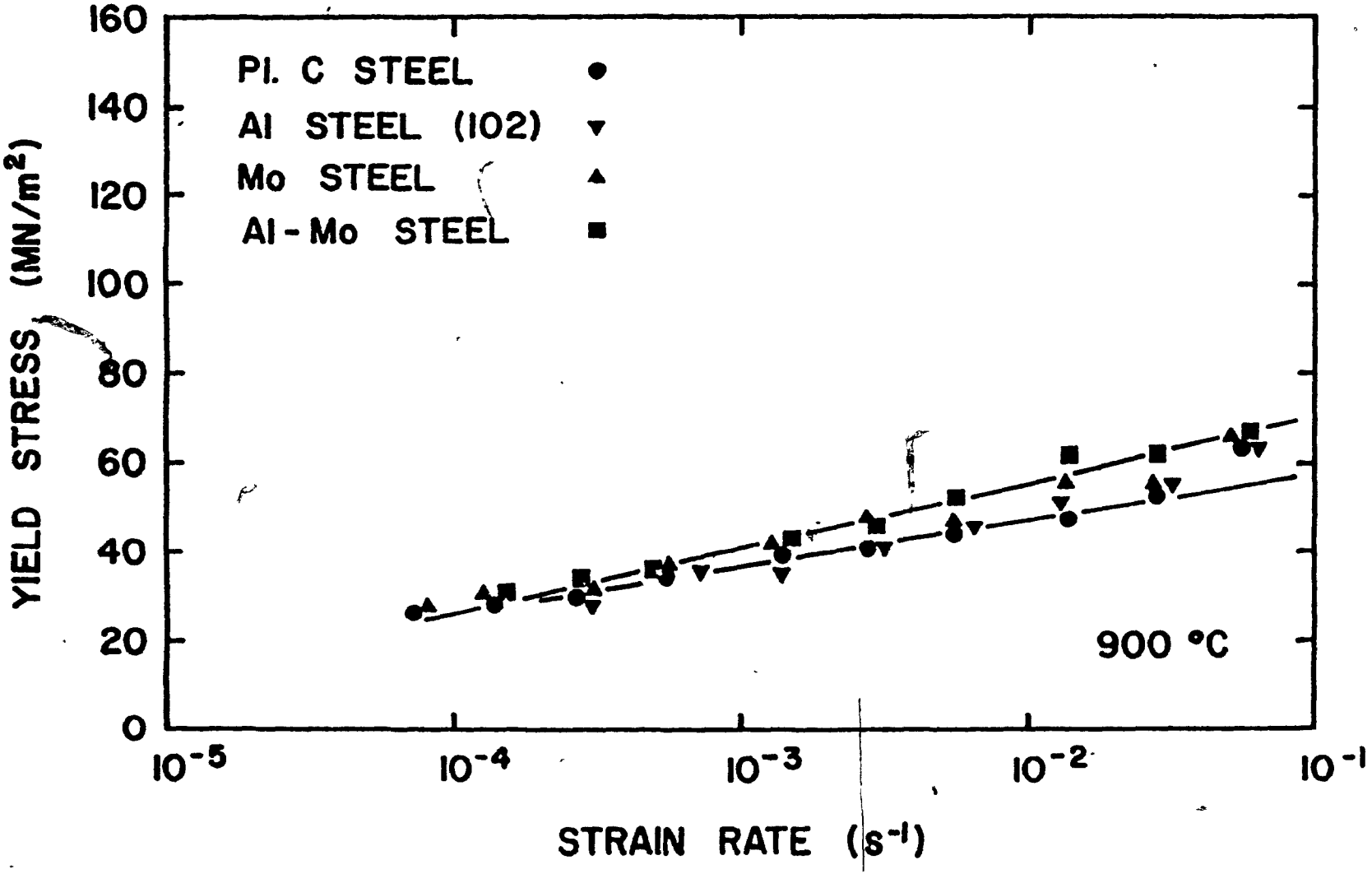

Figure 4.8b Dependence of yield stress on strain rate at 900°C for the three microalloyed steels and the plain C steel.

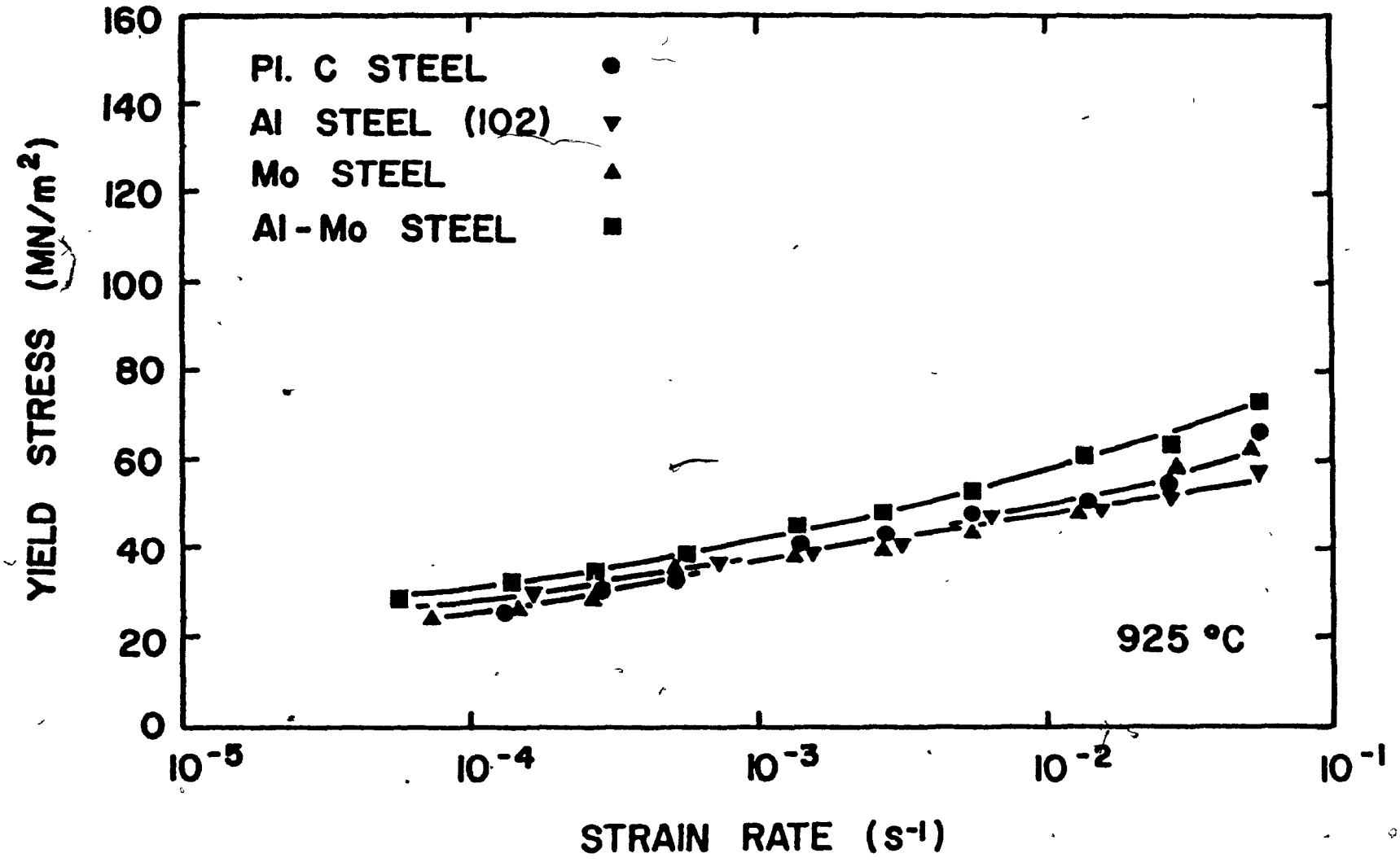

Figure 4.8c Dependence of yield stress on strain rate at 925°C for the three microalloyed steels and the plain C steel.

greater than indicated in Table 4.1.

4.5 DYNAMIC PTT CURVES

4.5.1 Approach to Determine Dynamic Precipitation

The method used here to detect dynamic precipitation involves the presence of a deviation or "hump" on the ϵ_p vs. $\log \dot{\epsilon}$ curves displayed in Section 4.2 (40, 66, 89). The schematic ϵ_p vs. $\log \dot{\epsilon}$ curve of Fig. 2.3 is reproduced as Fig. 4.9 for convenience. The dashed line A represents the solute case, i.e. the expected behaviour if there was no precipitation. The point at which the two curves A and B diverge at the high strain rate end of the plot defines the "start" of precipitation P_s. This is the strain rate at which precipitation starts before the peak strain is reached. The precipitation start time P_s is calculated from the ratio of the strain to strain rate as $P_s = \epsilon_{ps} / \dot{\epsilon}_s$. The curve marked C is parallel to A but shifted along the vertical axis until it becomes tangent to curve B. The precipitation finish time P_f is determined from the point of maximum divergence (point of tangency) as $P_f = \epsilon_{pf} / \dot{\epsilon}_f$. As the strain rate is decreased below ϵ_f, dynamic precipitation is completed at smaller and smaller strains and the amount of precipitate coarsening taking place during deformation to the peak stress increases, thus reducing the peak strain relative to ϵ_f.

Due to the considerably long testing times involved, data at the very low strain rate end of the deviations observed in Fig. 4.5 were not obtained. Consequently, only the start of precipitation could be detected in these steels.

4.5.2. Precipitation in Austenite

The P_s curves obtained for the two Al bearing steels are shown in Fig. 4.10. These curves indicate that the data points appear to be part of the lower branch of precipitation "C" curves. It is noticeable that the presence of Mo brings an earlier start to dynamic precipitation at the two higher temperatures. The results indicate that, at roughly 910°C, the start time of precipitation is about 15 s for the Al-Mo steel and 36 s for the Al

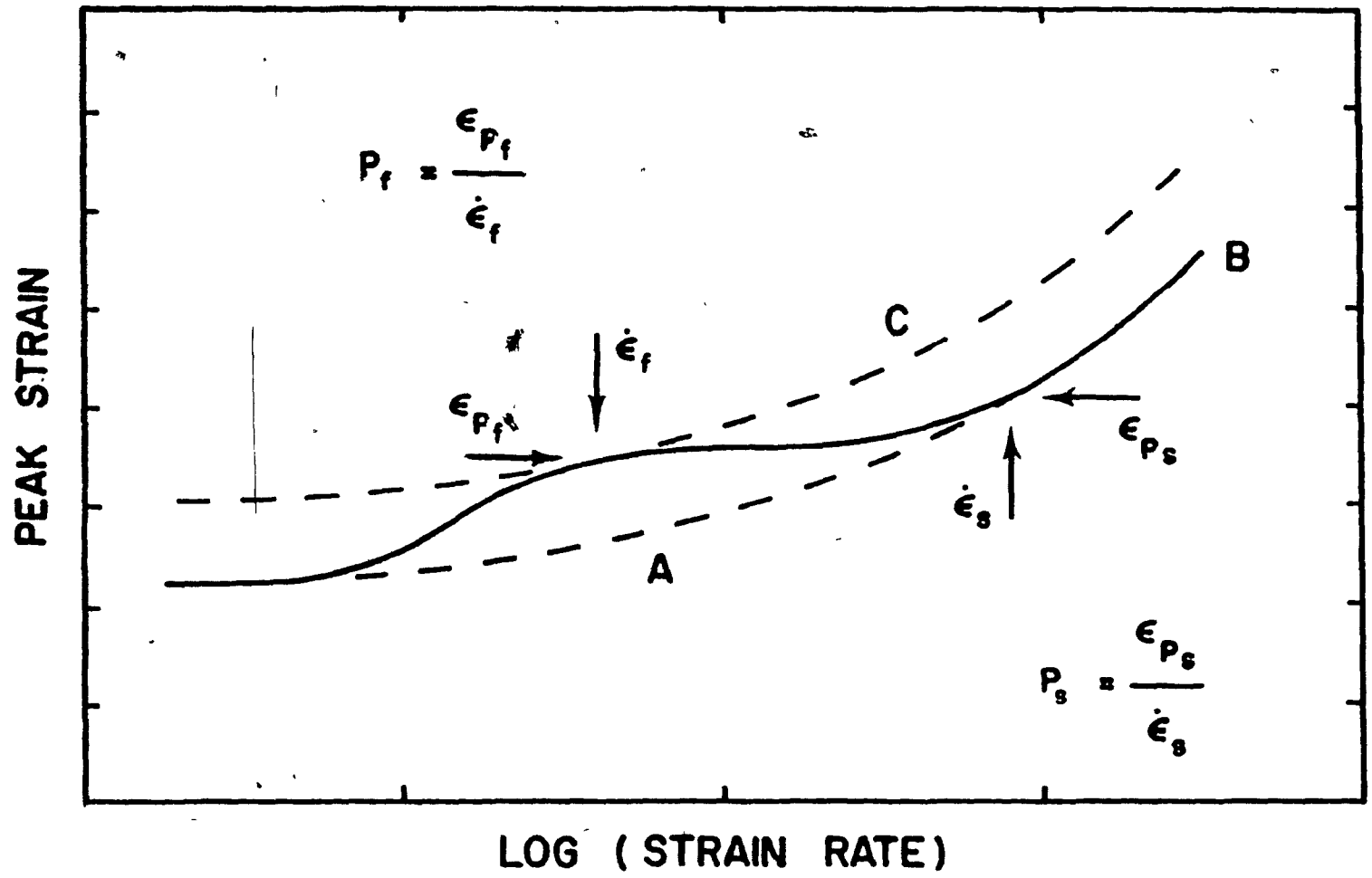

Figure 4.9 Schematic of ϵ_p vs. $\log \dot{\epsilon}$ curve to demonstrate the method of determining P_s and P_f times.

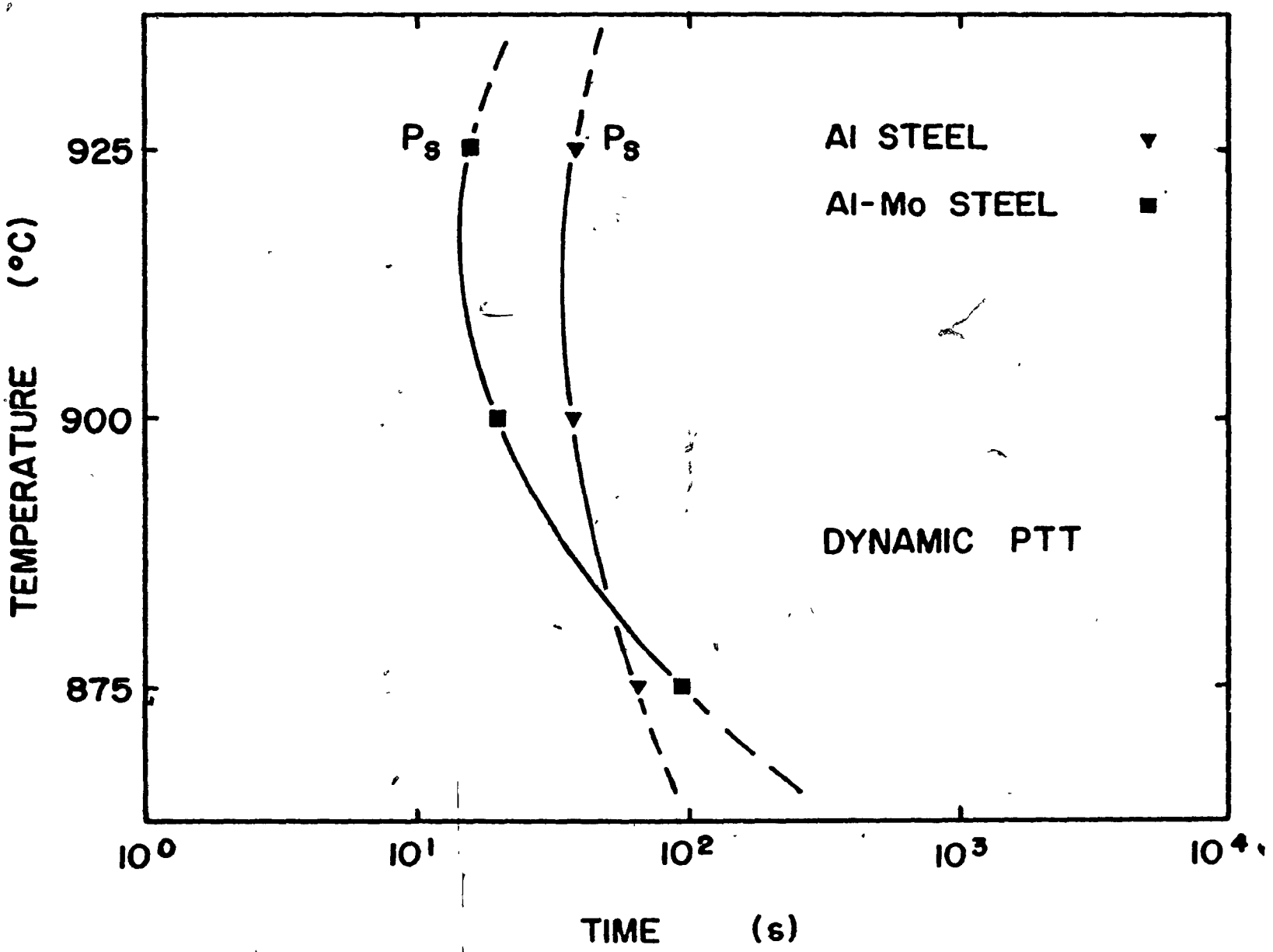

Figure 4.10 Dynamic P_s curves for the steels containing Al

steel. Compared to the Al-Mo steel, the wider opening of the "C" curve for the Al steel suggests a lesser dependence of precipitation on temperature for the range investigated. The order of P_s is reversed from 900 to 875°C, and precipitation appears earlier in the Al steel at 875°C. For each steel, what is believed to be the nose of the "C" curve is at roughly the same temperature (910 to 915°C). The corresponding times are 15 s for the Al-Mo steel and 35 s for the Al steel, more than twice as long.

CHAPTER 5

DISCUSSION

5.1 INFLUENCE OF ALUMINUM AND MOLYBDENUM ON DYNAMIC RECOVERY AND RECRYSTALLIZATION

From the relative peak strain values of the ϵ_p vs. $\log \dot{\epsilon}$ curves shown in Section 4.2, it can be seen that the addition of 0.2 wt.% Mo to a plain C steel increases the peak strain more (particularly at the higher strain rates as seen in Fig. 4.5) than 0.08 wt.% total Al. When the results are normalized for equal atom fractions (e.g. 0.1 atomic %), the stronger retarding effect on dynamic recrystallization comes from the addition of Mo as shown in Table 5.1. The combined addition of Al and Mo increases the peak strain relatively close to the sum of the individual contributions i.e.

$$\epsilon_p^{Al} + \epsilon_p^{Mo} - 2\,\epsilon_p^{PLC} \gtrsim \epsilon_p^{Al\text{-}Mo} - \epsilon_p^{PLC}$$

except at 900°C.

Although difficult to observe on the ϵ_p vs $\log \dot{\epsilon}$ curves of Fig. 4.5, the increases in peak strain obtained when raising the strain rate from 1.4×10^{-4} to $1.4 \times 10^{-1} s^{-1}$ show a slight difference among the steels investigated (Section 4.1). For both the plain C and Mo steels, the peak strain increases by a factor of 2.2 while for both steels containing Al it rises by a factor of 1.8. These results suggest that the addition of Al to the plain C steel might somewhat reduce its strain rate sensitivity.

The delay on dynamic recovery obtained from the alloying additions is reflected by an increase in the yield stress. The strengthening effect brought about by the investigated alloying additions are listed in Table 4.1. On an atomic fraction basis, the amount of retardation on dynamic recovery expressed from these values shows that the addition of Mo has a stronger effect than Al. This order is similar to that of delaying dynamic recrystallization.

Table 5.1 Retardation Effect on Recrystallization Produced by Al and Mo Additions

Element	% Retardation Per 0.1 at.%	% Retardation Per 0.1 wt.%
* Al (in Al Steel)	13.2	27.4
Al (in Al-Mo Steel)	7.1	14.7
Mo (in Mo Steel)	41.1	24.0
* Mo (in Al-Mo Steel)	30.0	17.5

* Based on G. L. Wang's data, Ref. 102.

Note: The above numbers are based on the total Al level. The soluble Al levels are under study, and are expected to be 80% of the total amount.

5.1.1. Effects of Al and Mo in Solution

The presence of microalloying elements in solution influences the hot strength of steels and their effects have already been studied by several authors (66, 74, 98, 110, 111). The variations in yield stress and peak strain (two of the parameters used to detect alloying effects) are usually ascribed to solute segregation, either to dislocations in the case of recovery or to grain boundaries in the case of recrystallization (62).

A number of reasons exists as to why some of the microalloying elements have significant effects on the dynamic restoration processes while some others have weaker contributions. As the solute atoms differ in size and rigidity from the solvent atoms, elastic interactions result between the microalloying elements and the dislocations, accounting for a component of solution hardening. Other possibilities of interaction also exist among which the most important are: the differences in atomic size and in modulus, the electronic structure differences and clustering. These have already been discussed and reviewed in previous works (57, 102, 112).

5.1.2. Effects of Al and Mo as Precipitate Formers

In addition to its solute contribution, the ability of Al to form precipitates constitutes a second mechanism capable of raising the hot strength of steel. The deposition on sub-boundaries or dislocations of fine precipitates formed before the attainment of the peak strain can delay the onset of both dynamic recovery and recrystallization. By lowering the rate of recovery, the particles also retard the nucleation of recrystallization and are thus responsible for the higher values of peak strain and peak stress.

Fine particles are obtained following a soaking treatment where carbonitrides present in the steel are dissolved. In the case where complete dissolution is not achieved, less carbonitride forming elements become available for precipitation. Upon straining, a reduction in dynamic precipitation together with the presence of coarser and less effective undissolved particles lower the magnitude of retardation of dynamic recrystallization and therefore the increase in peak strain. When considering the Al steels, where the N content is 0.006 wt.%, the above explains the necessity to reheat the material to put all the carbonitrides in solution.

Thereafter, the occurence of precipitation in pre-strained austenite (i.e. on dislocations) generates particles that are fine enough to produce an increase in flow stress (94).

Electron microscopy was not performed on samples tested during this research but is likely to become the subject of another thesis. Although no information is yet available to describe the nature, size distribution and volume fraction of possible precipitates, it remains of interest to examine the ϵ_p vs. $\log \dot{\epsilon}$ results for both the Al-Mo steel and the Al steel concurrently studied by Wang (102), from now on referred to as the Al steels, (Fig. 4.5). When compared to the plain C and Mo steels, both curves reveal the presence of a deviation and seem to level off towards the low strain rate end of the graph (Section 4.2). These deviations suggest that an additional retardation effect complements the delay on dynamic recrystallization brought about by the solutes. By considering these deviations as precipitation "humps", they could reflect the onset of a precipitation for which the completion time is probably very long. However, the poorly defined shape of these humps raises some doubts about the occurence of AlN precipitation. This may be ascribed to the limited Al in solution available to form the particles.

A study carried out by Michel et al. (74) on a steel microalloyed with 0.084 wt.% Al and 0.016 wt.% N revealed the presence of a pronounced hump on the ϵ_p vs. $\log \dot{\epsilon}$ curves which was attributed to AlN dynamic precipitation. The completion of this well defined deviation took place around a strain rate of $10^{-2}s^{-1}$ at 875°C and $10^{-3}s^{-1}$ at 925°C. However, in the case of the investigated Al steels, no end is observed in the deviation of the ϵ_p vs. $\log \dot{\epsilon}$ curves.

It is interesting to note that the N level in Michel's steel is more than twice that of the present Al steels. The corresponding atomic ratio of Al/N for the former material is 2.6 while the latter steels have a ratio of 6.7. This indicates that, upon AlN precipitation, the amount of free Al remaining in solution should be appreciable in the present Al steels.

The N content of both Al steels (0.006 wt.%) does not permit a great potential for AlN precipitation, especially in situations where alloying

elements other than Al, with a higher affinity for N, are also present. The complex Mo precipitates found in the Mo steel tested by Bacroix were observed to take place almost exclusively around fine nuclei constituted of TiN (109). The presence of residual Ti ($\leq$ 50 ppm) in the steel led to the formation of TiN at high temperatures with a consequent decrease of the initial amount of N available for the precipitation of AlN.

In the case of Bacroix's Mo steel, the above explains why almost no precipitation effect was detected on the ϵ_p vs. $\log \dot{\epsilon}$ curves, except at 875°C where a very weak deviation was detected (Fig. 5.1). This deviation was mostly attributed to the presence of fine complex Mo precipitates (109). Although the size of TiN particles was sufficiently small (<5 nm), the fact that they were probably not dynamicaly formed together with their low volume fraction is why they did not delay dynamic recrystallization (109, 113). Furthermore, the few AlN particles observed in this steel were found to be joined with other species such as Ti or MnS and to be of a size unable to affect recrystallization. Some of these precipitates were even detected in undeformed austenite which indicates the presence of undissolved AlN precipitates. This is interesting since the same reheating conditions were followed with the Al steels investigated here. The fact that the Al level is higher in the latter materials for a same N content as Bacroix's Mo steel suggests that some undissolved AlN precipitates could be present in the Al steels of this study. More likely is the possible presence of Al oxides coming from residual slag particles. The above could have affected the level of soluble Al available for AlN precipitation or for solute retardation of recrystallization.

Considering that the investigated Al steels were prepared by the same methods and equipment as Bacroix's Mo steel, the possibility of contamination by elements such as Ti has to be investigated. In the case where Ti is present in the Al steels, the deviation observed in the ϵ_p vs. $\log \dot{\epsilon}$ curves could be partly explained by the formation of some complex AlN-Ti or AlN-MnS particles with TiN precipitates. In the case of the Al-Mo steel, a definite retardation effect should be brought about by the formation of fine complex Mo particles around TiN precipitates. In both Al steels, other contributions could arise from the presence of undissolved AlN precipitates together with an appreciable amount of Al solute atoms.

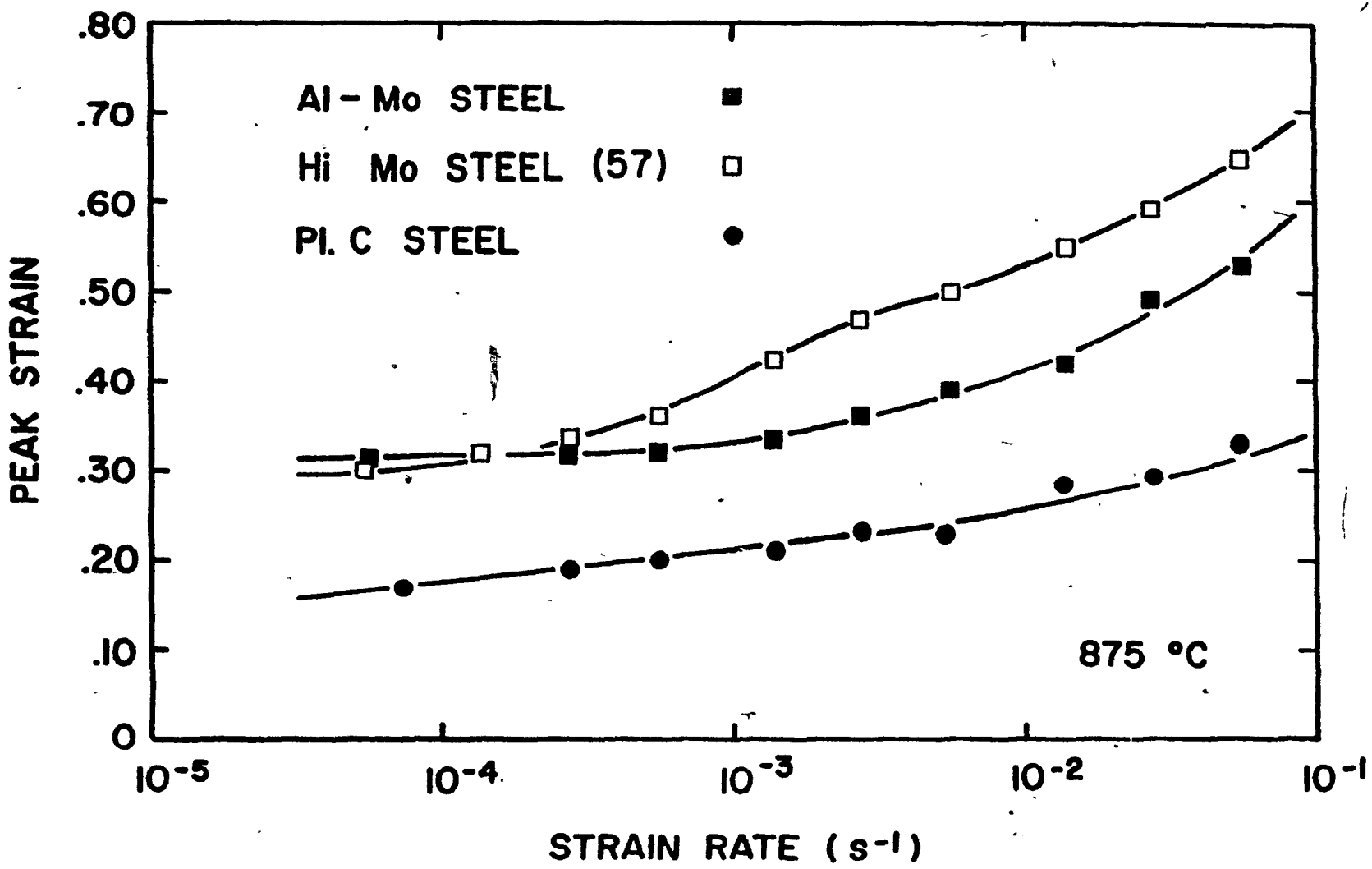

Figure 5.1a Dependence of peak strain on strain rate at 875°C for the Al-Mo steel and the Mo steel tested by Bacroix.

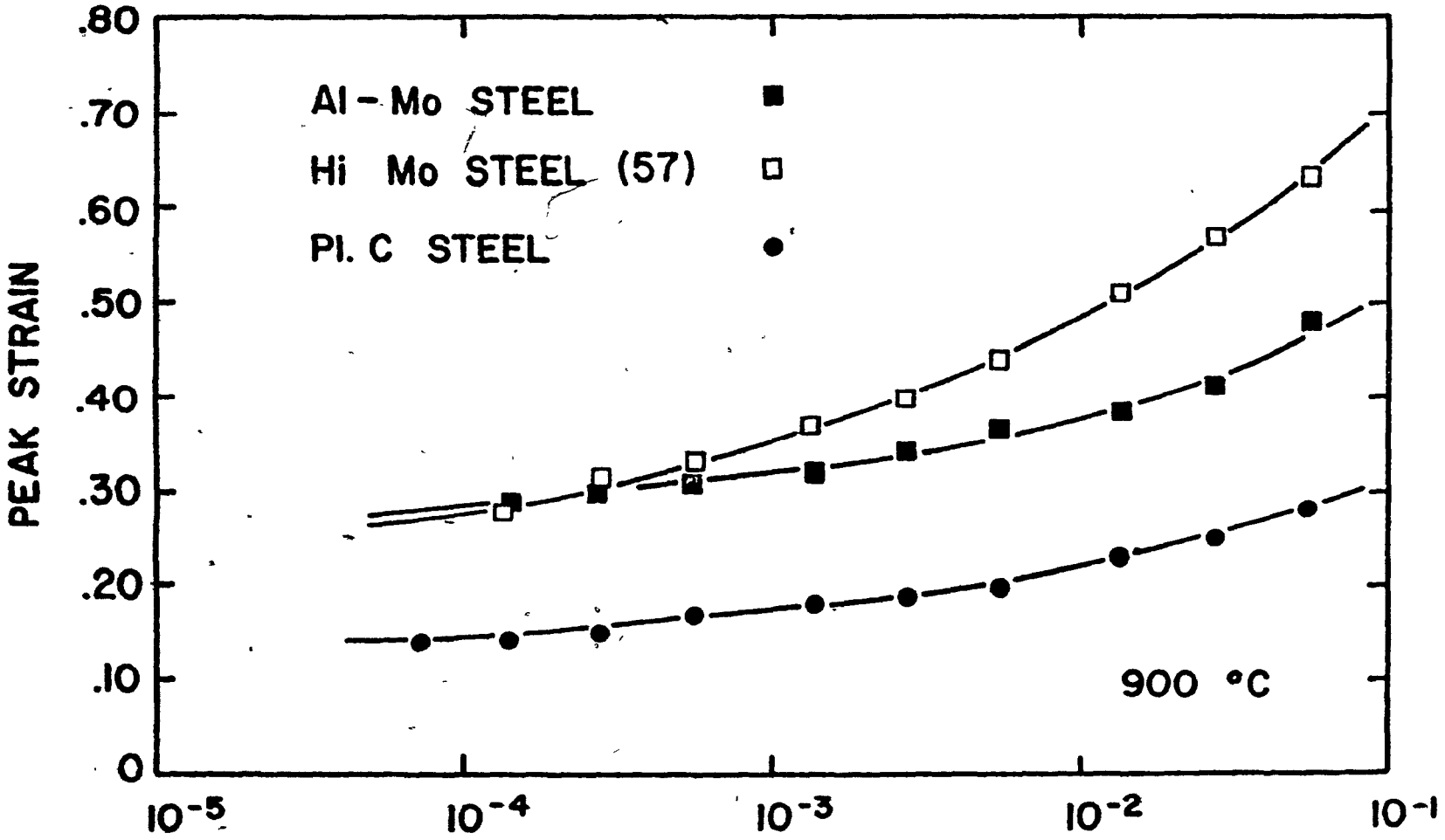

Figure 5.1b Dependence of peak strain on strain rate at 900°C for the Al-Mo steel and the Mo steel tested by Bacroix.

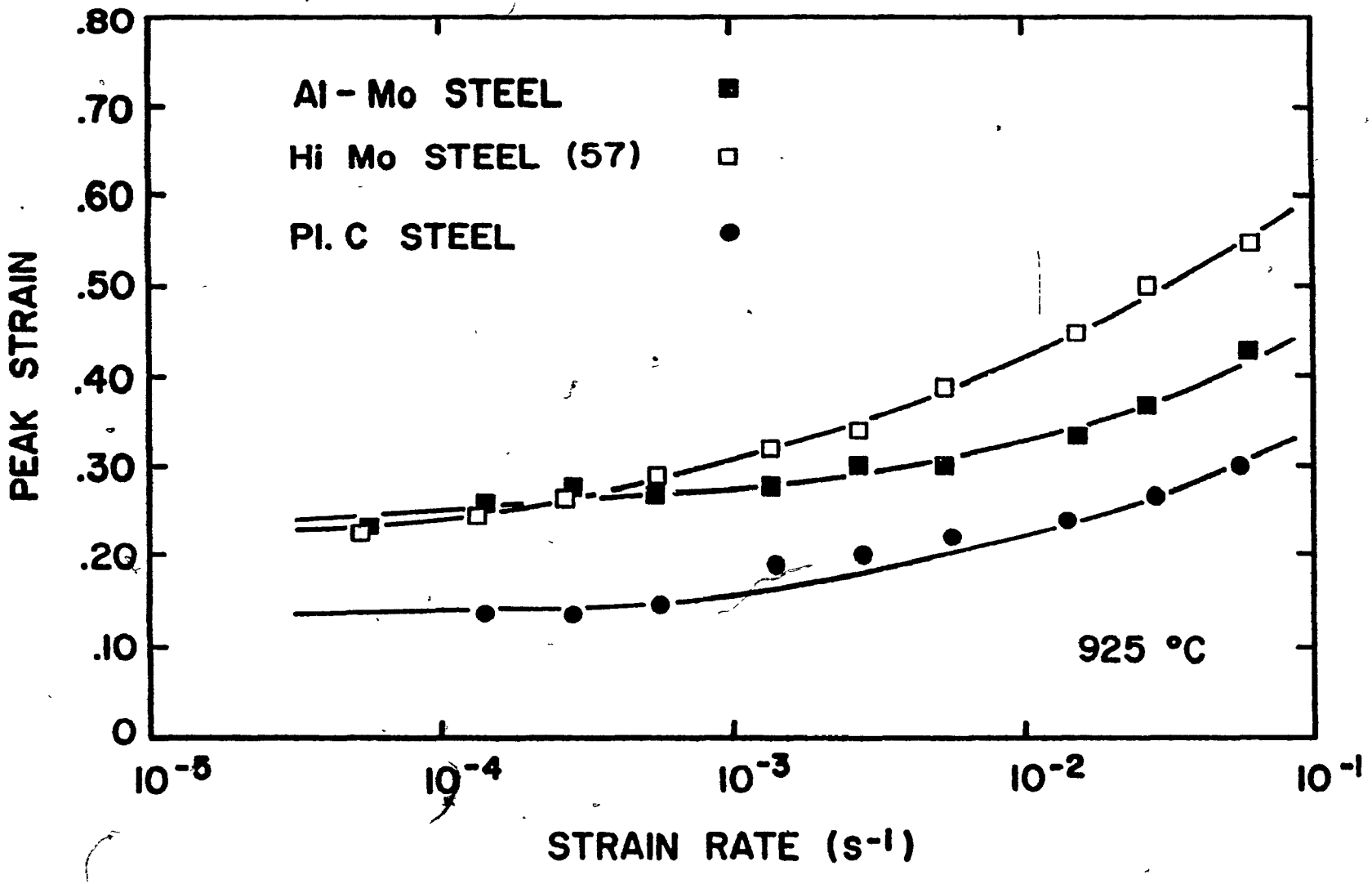

Figure 5.1c Dependence of peak strain on strain rate at 925°C for the Al-Mo steel and the Mo steel tested by Bacroix.

It is recognized that AlN is a phase which may have nucleating problems (114). Therefore, if aluminum is to be used as a "microalloying agent" to act as both solute and precipitate former, the presence of N gettering elements like Ti should be avoided in steel.

5.2 INFLUENCE OF MOLYBDENUM ON DYNAMIC PRECIPITATION

The dynamic PTT curves for the Al and Al-Mo steels are shown in Fig. 4.10. Both of these steels have a similar base composition but the Al-Mo material also contains 0.2 wt.% Mo (see Table 3.1). The results of Fig. 4.10 indicate that the addition of Mo to the Al steel slightly reduces the time required to onset dynamic precipitation at temperatures above 900°C. The effect is somewhat different from the observation reported by a previous study in which the addition of Mo was found to delay the onset of carbonitride precipitation (57). This effect was attributed to the probable reduction of the activity coefficients of both C and N caused by the Mo addition.

The physical significance of lowering the activity coefficient of an element in an alloy is that the material behaves as if there were less of that particular element present. For instance, the addition of Mn affects the activity coefficients of other alloying elements in this manner. A systematic study carried out by Koyama et al. demonstrated that Mn lowers the activity coefficients of C and N but it increases the ones of Nb and V in austenite to a lesser extent (115). The net result is a decrease in the carbide solution temperature (115). The effect of Mn on the solution temperature of Nb (CN) was discussed in detail by Akben et al. (66), and is schematically shown in Fig. 5.2. It reveals that, for a given temperature, the higher the concentration of Mn, the lower is the amount of supersaturation (with regard to Nb(CN) precipitation) which, in turn, decreases the driving force for precipitation.

In the present investigation, why the addition of Mo to the Al steel results in reducing the start time for dynamic precipitation is not clear. As in the case for Mn with Nb or V, it is possible that the presence of Mo increases the activity coefficient of other precipitating species such as Al but, to a much greater degree than it reduces those of C and N. This way,

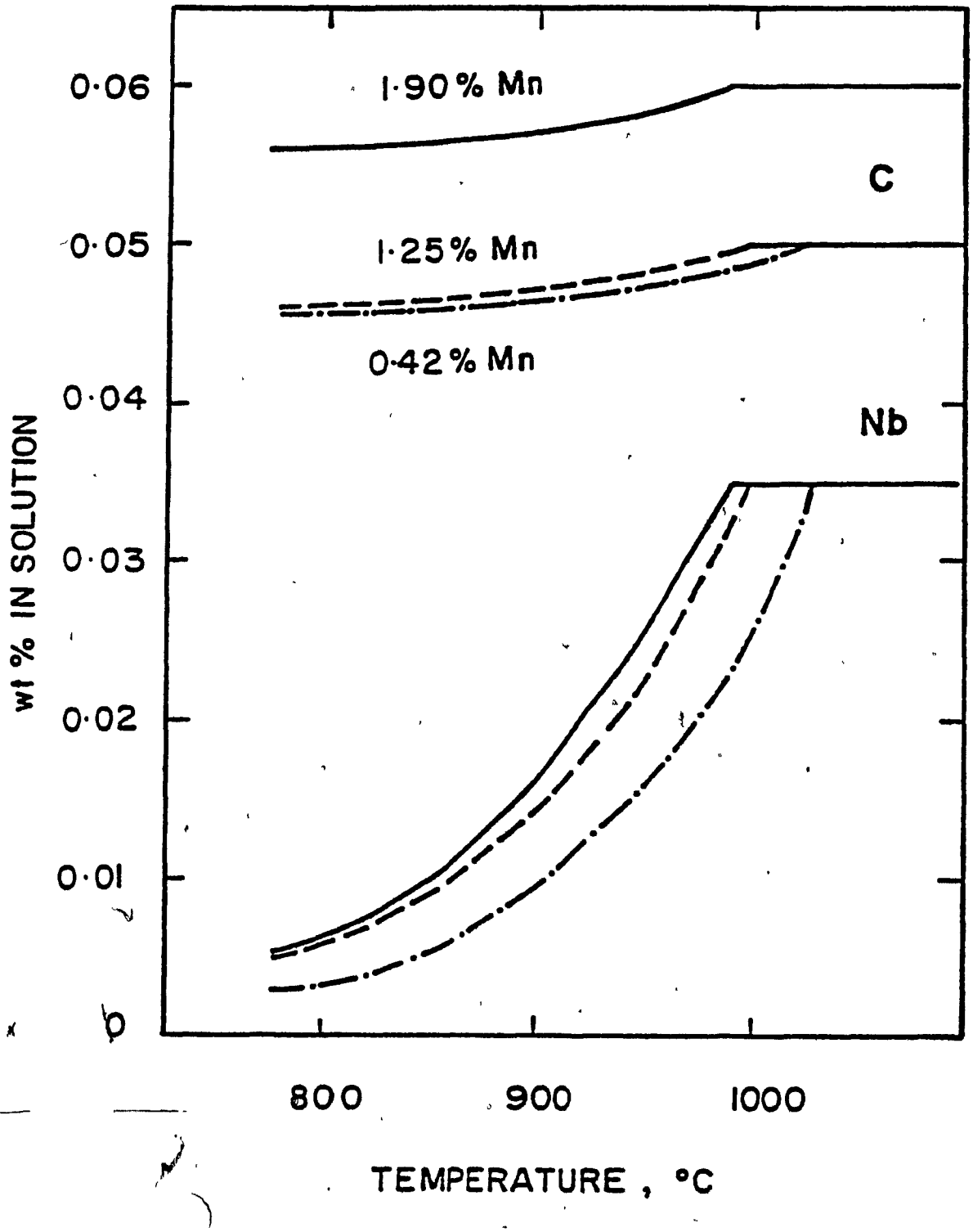

Figure 5.2 Calculated equilibrium solubility of Nb and C in three austenites containing 0.42, 1.25 and 1.90 % Mn from (98).

it could accelerate the onset of AlN precipitate formation. Unfortunately, no thermodynamic evidence concerning such an effect exists in the literature to confirm or contradict this hypothesis.

The shift of the P_s curve for the Al-Mo steel towards shorter times could also be attributed to the possible presence of complex Mo precipitates, as observed by L'Ecuyer et al. (109), on a steel similar to the Mo steel of this study. The presence of such complex precipitates could alter the overall formation of other precipitates in the steel as to when they appear in time.

Furthermore, the curvature of the P_s "C" curve for the Al-Mo steel differs from that of the Al steel (Fig. 4.10). As indicated in Fig. 5.3, these P_s curves have two main components: the part above the "nose" is controlled by the nucleation of precipitates whereas the lower part is controlled by the diffusion of the particle forming species. Mo is regarded as a slow diffusing element in γ-iron (85). It can thus decrease the diffusion rate of the elements with which it associates. The sharper trend of the Al-Mo steel precipitation curve towards longer times suggests that Mo decreases the diffusivity of the precipitating species.

5.3 EFFECT OF THE PARTIAL SUBSTTTUTION OF MOLYBDENUM BY ALUMINUM

Although molybdenum has been widely used in high strength low alloy steels for grain refinement and solution strengthening, its effectiveness is somewhat shadowed by a relatively high alloying cost when compared to other common microalloying elements. On the other hand, less expensive aluminum has a relatively poor solute effect in retarding recrystallization, but when combined with nitrogen as finely dispersed AlN particles, it effectively delays austenite recrystallization (74). It is therefore of interest to examine if, by substituting aluminum as a microalloying agent, the amount of more expensive molybdenum contained in a HSLA steel can be reduced without substantially accelerating recrystallization.

Ideally, the goal is to maintain in the Al-Mo steel a similar recrystallization start time (i.e. produce about the same amount of retardation of recrystallization) as in a steel with a higher Mo content

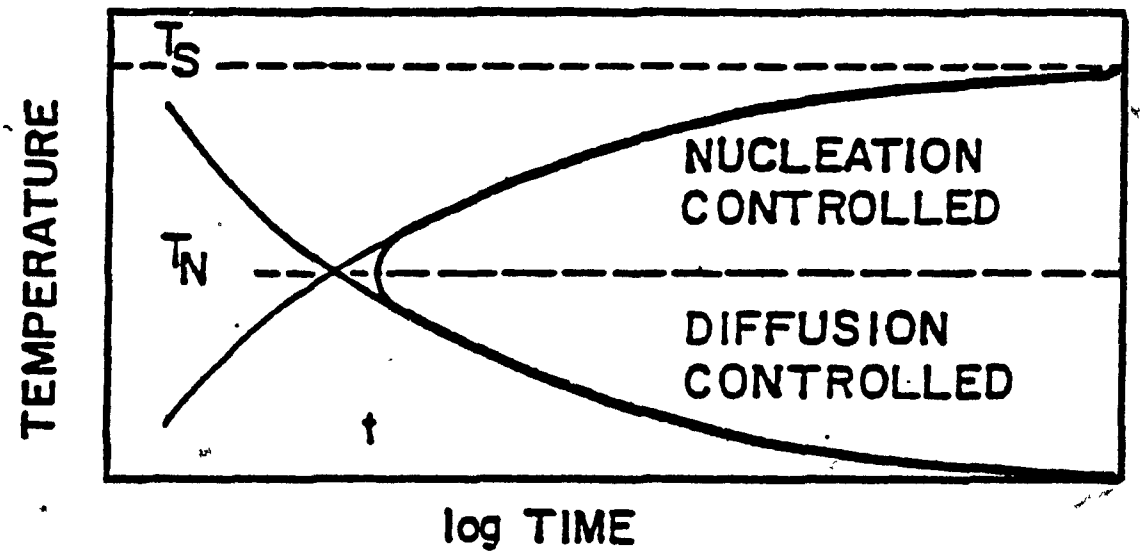

Figure 5.3 Illustration of the contributions of the nucleation and diffusion controlled branches of precipitation on the shape of the PTT curves.

throughout the strain rate range investigated, accompanied by an additional localized retardation effect brought about by the precipitation of AlN. The overall contribution in retarding recrystallization could possibly make the steel suitable for controlled rolling schedules.

For this purpose the results obtained from the investigated Al-Mo steel are compared to the ones from the Mo steel tested by Bacroix et al. (68). The latter had a similar base composition, a higher Mo (0.3 wt.%) and a lower Al content (0.065 wt.%) as compared to the present Al-Mo steel.

The result of the peak strain ϵ_p vs. log strain rate for these two steels and the reference plain C steel are represented in Fig. 5.1 for the three temperatures of interest. In all three cases, it can be observed that for strain rates higher than $1 \times 10^{-4} s^{-1}$, the Mo steel tested by Bacroix offers a stronger retarding effect on recrystallization than the Al-Mo steel of the present work. At strain rates below $1 \times 10^{-4} s^{-1}$, the two microalloyed steels appear to recrystallize at about the same strains. Note the absence of a precipitation hump in the curves of Bacroix's Mo steel except at 875°C, where a slight deviation can be observed. This suggests that no particularly strong retardation effect can be attributed to precipitation.

The above comparison indicates that by reducing the level of Mo from 0.3 to 0.2 wt.% and raising the level of Al from 0.065 to 0.08 wt.%, a loss of delaying effect on recrystallization is incurred.

Note that the grain sizes are approximately the same (100 μm) in these two materials. Regardless of the temperature, the percentage loss defined as:

$$\% \text{ Loss} = \frac{\epsilon_p^{\text{HiMo}} - \epsilon_p^{\text{Al-Mo}}}{\epsilon_p^{\text{HiMo}}} \times 100\%$$

raises from 0 at a strain rate of approximately $10^{-4} s^{-1}$, up to about 30% at $10^{-1} s^{-1}$ (Fig. 5.1). The loss of retardation probably results from a lower concentration of effective solutes, i.e. the replacement of some of the strong solute retardant Mo by the weaker solute contribution of Al (Section 4.2). The larger differences obtained with increasing strain rates might come from the greater difficulties in the rearrangement of solutes in the matrix.

Although no appreciable precipitation effect is observed on the curves of both Mo steels, the deviation on the Al-Mo steel curves, mentioned earlier in Section 4.2, is well defined besides the curves of Bacroix's Mo steel (Fig. 5.1).

This deviation, which mainly takes place at strain rates below $10^{-2}s^{-1}$, indicates that an additional retardation becomes effective in the Al-Mo steel. This extra retardation, probably resulting from dynamic precipitation, reduces the differences in peak strain between the two Mo steels. However, it is only at strain rates below $10^{-4}s^{-1}$ that the Al-Mo steel begins to show higher peak strains than Bacroix's Mo steel.

In the present context involving Bacroix's Mo steel and the investigated Al-Mo steel, the substitution of Al to partially replace the Mo content decreases the retardation effect on recrystallization and does not bring any appreciable dynamic precipitation effect. For these reasons, the investigated Al-Mo steel does not appear as a more suitable steel for controlled rolling applications than a 0.30 % Mo steel.

CHAPTER 6

CONCLUSIONS

The investigation described in this thesis dealt with the influence of aluminum and molybdenum additions on the kinetics of dynamic recrystallization and microalloy carbonitride (presumably (AlN)) precipitation in HSLA steels. A series of compression tests were performed in the temperature range 875-925°C. From the results, precipitation start times, and the influence of various chemistries on these kinetics were estimated for these materials. The following general conclusions were drawn from this study:

1) The addition of a high level of Al (0.08wt%, total) or 0.20% Mo alone or in combination to a plain C steel, results in retardation of dynamic recrystallization. The effect is stronger when the dual addition is made.

2) It is believed that some AlN particles remained undissolved, more likely the oxides. This has affected the level of soluble Al available for AlN precipitation or for solute retardation of recrystallization. It is estimated that one third of the total Al (by weight) is unavailable for this reason.

3) The precipitation start curves indicate that the addition of Mo to the Al steel (i.e. in the Al-Mo steel), reduces roughly by one-half the time required to onset dynamic precipitation. This may be attributed to Mo increasing the activity coefficients of the precipitating species.

4) The solute strengthening due to the addition of these two elements is roughly 1.3% and 6.5% per 0.1 atomic % addition of Al and Mo respectively. On a weight % basis, these numbers are 6 and 13% respectively.

5) Preliminary results of this study indicate that partial substitution of Al for the strong solute Mo may not be readily achieved. This may largely be because the steel-making practices do not readily allow for control of soluble Al levels.

REFERENCES

1. "Microalloying '75", Union Carbide Corporation, New York, N.Y. (1977).
2. "Alloys for the Eighties", Climax Molybdenum Company, Greenwich, Ct.
3. C. Parrini, N. Pizzimenti and A. Pozzi: Ref. 1, p. 288.
4. M. Cohen and S. S. Hansen: "MiCon 78: Optimization of Processing, Properties and Service Performance Through Microstructural Control", ASTM STP 672 (1979), p. 34.
5. W. C. Leslie: "The Physical Metallurgy of Steels", 1st ed., McGraw Hill Book Company, New York, N.Y. (1981), p. 77.
6. W. B. Morrison and J. A. Chapman: Phil. Trans. Roy. Soc. Series A, 282 (1975), p. 289.
7. F. B. Pickering: Ref. 1, p. 9.
8. K. J. Irvine: "Strong, Tough Structural Steels", The Iron and Steel Institute, Publication 104, (1967), p. 1.
9. J. N. Cordea: Symposium on Low Alloy High Strength Steels, Numberg, BRD, (1970), Metallurg. Companies, p. 61.
10. E. O. Hall: Proc. Phys. Soc., Series B, 64 (1951), p. 747.
11. N. J. Petch: J. Iron and Steel Inst., 174 (1953), p. 25.
12. N. J. Petch: Proc. Swampscott Conference, MIT Press (1955), p. 154.
13. I. Tamura: Proc. of the International Conference on Steel Rolling, ISIJ, Tokyo, 1 (1980), p. 59.
14. H. J. Wiester and H. Ulmer: Stahl und Eisen, 69 (1959), p. 1120.
15. R. W. Vanderbeck: Weld. J., 37 (1958), p. 114.
16. J. K. Macdonald, G. E. Wood and A. A. Towers: Ref. 13, 2, p. 921.
17. I. Kozasu, C., Ouchi, T. Sampei and T. Okita: Ref. 1, p. 120.
18. M. Cohen and W. S. Owen: ibid., p. 2.
19. K. J. Irvine, T. Gladman, J. Orr and F. B. Pickering: J. Iron and Steel Inst., 208 (1970), p. 717.
20. S. Yamamoto, C. Ouchi and T. Osuka: "Thermomechanical Processing of Microalloyed Austenite", Eds. A. J. De Ardo, G. A. Ratz and P. J. Wray, AIME, Warrendale, PA., (1982), p. 613.

21. T.M. Hoogendoorn and M. J. Spanraft: "Microalloying 75", Union Carbide Corporation, New York, N.Y. (1977), p. 120.

22. J. M. Gray and R. B. G. Yeo: ASM Transactions Quaterly, 61 (1968), p. 255.

23. J. D. Jones and A. B. Rothwell: "Deformation Under Hot Working Conditions", Iron and Steel Insititue, Publication 108 (1968), p. 78.

24. T. Mavropoulos: M. Eng. thesis, McGill University, Montreal, (1983).

25. A. M. Sage: "Proc. of Int'l. Conference on Hot Working and Forming Processes", Sheffield (1979), C. M. Sellars and G. J. Davies ed., The Metals Society, England, p. 119.

26. "Hot Working and Forming Processes", Eds., C. M. Sellars and G. J. Davies, Metals Soc., London, England (1980).

27. T. Tanaka, N. Tabata, T. Hatumora and C. Shiga: Ref. 21, p. 115.

28. T. Tanaka, T. Funakoshi, M. Vega, J. Tsuboi, T. Yasuda and C. Utahashi: ibid., p. 399.

29. D. R. Di Micco and A. T. Davenport: "Thermomechanical Processing of Microalloyed Austenite", Eds. A. J. De Ardo, G. A. Ratz and P. J. Wray, AIME, Warrendale, PA., (1982), p. 59.

30. J. H. Little, J. A. Chapman, W. B. Morrison and B. Mintz: "The Microstructure and Design of Alloys", 3rd Int. Conf. on the Strength of Metals and Alloys, Cambridge, England, Institute of Metals and ISI (1973), Vol. I, p. 80.

31. R. A. P. Djaic and J. J. Jonas: J. Iron and Steel Inst., 210 (1972), p. 256.

32. D. J. Towle and T. Gladman: Metal Science, 13 (1979), p. 246.

33. J. J. Jonas, C. M. Sellars and W. J. Mc. G. Tegart: Met. Rev., 14 (1969), p. 1.

34. C. M. Sellars and W. J. Mc. G. Tegart: Met. Rev., 17 (1972), p. 1.

35. D. J. Michel, J. Moteff and A. J. Lovell: Acta Met., 21 (1973), p. 1269.

36. J. J. Jonas and M. J. Luton: "Advances in Deformation Processing", J. J. Burke and V. Weiss ed., Plenum Publishing Corporation (1978), p. 128.

37. C. Rossard: Proc. 3rd Int. Conf. on the Strength of Metals and Alloys, Cambridge, England, 2 (1973), p. 175.

38. C. M. Sellars and J. A. Whiteman: The Metallurgist and Materials Technologist, 10 (1974), p. 35.

39. H. J. McQueen and J. J. Jonas: "Treatise on Materials Science and Technology", R. J. Arsenault ed., Academic Press, New York, N.Y., 6 (1975), p. 393.

40. L. Weiss and J. J. Jonas: Met. Trans., 10A (1979), p. 831.

41. A. LeBon, J. Rofes-Vernis and C. Rossard: Met. Sci., 9 (1975), p. 36.

42. C. Ouchi and T. Okita: Tetsu-to-Hagane, 62 (1976), p. 208.

43. T. Sakai, M. G. Akben and J. J. Jonas: "Thermomechanical Processing of Microalloyed Austenite", Eds. A. J. De Ardo, G. A. Ratz and P. J. Wray, AIME, Warrendale, PA., (1982), p. 237.

44. J. P. Sah, G. J. Richardson and C. M. Sellars: Met. Sci., 8 (1974), p. 325.

45. J. J. Jonas and M. J. Luton: "Advances in Deformation Processing", J. J. Burke and V. Weiss ed., Plenum Publishing Corporation (1978), p. 215.

46. M. J. Luton and C. M. Sellars: Acta Met., 17 (1969), p. 1033.

47. A. B. LeBon and L. N. de Saint Martin: "Microalloying 75", Union Carbide Corporation, New York, N.Y. (1977), p. 90.

48. M. J. Lafrance, F. A. Caron, G. R. Lamant and J. Leclerc: ibid., p. 367.

49. C. M. Sellars and J. A. Whiteman: Met. Science, 13 (1979), p. 187.

50. F. Haessner: "Recrystallization of Metallic Materials", F. Haessner ed., Dr. Rieder-Verlag GMBH, Stuttgart (1978), p. 1.

51. J. Everett, A. Gittins, G. Glover and M. Toyama: "Proc. of Int'L Conference on Hot Working and Forming Processes", Sheffield (1979), C.M. Sellars and G. J. Davies ed., The Metals Society, England, p. 16.

52. R. A. P. Djaic and J. J. Jonas: J. Iron & Steel Inst., 210 (1972), p. 1.

53. R. A. P. Djaic and J. J. Jonas: Metall. Trans., 4A (1973), p. 621.

54. T. Tanaka, T. Enami, M. Kimura, Y. Saito and T. Hatomura: Ref. 43, p. 145.

55. J. J. Irani, D. Button, J. D. Jones and A. B. Rothwell: "Strong, Tough Structural Steels", The Iron and Steel Institute, Publication 104 (1967), p. 110.

56. H. P. Stuwe: Ref. 50, p. 11.

57. B. Bacroix: M. Eng. Thesis, McGill University, Montreal (1982).

58. W. J. Mc. G. Tegart and A. Gittins: "The Hot Deformation of Austenite", J. B. Ballance, ed., AIME, N.Y. (1977), p. 1.

59. M. Zidek, B. Kubickova and J. Raab: Hutnicke Listy, 24 (1969), p. 98.

60. J. L. Robbins, O. C. Sheperd and O. D. Sherby: ASTM Quarterly Trans., 60 (1967), p. 205.

61. O. Dimitrov, R. Fromageau and C. Dimitrov: "Recrystallization of Metallic Materials", F. Haessner ed., Dr. Rieder-Verlag GMBH, Stuttgart (1978), p. 137.

62. L L. Dillamore: ibid., p. 223.

63. E. Hornbogen and U. Koster: ibid., p. 159.

64. T. Chandra, L Weiss and J. J. Jonas: Met. Sci., 16 (1982), p. 97.

65. E. L. Brown, A. J. De Ardo and J. H. Bucher: "The Hot Deformation of Austenite", J. B. Ballance, ed., AIME, N.Y. (1977), p. 250.

66. M. G. Akben, L Weiss and J. J. Jonas: Acta Met., 29 (1981), p. 111.

67. M. G. Akben, T. Chandra, P. Plassiard and J. J. Jonas: Acta Met., 32 (1984), p. 591.

68. B. Bacroix, M. G. Akben and J. J. Jonas: "Thermomechanical Processing of Microalloyed Austenite", Eds. A. J. De Ardo, G. A. Ratz and P. J. Wray, AIME, Warrendale, PA., (1982), p. 293.

69. M. G. Akben, B. Bacroix and J. J. Jonas: Acta Met., 31 (1983), p. 161.

70. R. W. K. Honeycombe: Metall. Trans. (1976), 7A, p. 915.

71. M. Korchynsky and H. Stuart: Symposium on Low Alloy High Strength Steels, Nurnberg, BRD, (1970), Metallurg. Companies, p. 17.

72. T. N. Baker: "Hot Working and Forming Processes", C. M. Sellars and G. J. Davies, eds., Sheffield, England (1979), p. 32.

73. A. T. Davenport, R. E. Miner and R. A. Kot: "The Hot Deformation of Austenite", J. B. Ballance, ed., AIME, N.Y. (1977), p. 186.

74. J. P. Michel and J. J. Jonas: Acta Met., 29 (1981), p. 513.

75. B. C. Woodfine and A. G. Quarrell: J. Iron & Steel Inst., 195, (1960), p. 409.

76. L. A. Erasmus: J. Iron & Steel Inst., 202 (1964), p. 32.

77. M. Fukagawa, Y. Saiga and K. Tachimoto: Trans. Iron Steel Inst. Japan, Suppl. 11 (1971), p. 1092.

78. M. T. Leger: Fonderie, 354 (1976), p. 107.

79. S. Hasebe: Tetsu-to-Hagane, 3 (1963), p. 200.

80. G. D. Funnell and R. J. Davies: Metals Technol., 5 (1978), p. 150.

81. G. D. Funnell: Preprint from Hot Working Int'l. Conf., Sheffield, 2, (1979), p. 12.1.

82. C. Ouchi, K. Tsukada and J. Tanaka: "Vanadium in High Strength Steel", Publication No. 140, Vanitec, London (1979), p. 37.

83. M. Fukuda, T. Hashimoto and K. Kunishige: "Microalloying 75", Union Carbide Corporation, New York, N.Y. (1977), p. 136.

84. H. Watanabe, Y. E. Smith and R. D. Pehlke: "The Hot Deformation of Austenite", J. B. Ballance, ed., AIME, N.Y. (1977), p. 140.

85. Y. Desalos, R. Laurent, M. Lena and B. Thomas: Memoires Techniques de la Revue de Metallurgie, 12 (1978), p. 673.

86. B. Bacroix, M. G. Akben and J. J. Jonas: Proc. of the International Symposium on the Thermomechanical Processing of Microalloyed Austenite, AIME, Pittsburg, PA (1981), p. 293.

87. W. Kanazawa, A. Nakashima, K. Okamoto, K. Tanabe and S. Nakazawa: Trans. ISIJ., 8 (1967), p. 113.

88. J. L'Ecuyer, G. L'Esperance, M. G. Akben and B. Bacroix: Acta Met., in press.

89. J. J. Jonas and L. Weiss: Met. Sci., 13 (1979), p. 238.

90. M. J. Luton, R. Dorvel and R. A. Petkovic: Metall. Trans., 11A (1980), p. 411.

91. C. M. Sellars: "Recrystallization and Grain Growth of Multiphase and Particle Containing Materials", N. Hansen, A. R. Jones and T. Leffers eds., Riso National Laboratory, Denmark (1980), p. 291.

92. T. Chandra, M. G. Akben and J. J. Jonas: Sixth International Conference on the Strength of Metals and Alloys, Melbourne, Australia, August (1982), 1, p. 499.

93. L. Meyer, F. Heisterkamp and W. Mueschenborn: Ref. 83, p. 153.

94. M. J. White and W. A. Owen: Met. Trans., 11A (1980), p. 597.

95. L. Weiss and J. J. Jonas: Met. Trans. 11A (1980), p. 403.

96. L. Wiess: Ph.D. Thesis, McGill University, Montreal (1978).

97. R. Simoneau, G. Begin and A. H. Marquis: Met. Sci., 12 (1978), p. 381.

98. M. G. Akben: Ph.D. Thesis, McGill University, Montreal (1980).

99. R. K. Amin, G. Butterworth and F. B. Pickering: "Proc. of Int'l. Conference on Hot Working and Forming Processes", Sheffield (1979), C. M. Sellars and G. J. Davies ed., The Metals Society, England, p. 27.

100. S. S. Hansen, J. B. Vandersande and M. Cohen: Met. Trans., 11A (1980), p. 387.

101. T. M. Hoogendoorn and M. J. Spanraft: "Microalloying 75", Union Carbide Corporation, New York, N.Y. (1977), p. 75.

102. G. L. Wang: M. Eng. Thesis, McGill University, Montreal (1986).

103. M. J. Luton: Ph.D. Thesis, McGill University, Montreal (1971).

104. J. P. Immarigeaon: Ph.D. Thesis, McGill University, Montreal, (1974).

105. R. A. Petkovic-Luton: Ph.D. Thesis, McGill University, Montreal, (1975).

106. L. S. Darken, R. P. Smith and E. W. Filer: Trans. Metall. Soc. AIME, 191 (1951), p. 1174.

107. Metals Handbook, 8th Edition, ASM, Metals Park, Ohio, 8 (1973), p. 64.

108. M. J. Luton, J. P. Immarigeon and J. J. Jonas: J. Phys. E. (Sci. Instr.), 7 (1974), p. 862.

109. J. D. L'Ecuyer, G. L'Esperance, M. G. Akben and B. Bacroix: Acta Met., in press.

110. R. L. Fleischer: Acta Met., 11 (1963), p. 203.

111. F. B. Pickering: Conf. Proc. of Internat. Conf. on Technology and Applications of HSLA Steels, ASM, Philadelphia, PA (1983), p. 1.

112. M. G. Akben and J. J. Jonas: ibid., p. 149.

113. L. A. Leduc and C. M. Sellars: "Thermomechanical Processing of Microalloyed Austenite", Eds. A. J. De Ardo, G. A. Ratz and P. J. Wray, AIME, Warrendale, PA., (1982), p. 641.

114. F. Vodopivec: J. Iron & Steel Inst., 211 (1973), p. 664.

115. S. Koyama, T. Ishii and K. Narita: Journal of the Japan Institute of Metals, 35 (1971), p. 1089.